AD-A110 021 SOUTHWEST RESEARCH INST SAN ANTONIO TX ARMY FUELS AN--ETC F/G 21/7
EVALUATION OF THE EFFECTS OF ALCOHOL FUELS ON SPARK IGNITION EN--ETC(U)
DEC 81 H W MARBACH, E C OWENS, T W RYAN DAAK70-79-C-0175
UNCLASSIFIED AFLRL-150 NL

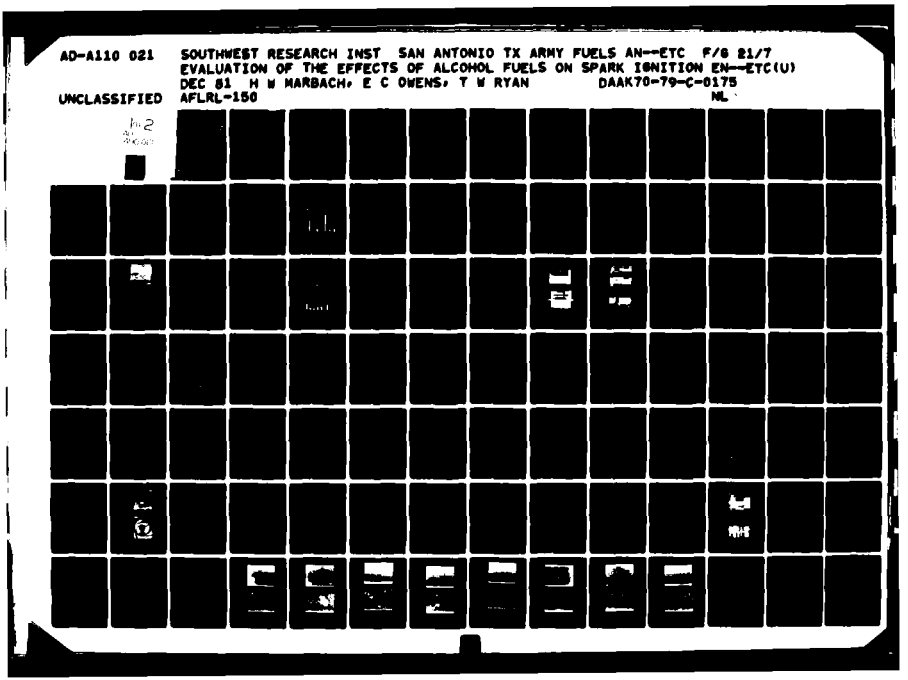

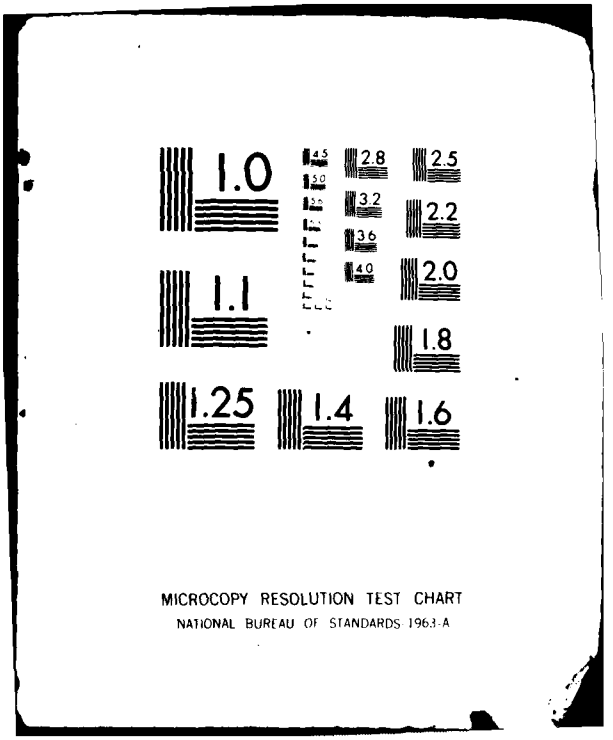
1.0
1.1
1.25
1.4
1.6
1.8
2.0
2.2
2.5
2.8
3.2
3.6
4.0
4.5
5.0
MICROCOPY RESOLUTION TEST CHART
NATIONAL BUREAU OF STANDARDS 1963-A

EVALUATION OF THE EFFECTS OF ALCOHOL FUELS ON SPARK IGNITION ENGINE WEAR

FINAL REPORT
AFLRL No. 150

(12)

By

H.W. Marbach, Jr.
E.C. Owens
T.W. Ryan III
E.A. Frame
D.W. Naegeli
Energy Systems Research Division
Southwest Research Institute
San Antonio, Texas

LEVEL II

For

U.S. Army Mobility Equipment
Research and Development Command
Fort Belvoir, Virginia
Contract No. DAAK70-79-C-0175
and
U.S. Department of Energy
Automotive Technology Development Division
Alternate Fuels Utilization Branch
Washington, D.C.
Interagency Agreement No. DE-AI01-79CS50030

Approved for public release; distribution unlimited

December 1981

Disclaimers

The findings in this report are not to be construed as an official Department of the Army position unless so designated by other authorized documents.

Trade names cited in this report do not constitute an official endorsement or approval of the use of such commercial hardware or software.

DDC Availability Notice

Qualified requestors may obtain copies of this report from Defense Documentation Center, Cameron Station, Alexandria, Virginia 22314.

Disposition Instructions

Destroy this report when no longer needed. Do not return it to the originator.

UNCLASSIFIED

SECURITY CLASSIFICATION OF THIS PAGE *(When Data Entered)*

REPORT DOCUMENTATION PAGE		READ INSTRUCTIONS BEFORE COMPLETING FORM
1. REPORT NUMBER AFLRL No. 150	2. GOVT ACCESSION NO. AD-A110 021	3. RECIPIENT'S CATALOG NUMBER
4. TITLE *(and Subtitle)* EVALUATION OF THE EFFECTS OF ALCOHOL FUELS ON SPARK IGNITION ENGINE WEAR		5. TYPE OF REPORT & PERIOD COVERED September 1979-September 1981 Final Report 6. PERFORMING ORG. REPORT NUMBER AFLRL No. 150
7. AUTHOR(s) H. W. Marbach, Jr. T.W. Ryan III E.C. Owens E.A. Frame D.W. Naegeli		8. CONTRACT OR GRANT NUMBER(s) DAAK70-79-C-0175 Interagency Agreement No. DE-AI01-79CS50030
9. PERFORMING ORGANIZATION NAME AND ADDRESSES U.S. Army Fuels and Lubricants Research Lab P.O. Drawer 28510, Southwest Research Institute San Antonio, Texas 78284		10. PROGRAM ELEMENT, PROJECT, TASK AREA & WORK UNIT NUMBERS
11. CONTROLLING OFFICE NAME AND ADDRESS U.S. Army Mobility Equipment Research and Development Command, DRDME-GL Ft. Belvoir, VA 22060		12. REPORT DATE December 1981 13. NUMBER OF PAGES 117
14. MONITORING AGENCY NAME & ADDRESS *(if different from Controlling Office)*		15. SECURITY CLASS. *(of this report)* Unclassified 15a. DECLASSIFICATION/DOWNGRADING SCHEDULE

16. DISTRIBUTION STATEMENT *(of this Report)*

Approved for public release; distribution unlimited

17. DISTRIBUTION STATEMENT *(of the abstract entered in Block 20, if different from Report)*

18. SUPPLEMENTARY NOTES

This work was conducted under Interagency Agreement No. DE-AI01-79CS50030 between DOD/US Army MERADCOM and the U.S. Department of Energy, Alternate Fuels Utilization Branch.

19. KEY WORDS *(Continue on reverse side if necessary and identify by block number)*

alcohol
methanol
ethanol
formic acid
cylinder bore wear
lubrication

20. ABSTRACT *(Continue on reverse side if necessary and identify by block number)*

An investigation of the effects of alcohol fuels on spark ignition engine wear and deposition was jointly sponsored by the U.S. Department of Energy and the U.S. Army Mobility Equipment Research and Development Command. Tests were conducted using neat methanol, anhydrous ethanol, and alcohol blends as fuel in a 2.3-liter engine using a modified ASTM Sequence V-D test procedure. This dynamometer testing indicates that alcohol fuels reduce the buildup of engine deposits. Also, it was found that neat methanol greatly

DD FORM 1 JAN 73 1473 EDITION OF 1 NOV 65 IS OBSOLETE

UNCLASSIFIED

SECURITY CLASSIFICATION OF THIS PAGE *(When Data Entered)*

20. ABSTRACT (continued)

increases engine wear rates at operating temperatures below 75°C, while anhydrous ethanol and alcohol-gasoline blends do not increase wear rates over that of unleaded gasoline. Tests were then conducted to evaluate the effects of methanol fuel on ten fully formulated lubricants and one lubricant with twelve additive composition changes. A 20-hour steady-state test was developed which shows that engine wear is inversely related to engine oil temperature when using methanol as fuel. The study shows that one lubricant appears to best control methanol-related engine wear, but still not to acceptable levels.

The mechanisms leading to this excessive wear were investigated using both engine and bench tests. Engine tests using prevaporized superheated methanol indicated that the wear results from reactions between the combustion products and the cast iron cylinder liner, where the presence of liquid methanol in the combusion chamber appears to be an important part of the mechanism. These reactions were investigated using a spinning disc combustor.

The spinning disc combustor was used to provide a source of burning methanol droplets which were subsequently quenched on a water-cooled cast iron surface. The condensate which formed on the cast iron surface was collected and analyzed for chemical composition. Infrared analysis indicated the presence of large quantities of iron formate, a reaction product of iron an formic acid. Additional spinning disc tests were performed to investigate the effects of surface material on the formation of formic acid.

FOREWORD

This work was conducted during the period September 1979 through September 1981 and was funded by a DOE-DOD Interagency Agreement No. DE-AI01-79CS50030 originated by the U.S. Department of Energy, Alternate Fuels Utilization Branch. The work directives and direct contract arrangements with U.S. Army Fuels and Lubricants Research Laboratory (USAFLRL) were made via contract DAAK70-79-C-0175, issued by the U.S. Army Mobility Equipment Research and Development Command (USAMERADCOM), Energy and Water Resources Laboratory, Fort Belvoir, VA. The DOE technical monitor was Mr. E.E. Ecklund and the USAMERADCOM technical monitor was Dr. J.V. Mengenhauser.

ACKNOWLEDGMENTS

The authors would like to acknowledge the significant contributions of Mr. J.T. Ford for his work in conducting the various engine tests and Mr. E.R. Lyons for his efforts in the rating and inspection of test engines. Special recognition is also made of the chemical and engine laboratory personnel at U.S. Army Fuels and Lubricants Research Laboratory (USAFLRL), and the following individuals whose talents contributed to this report: Ms. Elisabeth Robinett (editorial assistance), Ms. Silva Hayes (word processing), and Ms. Judy Caldwell (illustrations and drafting).

TABLE OF CONTENTS

LIST OF TABLES

LIST OF ILLUSTRATIONS

LIST OF ILLUSTRATIONS (cont'd)

I. INTRODUCTION

A national desire to reduce the volume of imported petroleum has generated extensive interest in the use of alcohols as fuels for spark ignition engines. Because of its naturally high octane number, methanol is extremely attractive as a substitute for petroleum-derived gasoline. Another attractive feature of methanol is that it can be derived from the vast United States coal resources. Also, interest exists in the production of ethanol from agricultural products for use as a gasoline extender and blending agent.

While large amounts of data have been accumulated on the combustion-related aspects of the use of these alcohols as fuels, the effects of methanol and ethanol on engine lubrication and durability have had limited investigation.(1-5)* As a result, the U.S. Department of Energy, in conjunction with the U.S. Army, funded an investigation into effects of these alcohols on engine lubrication and wear.

II. BACKGROUND

Historically, interest in the use of methanol as an automotive fuel has been highest during periods of petroleum shortages. Alcohols were widely used as engine fuels at the turn of the century, in the 1920's, and during World War II.(6) In all cases, the interest waned when the more economical petroleum fuels became available. In certain applications, such as racing, and in some geographical areas, the use of alcohol has continued.

Over the past two decades, it has become obvious that world resources of petroleum are being depleted faster than new reserves can be found. In view of this, the interest in alcohol fuels has once again been renewed, and several recent investigations have been undertaken concerning the performance and emissions characteristics of the alcohols and alcohol-gasoline blends. Both methanol and ethanol have been studied. Methanol, however, appears to

*Underlined numbers in parentheses refer to references listed at the end of this report.

be the better long-term replacement for gasoline because of the potential to produce it from coal at a relatively attractive cost.

Several studies(7-9) have been performed to examine the performance and emissions characteristics of methanol-fueled spark-ignition engines. Ingamells and Lindquist(10) have documented the incompatibility of methanol and certain fuel system components found in typical automobiles. The material compatibility problems exist whenever methanol comes into contact with lead, magnesium, aluminum, and some plastics. The effects of methanol on internal engine wear and lubricant degradation have only recently been addressed.

The U.S. Army Fuels and Lubricants Research Laboratory (AFLRL) investigation of the effects of alcohol fuels on the oil-wetted portions of an engine was started under U.S. Army Contract DAAK70-78-C-0001 using a single-cylinder Coordinating Lubricants Research (CLR) engine fueled with pure (technical grade) methanol. Based on research by Conoco(5) and a limited number of radioactive tracer engine tests by AFLRL(11), the initial investigations concentrated on low engine temperature operations. A series of 38 engine tests indicated that, in the CLR engine, the use of pure methanol greatly increased the top bore wear, top ring wear, and the rate at which iron wear particles accumulated in the engine oil.(11-14) The CLR engine is significantly different from current engine designs. Therefore, to confirm these initial CLR engine results in a full-scale modern engine, a test stand capable of conducting the ASTM Sequence VD (then PV-1)(15) test was set up. This test consists of cyclic low- and mid-range engine operating temperatures, and was developed to correlate the performance of engine oils to results obtained in actual consumer use during commuter-type service in the northern United States.

III. DETAIL OF TEST PROCEDURES

A. Lubricants and Fuels

A wide range of lubricant types and lubricant additive compositions was used

for this program (Table 1). The lubricants and additives are discussed in the appropriate sections of this report.

TABLE 1. TEST LUBRICANTS

Lubricant Code	Specification	Lube Type	Description
A	MIL-L-46152	10W-30	Army Fielded Oil
B	SE	10W-30	Factory Fill
C	MIL-L-21260B	Grade 30	Army Fielded Oil (Preservative Engine Oil)
D	MIL-L-46167	Synthetic 5W-20	Army OEA & Arctic HPTF
E	Experimental	10W-30	Extra Preservative Zinc
F	CD	15W-40	Commercial
G	CD	Synthetic 10W-30	Commercial
H	MIL-L-46167	Synthetic 5W-20	Army OEA & Arctic HPTF
I	SF	10W-40	Commercial
J	Experimental	20W-40	Experimental
A1-11	Experimental with twelve different additive compositions (Table 12)		

The three fuels used in this program were (1) Phillips J unleaded gasoline (Table 2) which is the reference fuel used in the ASTM Sequence VD Test; (2) denatured anhydrous ethanol [3785 liters (100 gallons) anhydrous ethanol plus 3.785 liters (1 gallon) unleaded gasoline] meeting BATF Formula 28A; and (3) commercial, technical grade methanol meeting Federal Specification O-M-232d Grade A.

The ethanol and methanol were purchased in 55-gallon drums. Even though large quantities of alcohol were used during this program, the alcohol was procured in drums to preclude problems of water absorption which may occur in bulk delivery and storage. All the drums were stored in a covered area and sealed until ready for use. A drum was opened and a sample collected; it was then connected to the in-house fuel supply system and the air vent was connected to a "Drierite" cylinder to exclude moisture.

TABLE 2. PROPERTIES OF PHILLIPS J UNLEADED GASOLINE

Property	Method	Value
Gravity, API, 15.6°C	D 287	52.8
Gravity, Specific, 15.6°C	D 1298	0.7678
Copper Corrosion, 3 hr at 100°C	D 130	1A
Reid Vapor Pressure, kg/m^2	D 323	43.9
Octane Number, Research	D 2699	95.9
Octane Number, Motor	D 2700	85.0
(R+M)/2		90.5
Total Sulfur, wt%	D 1266	0.020
Gum, mg/100 ml	D 381	0.6
Oxidation Stability, min	D 525	1200+
Distillation, % Evap, °C	D 86	
IBP		32
5%		41
10%		48
15%		54
20%		60
30%		77
40%		97
50%		114
60%		119
70%		127
80%		139
90%		162
95%		181
EP		210
Recovery, %		98.5
Residue, %		0.5
Hydrocarbon Types, vol%	D 1319	
Saturates,		42
Olefins		12
Aromatics		46

B. Modified ASTM Sequence VD Test

The multicylinder engine installation was designed to conform with the then current PV-1 installation. The engine was a 2.3-liter overhead cam four-

cylinder design and was set up in accordance with the PV-1 procedures (Appendix A), except that all engine blocks were bored 0.51 mm oversize and fitted with appropriate pistons and rings. At the conclusion of each test, all the inspected engine parts were replaced with new parts, except for the plated oil pan and rocker cover. Also, other engine parts were replaced when they failed to conform to specification.

Some modifications in the operating procedure were made to better suit the AFLRL test objectives. The most significant modification was to increase the oil sump volume to 3.8 liters (3.55 kilograms) to (1) make the test less severe, (2) make the test more representative of what actual field conditions were believed to be, and (3) improve test repeatability. Other changes included uncontrolled intake air temperature and humidity, replacing all the iron metal in the blowby measurement and oil filler pipe plumbing with stainless steel, and continuous monitoring of exhaust oxygen and carbon monoxide for more frequent air/fuel ratio adjustments. Also, the stage I and II engine-oil-in temperature was reduced by 8°C (15°F).

To compensate for the differences in stoichiometry between methanol, ethanol, and Phillips J unleaded gasoline, three different carburetors were used, one for each of the three fuels. Exhaust emissions, O_2, HC, and CO were monitored with Beckman O_2 and Barnes Emission Analyzers and were used to ensure the same equivalence ratio with each fuel. No attempt was made to increase the heat supplied to the intake manifold or to compensate for the increased heat required to vaporize the alcohol fuels.

The previous CLR work indicated that there were two iron wear particle generation methods. Iron was produced by wear at the rubbing surfaces and by rust formation in nonrubbing areas. With the CLR, rust contributed significantly to the total iron content of the used engine oil. This rust obscured the results of changes in oil formulation, since the integrating effect of iron wear metals accumulation was being used to indicate the extent of engine wear in a relatively short period of time. Rust was minimized in the CLR by substituting stainless steel for iron components in several areas within the engine installation. This approach of suppressing rust and concentrating on

wear was carried over into the 2.3-liter engine installation by using either plated or stainless steel components whenever possible within the nonrubbing oil-wetted areas.

The minimization of rust sites in this study means that oil formulations developed may control wear but not rusting. Rust formation may be a problem in actual service and will have to be addressed. This future work perhaps should use a Sequence IID-type test procedure, if methanol-based fuels are to be introduced. A total of forty tests were performed with the modified Sequence VD procedure (Appendix D).

C. 2.3-Liter Engine 20-Hour Steady-State Test

A simple test procedure was developed with the multicylinder 2.3-liter engine to determine the effects of engine operating temperature on wear metal generation with various fuels.

Three steady-state operating conditions were evaluated to determine which condition yielded the highest wear rates in a 20-hour period. As shown in Table 3, the conditions with the highest engine speed and load (A) produced

TABLE 3. PRELIMINARY STEADY-STATE OPERATING CONDITIONS

	Conditions		
	A	B	C
Load, N-m	94.9	16.3	10.8
Speed, rpm	2500	1500	750
Oil-In, °C	46	46	46
Coolant-Out, °C	43	43	43
Iron Wear, ppm			
Ethanol	12	23	--
Methanol	316	31	60
Unleaded Gasoline	17	30	--

the highest wear rate with methanol and were therefore adopted. The engine was then operated at this steady-state speed and load condition with various oil-in and coolant-out temperatures (Table 4) and the same equivalence ratio as the Sequence VD stages I and II.

TABLE 4. STEADY-STATE STAGE TEMPERATURES

	I	II	III	IV	V	VI	VII
Oil-In, °C	77	52	77	63	52	46	99
Coolant-Out, °C	68	43	68	54	43	43	91

Between each temperature stage, the engine was flushed for 1.5 hours with lubricant A at 99°C oil-in and 91°C coolant-out using the present test fuel. An oil sample was taken at the end of each flush for wear metal analysis. The engine was drained and fresh oil added for the next 20-hour test. Each temperature stage is conducted for a 20-hour period with a particular fuel keeping all other operating conditions the same as the Sequence VD stages I and II. Used oil samples (15 cc) were also taken at 10 minutes into the test, then at the 5-, 10-, 15-, and 20-hour intervals and analyzed for wear metals.

IV. ENGINE TEST RESULTS

A. Modified ASTM Sequence VD Tests

The engine test results with the CLR single-cylinder engine indicated that the use of methanol as a fuel greatly increased wear or rusting during tests which simulated the ASTM Sequence VC and ASTM Sequence IIC oil qualification tests. There were also indications that ethanol denatured with 0.99 percent gasoline and alcohol-gasoline blends may cause smaller increases in the level of iron wear particulates in the used oil, Figure 1. Because the CLR single-

cylinder engine is significantly different from current engine designs, a test stand capable of conducting the ASTM Sequence VD (then PV-1)(15) test was set up in order to confirm these initial results in a full-scale modern engine. This test procedure was developed to correlate the performance of engine oils to results obtained in actual consumer use. The results from this procedure evaluate oils in terms of protection provided against sludge and varnish deposits and valve train wear. This test is characterized by cyclic low- and mid-range engine operating temperatures with a relatively high rate of blowby. A PV-1 test was conducted in a Southwest Research Institute (SwRI) PV-1 development stand using the then current procedure (March 1979). The installation was modified by rejetting the carburetor and providing an additional fuel pump to ensure adequate fuel delivery.

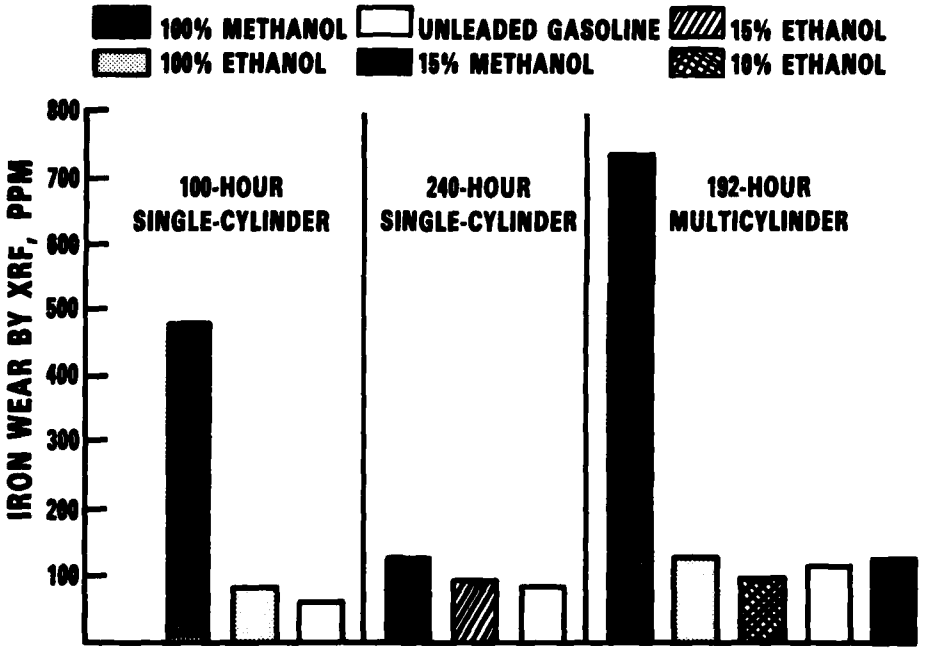

FIGURE 1. END OF TEST WEAR RESULTS SUMMARY

At the first oil sampling at 24 test hours, it was apparent that the engine was wearing rapidly. Wear metals measurements in the used oil indicated a 560-ppm iron concentration. The camshaft was examined since this is a known

site for high wear in this engine test. Visually, no unusual wear was noted in that area. A valve cover with a transparent section was installed, and the test was continued. Through this transparent section, it was observed that a yellowish milky oil-water-methanol emulsion would form during the idle portions of the test cycle. The oil would then revert to its normal appearance during the higher temperature periods. The scheduled 192-hour test eventually had to be terminated at 189 test hours due to excessively low oil pressure. At that point, the oil consumption and blowby had exceeded the test limits, and the lubricant iron content had reached 5850 ppm (0.58 percent). Disassembly of the engine showed extreme piston ring and cylinder bore wear, plus excessive wear throughout the engine. Some of this wear was certainly due to the wear metals acting as abrasives in the oil. The low oil pressure appeared to be due primarily to wear of the oil pump. These test results are summarized in Table 5.

TABLE 5. SUMMARY OF ENGINE INSPECTIONS FOR PV-1 TEST USING METHANOL AND FREO-200-3

Avg Sludge Deposits*	9.89
Varnish Deposits*	
Piston Skirts	9.89
Rocker Arm Cover	9.50
Cam Cover Baffle	9.70
Cylinder Wall (BRT)	7.94
Oil Pan	9.50
Avg Varnish*	9.11
Stuck Comp Rings, No.	2
Stuck Oil Rings, No.	
Stuck Lash Adj Bodies, No.	0
Stuck Lash Adj Plungers, No.	0
Blowby, cfm, Avg	2.00
Oil Consumption, liters	1.95
Wear	
Top Ring Gap Inc, Max mils	26.0
Top Ring Gap Inc, Avg mils	21.7
Rod Brg Wt Loss, Max mg	171.0
Rod Brg Wt Loss, Avg mg	151.3
Cam Follower Wt Loss Max, mg	575.7
Cam Follower Wt Loss Avg, mg	259.8
Cam Lobe Wear Max mils	34.7
Cam Lobe Wear Avg mils	9.8

* 10 = Clean

This test thus confirmed the high wear indications from the CLR tests. As a result, a test stand similar to the PV-1 stand was set up in the AFLRL lab. However, it was necessary to reduce the severity of the test. It was felt that increasing the engine oil charge would both improve the repeatability and decrease severity. In addition, all the iron metal in the blowby measurement and oil filler pipe plumbing was replaced with stainless steel to decrease rusting in those areas.(11) A comparison test was then conducted using the same reference lubricant (FREO-200-3) and Phillips J unleaded gasoline to determine the effects of these changes on test severity. The results of this test, when compared to the industry 90-percent confidence range for this lubricant and a representative test (which was slightly light on varnish), indicated the expected reduction in the level of deposits and reduction in total engine wear (Table 6). This test confirmed that the changes in operating procedure significantly reduced the engine wear.

TABLE 6. COMPARISON OF MODIFIED PV-1 TEST PROCEDURE WITH STANDARD PROCEDURE

Test Type	Modified	Commercial	Industry 90% Confid. Range
Fuel	Phillips J	Phillips J	Phillips J
Lubricant	FREO-200-3	FREO-200-3	FREO-200-3
Duration	192 Hours	192 Hours	192 Hours
Avg Sludge Deposits*	9.74	9.74	9.25-9.99
Piston Skirt Varnish*	7.45	7.55	6.14-7.46
Avg Varnish Deposits*	8.03	7.24	6.19-7.03
Top Ring Gap Incr, Max mils	5.0	7.0	
Top Ring Gap Incr, Avg mils	2.6	7.0	
Rod Brg Wt Loss, Max mg	20.9	47.5	
Rod Brg Wt Loss, Avg mg	18.1	41.2	
Cam Follower Wt Loss, Max mg	4.7	116.5	
Cam Follower Wt Loss, Avg mg	2.1	24.1	
Cam Lobe Wear, Max mils	0.7	3.6	
Cam Lobe Wear, Avg mils	0.5	1.25	

* 10 = Clean

Lubricant A, a 10W-30 Grade product qualified under MIL-L-46152, had been used for the earlier single-cylinder tests. Thus, a large amount of field data was available. Lubricant A was therefore used in these tests.(16) The unleaded gasoline used in the previous CLR-based testing was replaced by Phillips J fuel (Table 2), since this fuel had more closely controlled properties. The change in unleaded gasolines appeared to affect the engine wear results, with the Phillips fuel apparently increasing wear slightly, Figure 2.

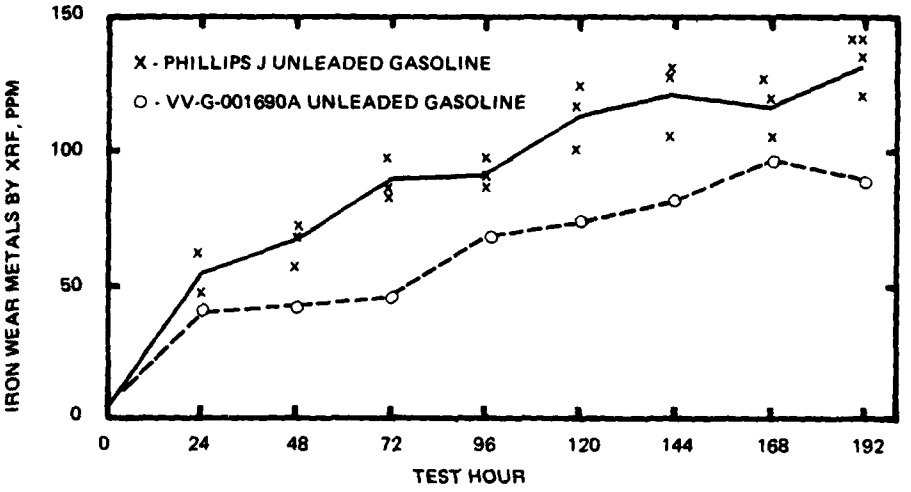

FIGURE 2. COMPARISON OF IRON WEAR METALS ACCUMULATION WITH TWO UNLEADED GASOLINES

The engine test has been found to be reasonably repeatable in evaluating wear as indicated by subsequent oil analysis. Figure 2 shows the accumulation of iron in the oil with lubricant A and Phillips J gasoline for these tests, and Table 7 summarizes the engine inspection data.

The wear rate with pure methanol and lubricant A also appears to be reasonably repeatable, but at a much higher level. The difference in wear rates between pure methanol and Phillips J unleaded gasoline as indicated by iron

TABLE 7. SUMMARY OF TEST RESULTS--LUBRICANT A AND PHILLIPS J GASOLINE

Test No.	5	15
Avg Sludge Deposits*	10.0	9.69
Piston Skirt Varnish*	7.96	7.71
Avg Varnish Deposits*	9.18	8.76
Top Ring Gap Inc, Max mils	4.0	5.0
Top Ring Gap Inc, Avg mils	1.0	2.5
Second Ring Gap Incr, mils, avg	3.0	4.0
Rod Brg Wt Loss, Max mg	61.5	29.0
Rod Brg Wt Loss, Avg mg	54.9	23.9
Cam Follower Wt Loss Max, mg	7.5	--
Cam Follower Wt Loss Avg, mg	5.1	--
Cam Lobe Wear Max mils	0.7	0.4
Cam Lobe Wear Avg mils	0.5	0.2
Iron Wear Metals at EOT, ppm by XRF	121	143

* 10 = Clean

wear metal accumulation is illustrated graphically in Figure 3. The average iron wear rate with methanol was approximately seven times the rate with Phillips J unleaded gasoline. Other differences in engine wear measurements

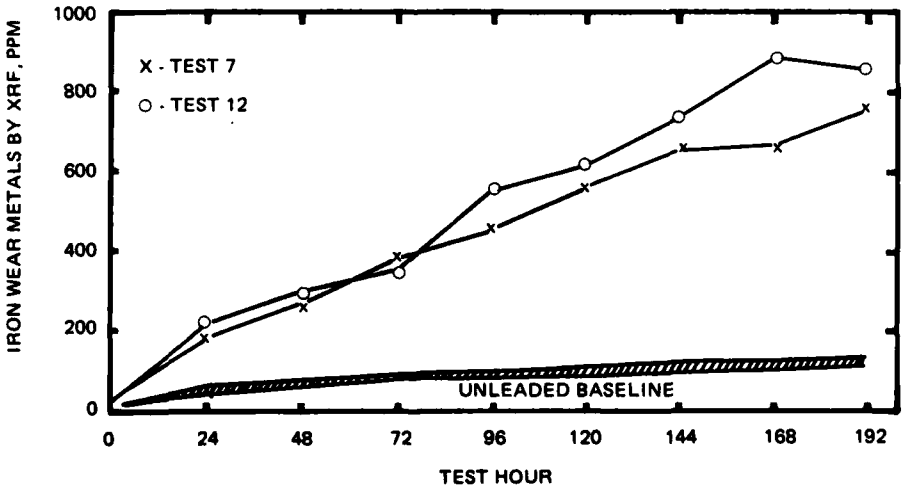

FIGURE 3. WEAR METAL ACCUMULATION RATE WITH NEAT METHANOL AND LUBRICANT A

and deposit levels are shown in Table 8. In general, the increased wear appeared to be primarily in the piston ring and cylinder bore area with the remainder of the engine unaffected. As expected, the engine varnish deposits were reduced. As noted earlier, the engine had relatively few locations for rust formation. No rusting was found on either the valve train gear or the bearing journals as had been the case in the PV-1 test run in the SwRI PV-1 development stand.

TABLE 8. POST-TEST INSPECTIONS--METHANOL AND LUBRICANT A

Test No.	7	12	Avg Baseline
Fuel	Methanol	Methanol	Phillips J
Lubricant	A	A	A
Duration, hr	192	192	192
Avg Sludge Deposits*	9.73	9.73	9.80
Piston Skirt Varnish*	9.91	9.93	7.91
Avg Varnish Deposits*	9.50	9.83	8.63
Top Ring Gap Inc, Max mils	13.0	9.0	3.3
Top Ring Gap Inc, Avg mils	7.0	6.0	1.8
Rod Brg Wt Loss, Max mg	72.4	46.5	37.5
Rod Brg Wt Loss, Avg mg	45.9	35.7	32.7
Cam Follower Wt Loss Max, mg	9.8	537.5	2.5
Cam Follower Wt Loss Avg, mg	4.3	116.4	1.7
Cam Lobe Wear Max mils	1.4	16.9	0.57
Cam Lobe Wear Avg mils	1.2	4.2	0.37

* 10 = Clean

Cursory used oil analysis, Table 9, showed no significant differences between the methanol and Phillips J fueled tests other than the wear metals and water content. With lubricant A, the final drain with methanol had almost seven times as much iron and at least twice as much copper as the engine fueled with Phillips J unleaded gasoline. This increased wear metal tends to indicate that the increased wear observed with methanol is occurring without permanently altering the bulk oil properties.

TABLE 9. USED OIL ANALYSES

Lubricant	FREO-200-3	A*	FREO-200-3	A*
Fuel	M**	M**	P**	P**
Tested By	SwRI	AFLRL	AFLRL	AFLRL
Properties				
K Vis, cSt				
at 40°C	53.6	63.9	42.3	57.3
at 100°C	ND	10.3	7.4	9.3
Flash Point, °C	ND	183	140	154
Total Acid No.	ND	3.8	7.4	4.2
Total Base No. (D 664)	ND	2.3	0.3	2.0
Insolubles, w/coag				
Pentane, wt%	ND	0.36	0.46	0.30
Toluene, wt%	ND	0.22	0.17	0.14
Wear Metals, ppm by AA				
Fe	5850	815	154	102
Cu	104	26	9	10
Cr	79	8	1	2
Pb	213	64	27	53
Water Content, wt%	ND	0.51	0.11	0.24

ND = Not determined.
* = Avg of two test.
** = M is methanol; P is Phillips J.

Earlier testing with the CLR single-cylinder engine indicated that denatured anhydrous ethanol and alcohol-gasoline blends may cause smaller increases in the level of iron wear concentration in the used lubricant than with neat methanol, Figure 1. Tests conducted with lubricant A and various fuels are summarized in Tables 10 and 11. These test fuels included anhydrous ethanol; 10 percent ethanol plus 90 percent Phillips J unleaded gasoline; neat methanol; and 10 percent methanol plus 90 percent Phillips J unleaded gasoline.

Both the end of test used oil analyses and the measured engine parts failed to reveal any increased wear with the anhydrous ethanol, ethanol-gasoline, and methanol-gasoline blend fuels.

TABLE 10. SUMMARY OF MODIFIED ASTM SEQUENCE VD TESTS WITH VARIOUS FUELS AND LUBRICANT A

	Ethanol	10% Ethanol + 90% Phillips J	Methanol	10% Methanol + 90% Phillips J	Phillips J
Top Bore Wear Avg, mm	0.0000	0.0051	0.0660	0.0051	0.0051
Mid Bore Wear Avg, mm	0.0025	0.0025	0.0025	0.0025	0.0025
Top Ring Gap Incr. Avg, mm	0.0254	0.0254	0.1778	0.0254	0.0254
2nd Ring Gap Incr. Avg, mm	0.0762	0.1016	0.1016	0.0508	0.0762
Rod Bearing, Wt Loss Avg, gm	0.0078	0.0595	0.0341	0.0192	0.0327
Cam Follower, Wt Loss Avg, gm	0.0038	0.0029	0.0559	0.0020	0.0005
Cam Lobe Wear Avg, mm	0.0102	0.0178	0.0635	0.0106	0.0106
Exhaust Valve Guide Wear Avg, mm	0.0432	0.0670	0.1041	0.0076	0.0356
Intake Valve Guide Wear Avg, mm	0.0051	0.0102	0.0152	0.0000	0.0127
EOT Wear Metals, ppm	AA	AA	AA	XRF	AA
Chrome	1	1	8	10	5
Copper	8	9	26	21	14
Iron	102	96	806	136	102
Lead	30	34	69	80	53
Sludge Rating Avg*	9.8	9.8	9.7	9.7	9.8
Varnish Rating Avg*	10.0	9.1	9.6	8.0	8.6
Piston Varnish Avg*	10.0	7.7	9.9	8.1	7.9
Intake Valve Deposits Avg	8.7	6.1	8.6	6.4	6.4

*10 = Clean
AA = Atomic Absorption Method
XRF = X-ray Fluorescence Method

TABLE 11. SUMMARY OF MODIFIED ASTM SEQUENCE VD USED OIL DATA WITH VARIOUS FUELS AND LUBRICANT A

	Method	Ethanol	10% Ethanol + 90% Phillips J	Methanol	10% Methanol + 90% Phillips J	Phillips J
Viscosity, cSt at 40°C	D 445	65.4	58.5	66.3	59.6	56.4
Viscosity, cSt at 100°C	D 445	10.0	9.9	10.4	10.3	9.4
Viscosity Index	D 2270	138	157	145	163	149
TAN	D 664	4.1	4.9	4.4	4.3	4.1
TBN	D 664	1.6	3.6	1.7	1.9	2.3
Flash Point, °C	D 92	210	156	190	152	163
Pentane Insolubles, wt% Method A	D 893	0.09	0.25	0.28	0.23	0.53
Toluene Insolubles, wt% Method A	D 893	0.07	0.12	0.16	0.10	0.22
Water, wt%	D 1744 mod.	0.29	0.12	0.41	0.28	0.22
Oil Consumption, kg		1.63	2.09	1.97	1.19	1.38

The engine tests conducted thus far using the modified ASTM Sequence VD procedure were shown to have acceptable repeatability. The use of methanol as a fuel greatly increased iron wear concentration in the used lubricant when compared to unleaded Phillips J gasoline. The increased wear occurs primarily in the top piston ring and upper cylinder bore area. The cam followers, cam lobes, bearings and exhaust valve guides show lesser increases, possibly due to abrasive wear. The ring and bore wear take place at the uppermost travel of the top ring on the cylinder wall and down approximately 0.64 cm (0.25 inch). The surface profile and microscopic photographs of this area indicate that corrosive attack played some part in the increased wear as shown in Figures 4 and 5. The distance between the top and second ring is approximately 5 mm, so apparently the second ring does not enter this area. Limited wear occurs on the second ring and further down the cylinder walls. The No. 1 cylinder bore has the greatest wear, followed by No. 4. No. 2 and No. 3 have progressively less wear. Most of the cam lobe and cam follower wear which takes place in the fourth cylinder area (valves 7 and 8) appears to be caused by an emulsion (methanol, water, oil) that comes from the blowby condenser and is deposited on that area of the engine.

1. Fully Formulated Lubricants--With the establishment of a test procedure that appeared to distinguish between neat methanol fuel and unleaded gasoline in terms of wear with lubricant A, the next activity concentrated on evaluating various lubricant formulations. Several lubricants, some of which had shown positive results in the single-cylinder CLR engine, were obtained. Appendices B and D list the lubricants and test numbers, along with physical and chemical inspections. The modified Sequence VD test was conducted on these lubricants using pure methanol as fuel. Lubricants B, C, D, E, and G were selected because of their good performances when screened in the CLR single-cylinder engine. Lubricants B, C, D, and E had less iron concentration than did lubricant A, while lubricant G had the same iron concentration as lubricant A in the CLR single-cylinder engine.(11) The second oil tested was lubricant B, with a magnesium-based detergent additive. The results of this test are shown in Appendix C. The test was halted at 152 hours due to high iron wear concentration. A level of approximately 2000-ppm iron in the used oil was selected as a shutdown point. At this high iron level, addi-

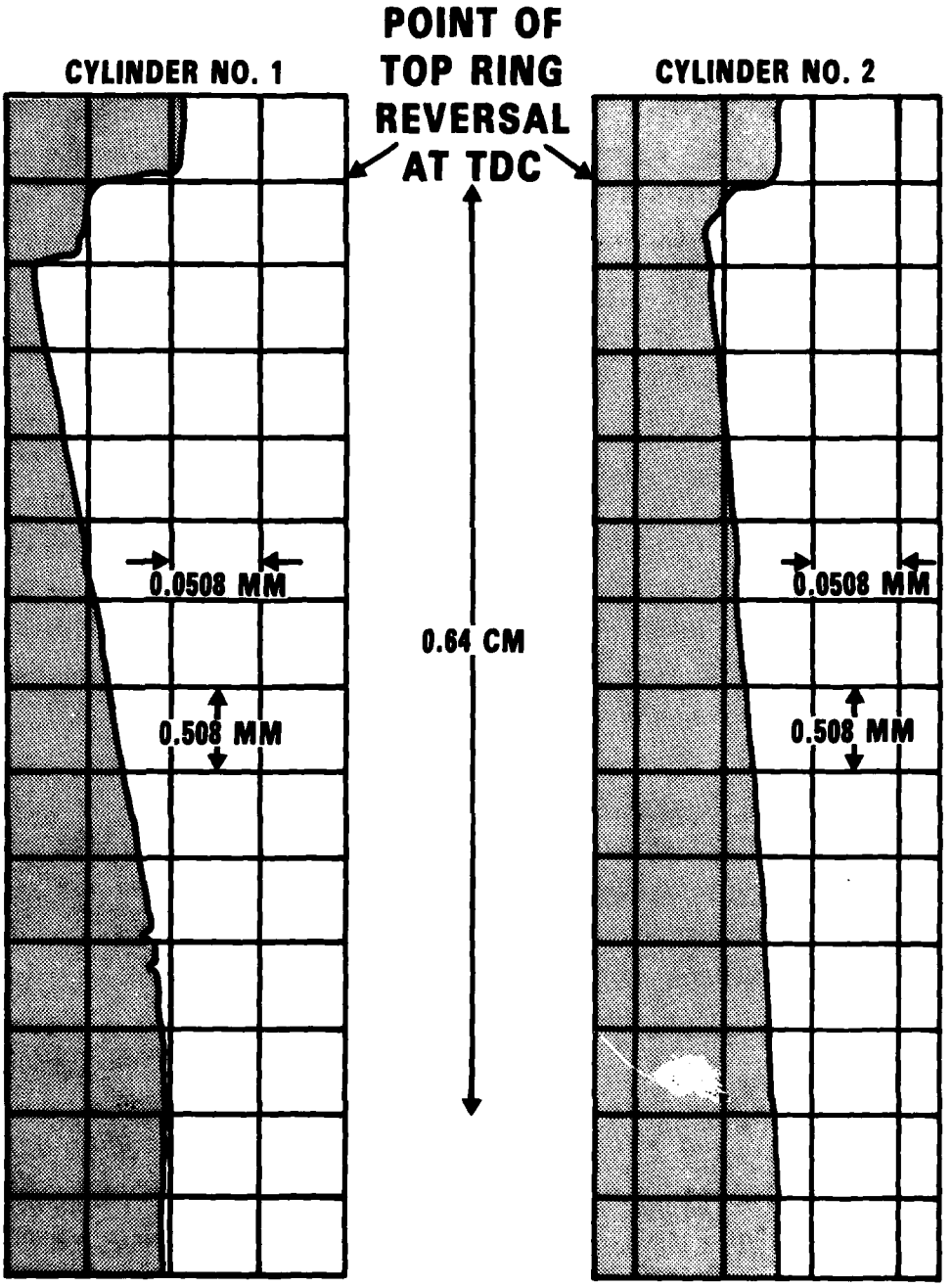

FIGURE 4. SURFACE PROFILE OF CYLINDERS FROM TEST USING NEAT METHANOL AND LUBRICANT A

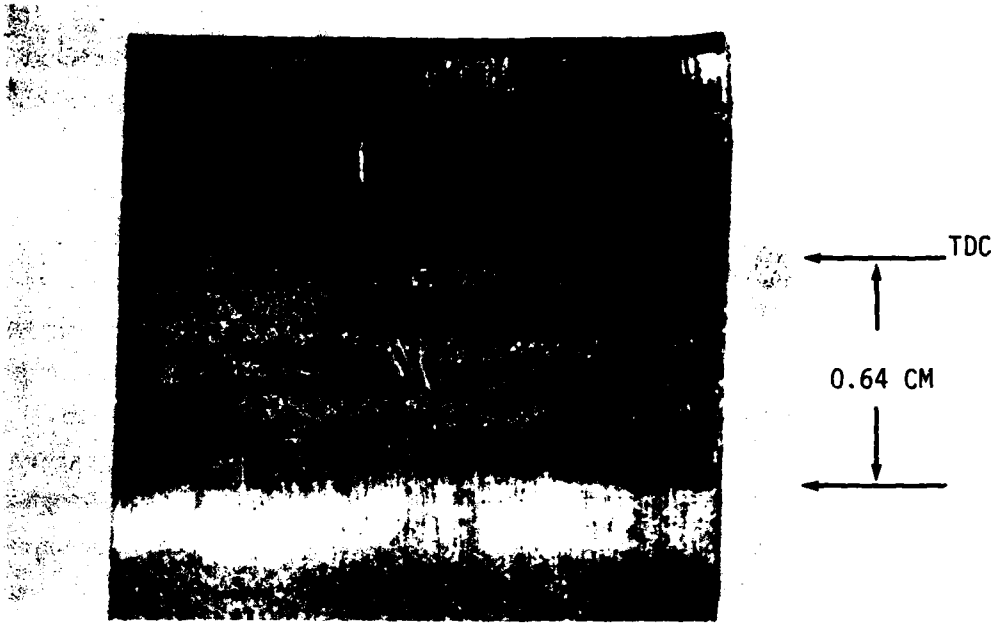

FIGURE 5. MICROSCOPIC PHOTOGRAPH OF CYLINDER WALL WEAR AREA

(5x Magnification)

tional wear could be coming from circulating abrasive iron particles in the used oil, which would mask the primary methanol-related wear. This test had twice the iron concentration, top bore and top ring wear, as did lubricant A and pure methanol.

The next test was conducted using lubricant C, a MIL-L-21260B preservative engine oil which had shown promise in reducing corrosion due to high-sulfur fuel.(17) Also, encouraging results were obtained with lubricant C in the single-cylinder CLR engine. The results from this test are shown in Appendix C. Lubricant C had a 75-percent increase in iron concentration when compared to lubricant A, which was higher than expected. The bore and ring wear were approximately the same as for lubricant A but with an increase in iron wear metals coming from cam follower and cam lobe wear.

The next oil tested was lubricant E, and the results are shown in Appendix C. Lubricant E is lubricant A plus the preservative engine oil additive package

(zinc) used in meeting MIL-L-21260B specification. This lubricant had a 97-percent increase in iron concentration compared to lubricant A. There was a slight increase in top bore and top ring wear, but again the cam follower and cam lobe wear were high relative to lubricant A.

From these data, it appeared that the CLR single-cylinder engine and the 2.3-liter engine did not correlate in wear rate results using neat methanol fuel. Therefore, another lubricant was selected for testing which had lower iron wear concentration in the CLR engine than lubricant A and has demonstrated good performance throughout the Army system. Lubricant D (MIL-L-46167), a synthetic diester product, contains a barium-based detergent-dispersant additive system and contains no zinc dithiophosphate. This lubricant resulted in an increase in used oil iron concentration of 130 percent as compared to lubricant A. There was again high wear in the top cylinder bores, cam lobes, and cam followers relative to lubricant A, as shown in Appendix C. In addition, there was a very high oil consumption rate. It is believed that some of the wear was due to an incompatibility between the antiwear additive chemistry of the lubricant and the 2.3-liter engine metallurgy.

Next, lubricant F was evaluated using methanol fuel (Appendix C). This lubricant, a commercially available 15W-40 grade mineral oil with a calcium-based additive system, had a 127-percent increase in iron concentration when compared to lubricant A. Lubricant F showed a slight decrease in top bore and top ring wear relative to lubricant A. However, there was a significant increase in cam follower and cam lobe wear. In addition, lubricant F had a 366-percent increase in lead concentration, indicating increased bearing wear.

Lubricant G, a 10W-30 synthetic oil with a calcium-based additive package, was the next lubricant evaluated. Lubricant G had a 75-percent increase in iron concentration when compared to lubricant A and methanol as fuel (Appendix C). The top bore and top ring wear were approximately the same, but the cam follower and cam lobe wear were significantly increased with lubricant G.

Lubricant H, a MIL-L-46167-qualified, 5W-20 synthetic polyalphaolefin oil, was evaluated using methanol fuel. This lubricant had unusual results in that the top ring wear was one of the highest, while the top bore wear was the lowest (Appendix C). Also, the highest top bore wear occurred in cylinder No. 4, where the No. 1 cylinder had the highest top bore wear for all other lubricants tested. This lubricant had higher cam follower and cam lobe wear than did lubricant A.

Then lubricant I, a commercial grade 10W-40 API Service Classification SF lubricant was evaluated using methanol fuel. This lubricant was selected because it was representative of typical SF quality oils. The results (Appendix C) show a 78-percent increase in iron concentration relative to lubricant A. There was also a 46-percent increase in top bore wear and an increase in mid bore wear with a 71-percent increase in top ring wear. In addition, there was a large increase in cam follower and cam lobe wear when compared to lubricant A.

The second to last lubricant evaluated was lubricant J, an experimental 20W-40 grade product which appeared to show some promise in wear reduction (Appendix C). Lubricant J had a 96-percent increase in iron concentration when compared to lubricant A. It also had a 54-percent decrease in top bore wear and a slight decrease in exhaust valve guide wear when compared to lubricant A. However, there was an increase in cam follower and cam lobe wear.

The last lubricant evaluated in this phase was lubricant K (Test 30), an experimental lubricant. This lubricant was lubricant A with a polytetrafluoroethylene resin treatment added as a friction reducer and coating. When the results from this lubricant were compared to lubricant A, lubricant K had more wear in all the measured wear areas.

In summary, none of the ten lubricants evaluated using neat methanol fuel exceeded the performance of lubricant A. However, lubricant A performance with methanol fuel still would not be adequate for low-temperature operation. The results also appear to show that the CLR single-cylinder engine and the

2.3-liter multicylinder engine do not correlate in iron wear accumulation when using neat methanol fuel (Figure 6). In the single-cylinder engine, lubricants B, C, D and E had less iron wear than lubricant A, while lubricant G had approximately the same iron wear as lubricant A. However, in the 2.3-liter multicylinder engine, all the lubricants had significantly more iron wear than did lubricant A.

2. Lubricant Composition Studies--For this phase of the program, discussions were held with several lubricant manufacturers regarding the engine wear problems experienced with methanol fuel. As a result of these discussions, one lubricant manufacturer expressed a desire to provide lubricant formulations for evaluations with alcohol-containing fuels. Throughout this

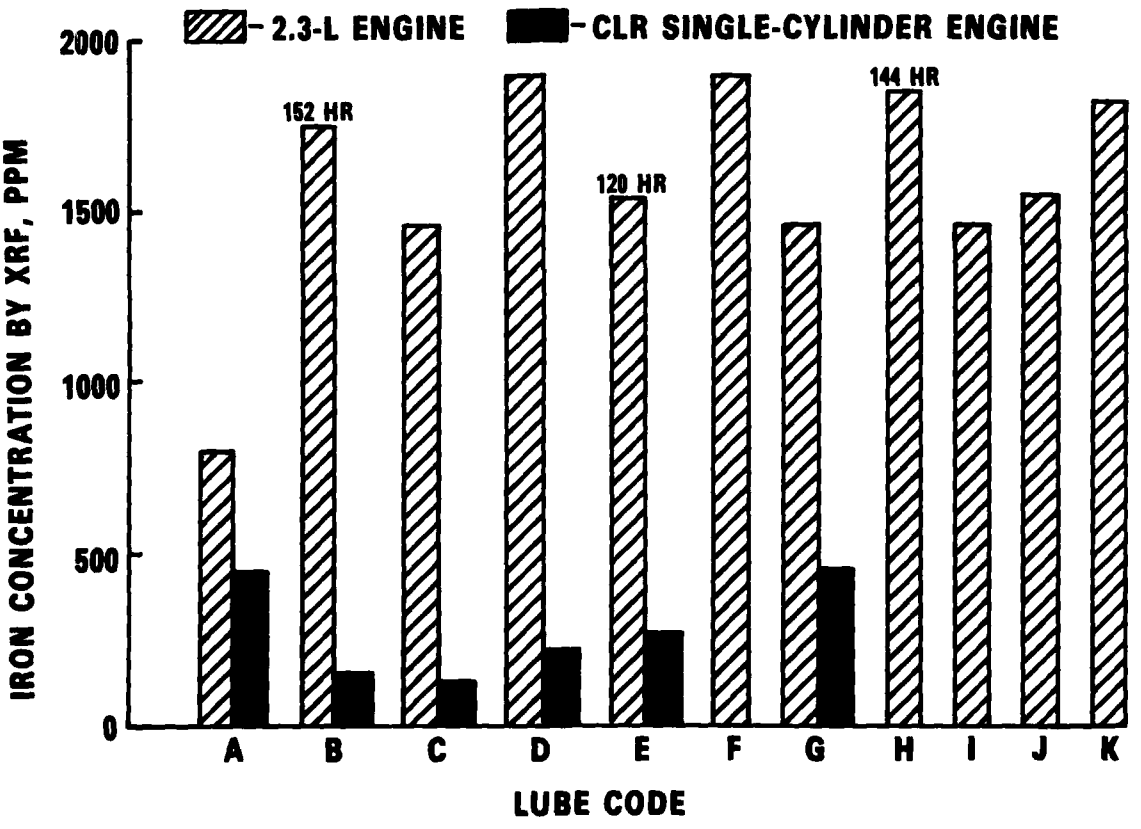

FIGURE 6. IRON WEAR METALS CONCENTRATION

phase, the manufacturer sent AFLRL a total of 11 lubricants for evaluation (Tables 12 and 13) which were based on lubricant A. These lubricants were used to evaluate the effects of lubricant composition on engine wear with methanol fuel. Neat methanol was used through this phase of the program. All evaluations were performed using the modified Sequence VD test, and the test and lubricant codes are listed in Appendix D. The new and used oil properties and the engine test wear results for this series of lubricant evaluations are presented in Appendices E and F. Lubricant A-1 (Test 16) was tested first with methanol fuel. This lubricant is the same as lubricant A with the phosphorus dispersant being replaced with a nitrogen (Type 1) dispersant (Table 13). The test was stopped at 40 hours because it had 2857 ppm lubricant iron wear concentration. When disassembled, it was found that the

TABLE 12. EXPERIMENTAL LUBRICANTS

Lubricant Number	Composition
A	P Disp, Ca Sulf, Alkyl ZDTP, Disp VII & Ashless Inh (1)
A-1	A with N Disp-1
A-2	A with N Disp-1 & Mg Sulf
A-3	A with Aryl ZDTP
A-4	A with N Disp-1 & Shear Stable OCP VII
A-5	A with N Disp-1, Ashless Inh (2), & Friction Modifier
A-6	A with Mg Sulf
A-7	A with Increased Ca Sulf
A-8	A without Disp
A-9	A with N Disp-2
A-10	A without VII, SAE-30
A-11	A with Less Shear Stable OCP VII

TABLE 13. EXPERIMENTAL LUBRICANTS

Lube Code	A	A	A	A-2	A-5	A-6	A-7	A-1	A-1	A-1	A-8	A-9	A-3	A-4	A-10	A-9	A-11
Test No.	1	5,15,20	7,12,33	21	22	26	28	29	32	34	35	36	37	40	41	42	43
PVI-Fuel	Unleaded Gasoline	Unleaded Phillips J	MeOH	MeOH	MeOH	MeOH	MeOH	Unleaded Phillips J	MeOH	MeOH	MeOH	MeOH	MeOH	MeOH	MeOH	MeOH	MeOH
Detergent Additive																	
Calcium	X	X	X	-	X	-	-	X	X	X	X	X	X	X	X	X	X
Increased Calcium	-	-	-	-	-	-	X	-	-	-	-	-	-	-	-	-	-
Magnesium	-	-	-	X	-	X	-	-	-	-	-	-	-	-	-	-	-
Dispersant Additive																	
Phosphorus	X	X	X	-	-	X	X	-	-	-	-	-	-	-	X	-	X
Nitrogen, Type 1	-	-	-	X	X	-	-	X	X	X	-	-	X	X	-	-	-
Nitrogen, Type 2	-	-	-	-	-	-	-	-	-	-	-	X	-	-	-	X	-
Other Additives																	
Anti-Wear	a	a	a	a	a	a	a	a	a	a	a	a	b	a	a	a	a
Friction Modifier	-	-	-	-	X	-	-	-	-	-	-	-	-	-	-	-	-
VI Improver	c	c	c	c	c	c	c	c	c	c	c	c	c	d	Grade 30	c	e
Inhibitor	f	f	f	f	g	f	f	f	f	f	f	f	f	f	f	f	f

X = Presence of particular additive
a = Alkyl zinc
b = Aryl zinc
c = Dispersant Polymethacrylate
d = Shear-stable olefin copolymer
e = Less shear-stable olefin copolymer
f = Inhibitor No. A
g = Inhibitor No. B

internal engine parts were very rusty (Figures 7 and 8) and had extreme wear for only 40 hours of operation. Next, lubricant A-2 was evaluated. This (Test 18) lubricant is the same as lubricant A-1 except that it uses a magnesium detergent instead of a calcium detergent (Table 13). This test was also halted at 34 hours due to high iron wear concentration of 1709 ppm. Again, rust was observed on the internal engine parts. The intake manifold, the blowby cooler, the oil cooler, and exhaust manifold cooler were checked for coolant leaks and for possible lubricant contamination. No leaks were found in the accessory equipment nor any unusual contamination in the used oil. The methanol was then checked for purity and was found to contain 99.9 percent methanol and 0.10 percent water, which is standard for commercial methanol. After checking the entire test stand, along with the various accessory equipment, a new test was started. A test was conducted (Test 19) to verify the test stand integrity using lubricant A and neat methanol fuel. The 24-hour test used-oil sample had 1033 ppm iron and 1749 ppm iron at 34 hours, which were still unexpectedly high for this fuel/lubricant combination. The engine was flushed twice and refilled with lubricant A, using Phillips J unleaded gasoline as fuel. At the 24-hour period, there was 84 ppm iron. This iron concentration is higher than the two previous tests with lubricant A but appears to fall within the range of repeatability. The engine was again drained, flushed, and filled with lubricant A and run, using a different shipment of neat methanol. At 24 hours, there was 195 ppm iron in used oil, which compared well with the 24-hour period of the two previous tests which had 184 and 218 ppm iron. From these data, it appeared that the methanol caused the increased wear. Therefore, Test 20, using lubricant A, was conducted using Phillips J unleaded gasoline as fuel. The iron wear concentration fell between the previous tests, indicating that no problems existed with the test stand, lubricant A, or Phillips J unleaded gasoline. It appears from the available data that the high wear in tests performed with lubricants A-1 and A-2 was caused by an unknown impurity in the methanol fuel. This methanol was further analyzed to determine any unidentified impurities.

The contaminated methanol was analyzed by Infrared Spectrophotometer (IR), Gas Chromatograph (GC), and the Gas Chromatograph/Mass Spectrometric (GC/MS)

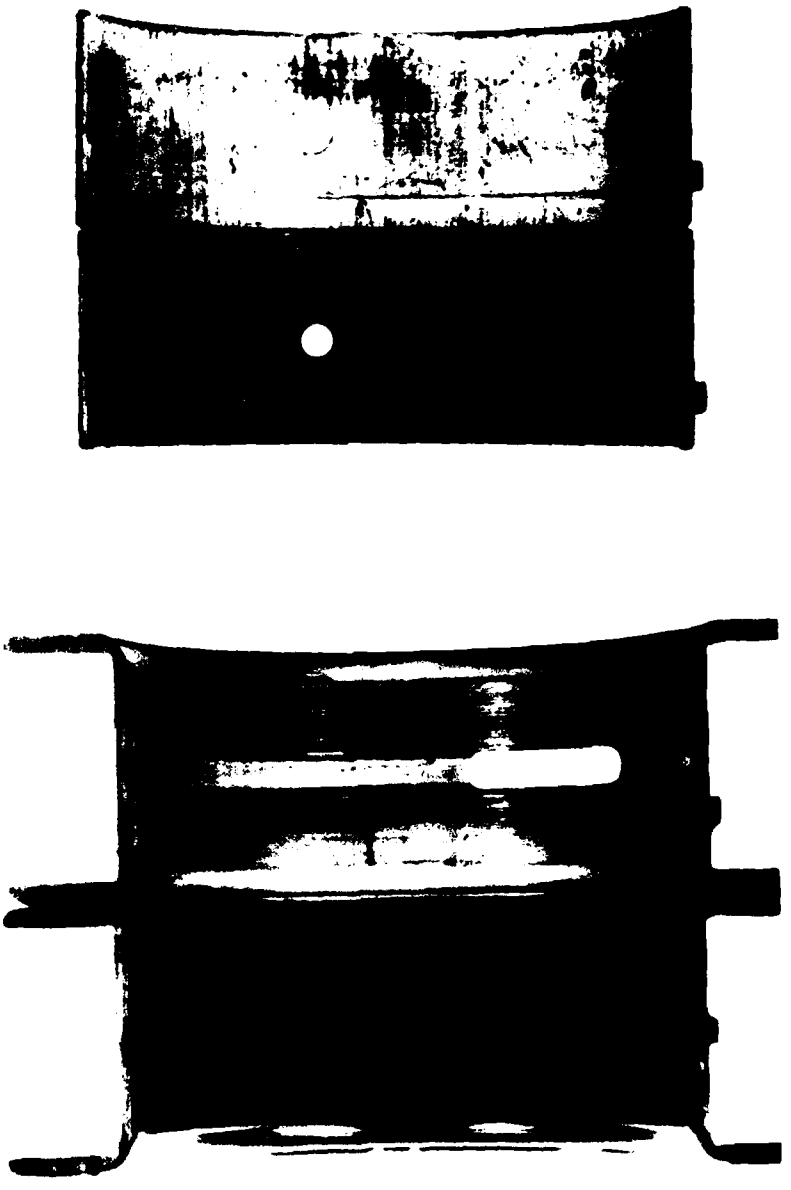

FIGURE 7. ROD BEARING FROM TEST 16

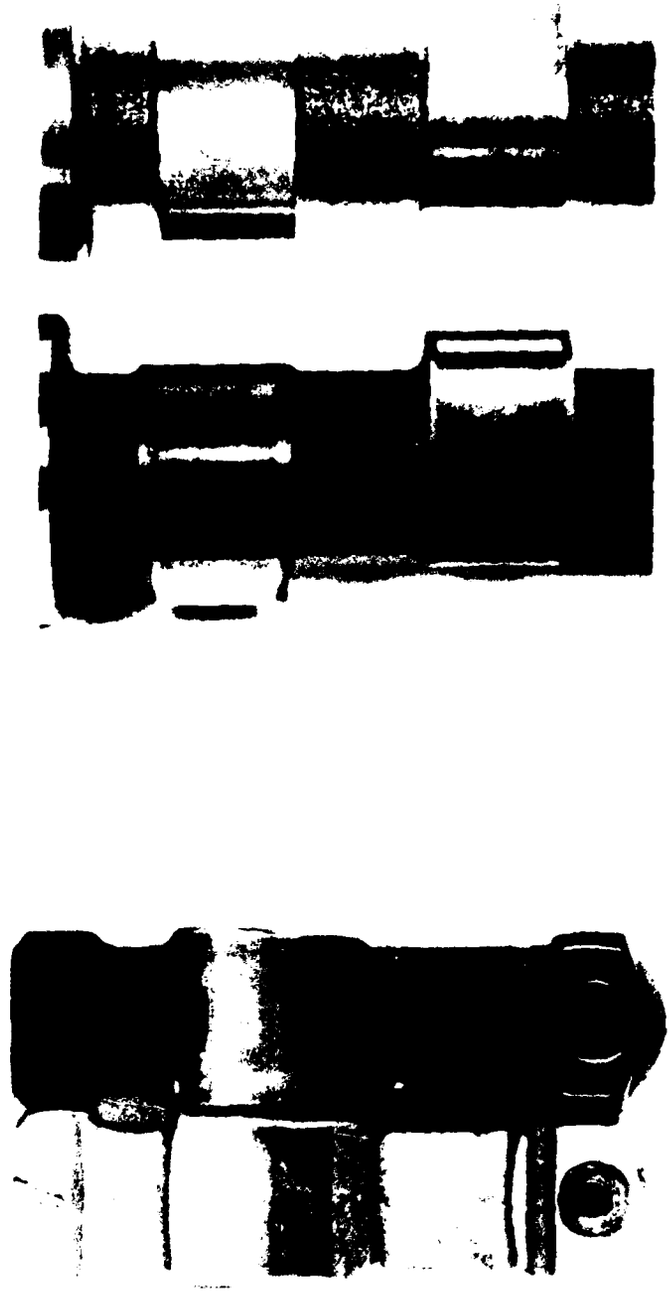

FIGURE 8. CAM AND ROCKER ARMS FROM TEST 16

methods. These analyses did not identify the impurities which caused the high iron wear. No more work was performed on the impure methanol because of economic consideration, and it was felt at that time that it was not in keeping with the objective of the program.

A new shipment of neat methanol was used to conduct the evaluation with a new batch of lubricant A-2. This Test 21 had considerably less wear iron concentration than did the first test with lubricant A-1 (with contaminated methanol). The test still had to be halted at 120 hours with 1792 ppm wear iron concentration and high top bore wear (Figure 10).

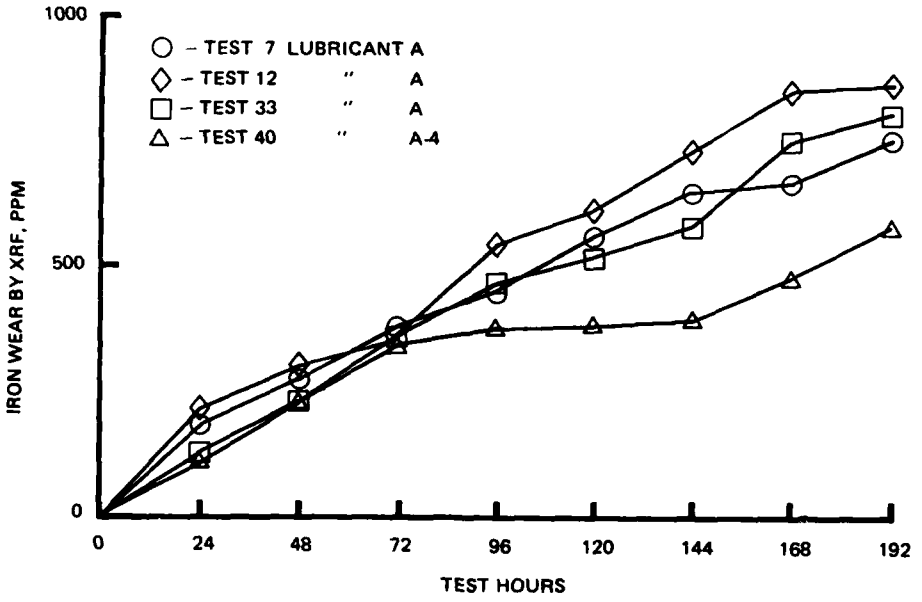

FIGURE 9. IRON WEAR ACCUMULATION RATE WITH NEAT METHANOL

Test 22 was performed with lubricant A-5 (Table 13) which had a nitrogen (Type 1) dispersant different inhibitor number (I-2) and a friction modifier. This test was also stopped early at 140 hours with 2242 ppm wear iron concentration, high top bore wear, and high cam follower wear. From the results obtained thus far, it appeared that the magnesium detergent and/or the nitrogen (Type 1) dispersant caused the increase in wear iron. Therefore, lubricant A-6 (Test 26) was evaluated. This lubricant is the same as lubricant A with a magnesium detergent, rather than the calcium detergent. The test ran the full 192 hours and had 1440 ppm wear iron concentration (Figure 10) and high top bore wear. Based on this work, calcium detergent and phosphorus dispersant appear to be more effective than the magnesium detergent and the nitrogen (Type 1) dispersant in counteracting the increase wear when using methanol fuel. Because of these results, lubricant A-7, Test 28, which had an increase in the calcium detergent when compared to lubricant A, was tested. The additional calcium gave the lubricant a higher total base number (TBN = 14.6). The additional calcium did not appear to have affected the iron wear rate because it fell in the zone bounded by two previously reported tests with lubricant A (Figure 10). It appeared that increased iron wear was observed when using the nitrogen (Type 1) dispersant. Test 29 with lubricant A-1 was conducted to determine whether the nitrogen (Type 1) dispersant would have as much effect on the iron wear when using unleaded Phillips J gasoline as with neat methanol. The results showed that the nitrogen dispersant did not increase the iron wear rate when using unleaded Phillips J gasoline. The iron wear data fell within the zone bounded by three other tests using unleaded Phillips J gasoline.

Because no valid test had been run while just changing the phosphorus/dispersant to nitrogen dispersant when using neat methanol fuel, it appeared necessary to observe this effect. Therefore, a second shipment of lubricant A-1 (Test 32) was evaluated. This lubricant had a lower iron wear rate than the two tests with lubricant A (Figure 10). This low wear rate was not expected since all other nitrogen (Type 1) dispersant containing lubricants had higher wear results. Due to these results, it appeared necessary to verify the test stand integrity. Test 33 was conducted using lubricant A and neat methanol fuel which resulted in good correlation with the two previous

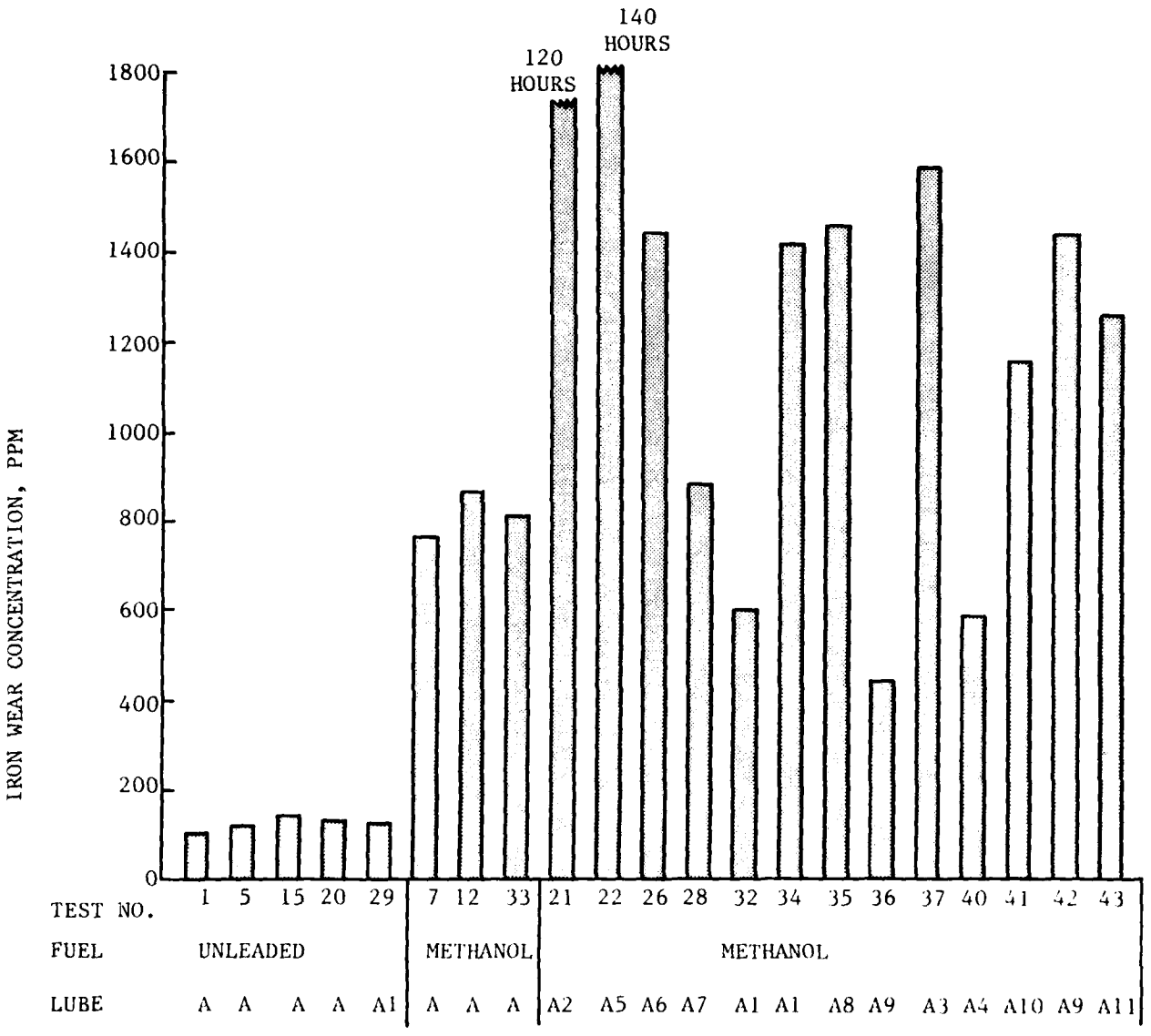

FIGURE 10. TEST RESULTS WITH EXPERIMENTAL OILS

tests, indicating no shift had occurred (Figure 9). A new shipment of lubricant A-1 was received and tested to verify the low iron wear rate with Test 32. Test 34 had a considerably higher iron wear rate (1280 ppm) than did Test 32 (599 ppm) with lubricant A-1 (Figure 10). This indicates a much higher sensitivity to variations in basestock composition or the nitrogen (Type 1) dispersant than would normally be anticipated.

This testing has shown that different dispersants have a significant effect on the engine oil iron concentration when using neat methanol as fuel. Therefore, Test 35 and Test 36 were performed to further investigate this effect. One lubricant, A-8, had no ashless dispersant and the other lubricant, A-9, contained a different nitrogen dispersant (Type 2) than used in previous tests. Test 35 was conducted using lubricant A-8 without an ashless dispersant. This lubricant produced an 80-percent increase in iron wear concentration with higher top bore wear when compared to Tests 7, 12, and 33, which used lubricant A with a phosphorus dispersant. Test 36 was conducted using lubricant A-9 with a different nitrogen (Type 2) containing dispersant. The use of this nitrogen (Type 2) dispersant reduced the iron concentration by 45 percent when compared to test using lubricant A, Figure 10.

The Sequence VD 2.3-liter engine has been shown to be sensitive in the valve train area to the type of zinc anti-wear additive when using unleaded gasoline fuel. Lubricant A, with phosphorus dispersant/calcium detergent, contains an alkyl-type zinc as does the calcium detergent/nitrogen (Type 1) dispersant lubricant A-1. Therefore, a lubricant containing an aryl-type zinc was used to investigate if this zinc-type sensitivity existed when using neat methanol fuel. Test 37 was conducted using lubricant A-3 (aryl zinc). It appears from the results of the used oil iron content that Test 37 (aryl zinc) was not substantially different than Test 34 (alkyl zinc), but it was much higher than Test 32 (alkyl zinc). All three lubricants used the calcium detergent/nitrogen (Type 1) dispersant additive. Both zinc types resulted in similar bore wear with Test 34 showing more. However, the cam follower and cam lobe wear (Appendix C) revealed thate was a significant increase resulted in wear with the aryl zinc-type additive in Test 37 with lubricant A-3. Therefore, it appears that valve train area wear resulting from aryl zinc occurs with both neat methanol fuel and unleaded gasoline.

Test 40 was conducted using lubricant A-4 which had the polymethacrylate viscosity index improver replaced with a shear stable olefin copolymer viscosity index improver. The results from this test show that the iron wear concentration increased at a constant rate until the 72-hour period (Figure 9). From the 72-hour period to the 144-hour period, there was an increase in iron wear concentration of only 51 ppm. From the 144-hour period on, it again approximated the rate of the first 72 hours. Part of this low iron wear rate after the 72-hour period can be explained by a larger than average oil addition at the 72-hour period. This normally affects the wear rate for only one 24-hour period and then resumes the original iron wear rate.

To investigate the effect of the viscosity index improvers, a grade 30 lubricant (without viscosity index improver) was tested. Lubricant A-10 contained the lubricant A additive system which was formulated to be grade 30 without a viscosity index improver. Test 41 results show that the iron wear concentration is below lubricant A rate until the 96-hour period, at which point it begins to increase more rapidly (Figure 10).

Test 42 was conducted using lubricant A-9. This duplicate test was run to verify the lower wear levels of Test 36 which had the lowest iron wear concentration. The lubricant A-9 has the same additive package as the lubricant used in Test 36. The lubricant is a different batch but is within the batch-to-batch limits of the manufacturer's specification. This lubricant uses the same calcium detergent but a different nitrogen dispersant (Type 2) than did the previous lubricants supplied. As can be seen from Figure 10, there was excessive iron wear during Test 42. The test results indicated a 222-percent increase in iron concentration when compared to the supposedly identical Test 36. A similar result was observed with Tests 32 and 34 (Figure 10). These earlier two tests used a lubricant with the same calcium detergent and the same nitrogen dispersant (Type 1) but were also from different batches meeting the specifications of the manufacturer. This earlier lubricant formulation is the same as those used in Tests 36 and 42 with the exception of a different nitrogen dispersant (see Table 14).

TABLE 14. LUBRICANTS CONTAINING DIFFERENT DISPERSANT BATCHES

	PVI-32 AL-9440 Batch 1	PVI-34 AL-10122 Batch 2	PVI-36 AL-10121 Batch 1	PVI-42 AL-10459 Batch 2
Calcium Detergent	X	X	X	X
Nitrogen Dispersant Type 1	X	X		
Nitrogen Dispersant Type 2			X	X

Test 32 had a 137-percent increase in iron concentration when compared to Test 34. It is evident that there is poor repeatability with the tests that used a lubricant with a nitrogen dispersant. However, those tests which used a lubricant with a phosphorus dispersant and a calcium detergent had good repeatability as in Test 7, 12, 28, and 33.

Test 43 was performed using lubricant A-11. Lubricant A-11 used a less shear-stable olefin copolymer than lubricant A-4 used in Test 40. Also, a phosphorus dispersant was used instead of a nitrogen-based dispersant. This test was conducted to compare the effects of different olefin copolymers when using different dispersants. Test 43 had a 115-percent increase in iron wear concentration compared to Test 40 lubricant A-4 (see Figure 10) which had an unusual iron wear concentration with a shear stable olefin copolymer additive.

B. 2.3-Liter Engine 20-Hour Steady-State Tests

Several 20-hour steady-state tests were conducted with four of the multicylinder 2.3-liter engines, Tests 17, 27, 39, and 44, to determine the effects of engine operating temperature on wear metal generation with various fuels. Lubricant A was used for this entire study. The fuels examined were neat methanol, methanol containing 11 percent deionized water, denatured anhydrous ethanol, denatured anhydrous ethanol with 11 percent deionized water, and Phillips J unleaded gasoline.

From these data (Figure 11), it appears that all the fuels had approximately the same wear metal generation rates until the oil sump temperature was lowered below 70°-80°C. Below this temperature range, the wear metal production increased rapidly, as illustrated in Figure 11. In this figure, the shaded region bounds an eight-test band generated using eight different batches of anhydrous methanol. This contrasts sharply with the denatured anhydrous ethanol and the gasoline results depicted by the dashed line.

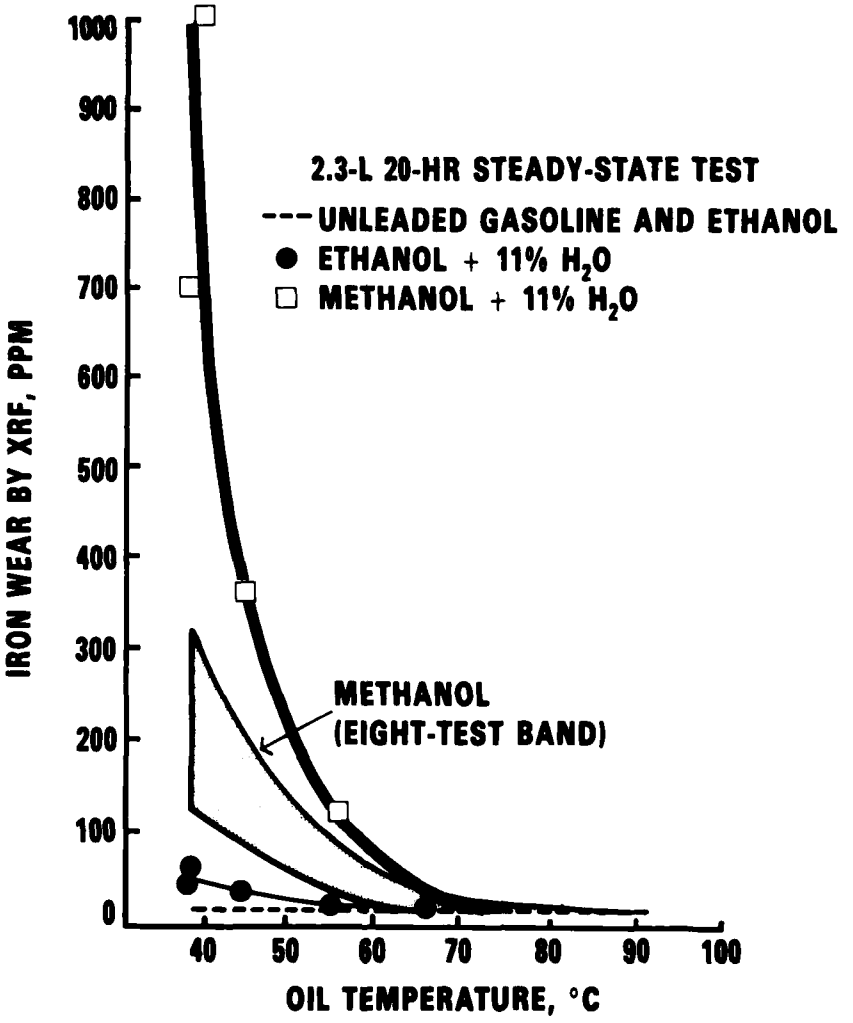

FIGURE 11. EFFECT OF OIL TEMPERATURE ON ENGINE IRON WEAR WITH VARIOUS FUELS

While this result with methanol confirmed the modified Sequence VD results, this study's results with ethanol conflicted with increased wear results reported by other researchers using "wet" ethanol. As a result, 11 percent water was added to both alcohol fuels, and these "wet" fuels were evaluated using this procedure, again holding the equivalence ratio constant. Tests conducted with "wet" ethanol fuel showed increased wear resulting from the water addition. For example, at 46°C oil-in temperature, this fuel produced 52 ppm of iron compared to 12 ppm iron wear metals with the anhydrous ethanol. The same type of wear increase was observed with the methanol, where the water addition increased iron wear metal production by about 300 percent over that observed with the neat methanol at temperatures below the 70°-80°C threshold. The water, ethanol, and methanol contents in the used lubricants were determined as shown in Tables 15 through 17. The increase in concentration of the alcohol and water in the lubricant coincides with the increased wear rate, but only when this accumulation is a byproduct of the combustion process. In previously reported data (13), alcohol and water were added directly to the lubricant in the crankcase of the CLR test engine with no apparent increase in iron wear.

The used lubricant from the 20-hour steady-state tests were analyzed for TAN and TBN by ASTM D 664, and the results are reported in Tables 15 through 17. As shown in Figure 12, it appears that as the TBN decreases, the iron wear increases. Figure 13 indicates that, in general as the oil temperature decreases, the TBN decreases, especially below about 65°C.

Three tests were also run with the oil-in temperature at 85°C and the coolant-out temperature at 49°C. These tests were performed to investigate if the increased iron wear levels could be produced with the engine water jacket colder and the oil warmer than the apparent 70°-80°C critical wear temperature with neat methanol. These data fell below the highest iron wear level for unleaded Phillips J gasoline in Figure 11 and appear to indicate that the engine oil temperature plays a more important role in the production of wear iron concentration than does the engine coolant temperature.

Thermocouples were installed in the 2.3-liter engine in the edge of the head

TABLE 15. ANALYSIS OF FINAL USED OIL SAMPLES FROM 2.3-LITER 20-HOUR STEADY-STATE TESTS USING ETHANOL AND LUBRICANT A

Oil-In Temp, °C	Iron Wear, ppm	TAN	TBN D 664	Vol% Ethanol	Vol% Water
		100% Ethanol			
77	15	2.3	8.8	0.01	0.26
52	10	2.4	8.0	0.02	0.26
77	18	2.6	8.9	0.01	0.24
63	13	2.7	8.9	0.01	0.28
52	13	2.8	8.2	0.02	0.27
46	12	2.6	6.6	0.02	0.26
99	12	2.6	8.2	0.01	0.21
		Ethanol + 11% Water			
46	45	2.2	5.6	0.06	1.08
77	12	2.1	7.3	0.03	0.22
63	17	2.2	7.0	0.03	0.22
52	34	1.9	5.7	0.07	0.45
46	56	2.3	6.8	0.19	6.62

New Lubricant TAN = 2.5
TBN (D 664) = 9.7
Vol% Ethanol = Ref 11
Vol% Water = ASTM Method D 1744 Modified

TABLE 16. ANALYSIS OF FINAL USED OIL SAMPLES FROM 2.3-LITER 20-HOUR STEADY-STATE TESTS USING METHANOL AND LUBRICANT A

Oil-In Temp, °C	Iron Wear, ppm	TAN	TBN D 664	Vol% Methanol	Vol% Water
		100% Methanol			
77	18	2.4	7.2	0.01	0.16
63	14	2.3	7.4	0.01	0.14
52	74	2.2	5.5	0.05	0.88
46	192	2.5	5.4	0.17	3.11
99	19	2.4	6.3	0.01	0.17
46	184	2.1	5.5	0.21	3.15
		Methanol + 11% Water			
77	10	3.1	6.3	0.02	0.14
63	120	3.6	4.5	0.09	1.43
96	704	4.5	3.3	1.10	50.82

New Lubricant TAN = 2.5
TBN (D 664) = 9.7
Vol% Methanol = Ref 11
Vol% Water = ASTM Method D 1744 Modified

TABLE 17. ANALYSIS OF FINAL USED OIL SAMPLES FROM 2.3-LITER 20-HOUR STEADY-STATE TESTS USING PHILLIPS J UNLEADED GASOLINE AND LUBRICANT A

Oil-In Temp, °C	Iron Wear, ppm	TAN	TBN D 664	Vol% Water
77	10	2.0	8.2	0.24
52	20	2.2	6.9	0.22
77	14	2.5	7.3	0.22
63	14	2.7	7.2	0.21
52	10	2.5	6.8	0.21
46	17	2.8	6.3	0.21
99	12	2.4	8.5	0.22

New Lubricant TAN = 2.5
TBN (D 664) = 9.7
Vol% Water = ASTM D 1744 Modified.

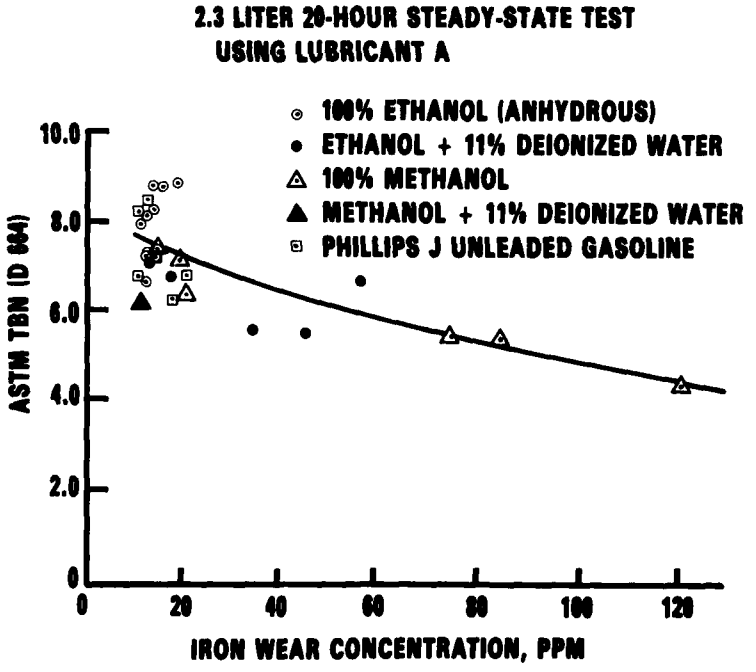

FIGURE 12. RELATIONSHIP OF TBN (D 664) TO IRON WEAR WITH VARIOUS FUELS

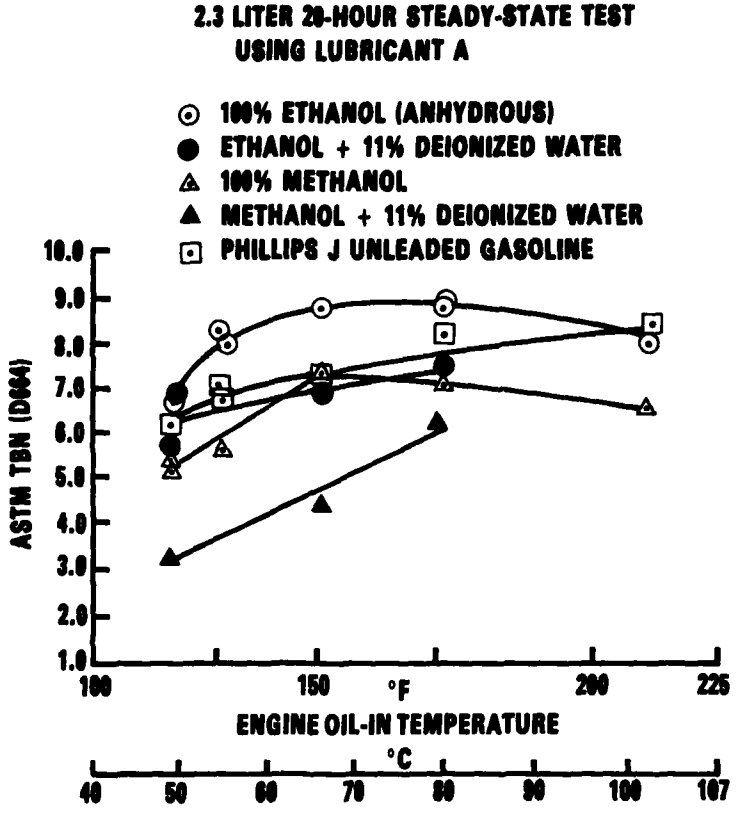

FIGURE 13. EFFECT OF OIL TEMPERATURE ON TBN (D 664) USING VARIOUS FUELS

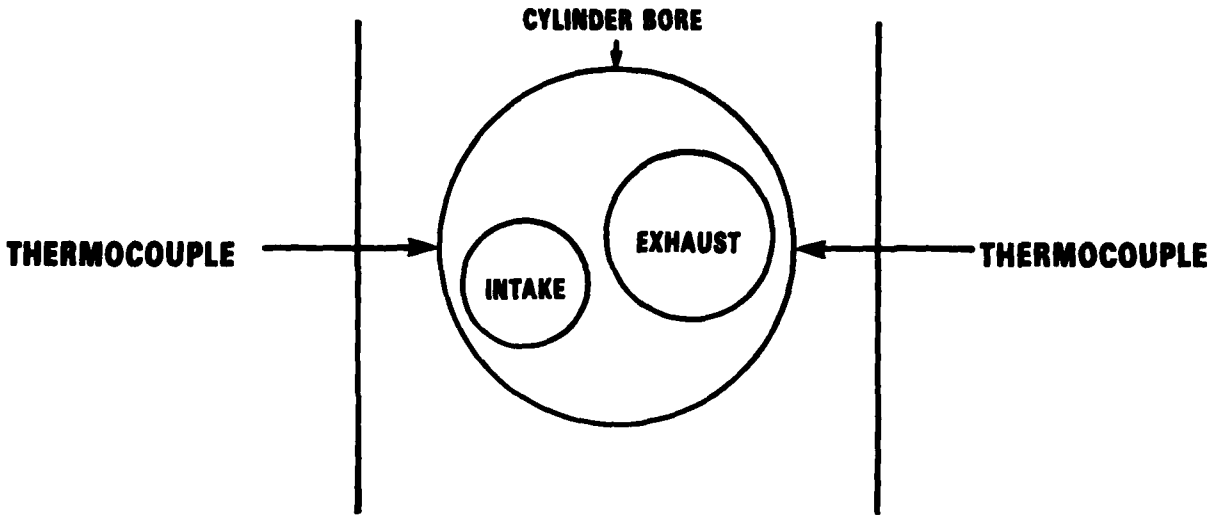

FIGURE 14. TOP VIEW DRAWING OF THE THERMOCOUPLE LOCATIONS

gasket between the head and cylinder block with one thermocouple on each side of the four cylinders (Figure 14). One thermocouple was also installed in each of the four intake manifold port passages at the engine block junction. These thermocouples were installed to determine the temperature differences between the various air/fuel mixtures and between the engine cylinders. The following fuels were used: anhydrous ethanol, neat methanol, Phillips J unleaded gasoline, ethanol + 11 percent deionized water, and methanol + 11 percent deionized water. The results are shown graphically in Figures 15 and 16. The temperatures in the head gasket/cylinder wall area appear hottest when using anhydrous ethanol, and coolest when using the alcohol/water mixtures; the Phillips J unleaded gasoline and neat methanol fell between the other two temperature ranges. The No. 1 cylinder was the coolest; No. 2 was warmer; and Nos. 4 and 3 were the hotter of the cylinders (typical results given in Table 18). These changes in temperature between the cylinder walls appear to be caused by the cylinder location relative to coolant inflow from

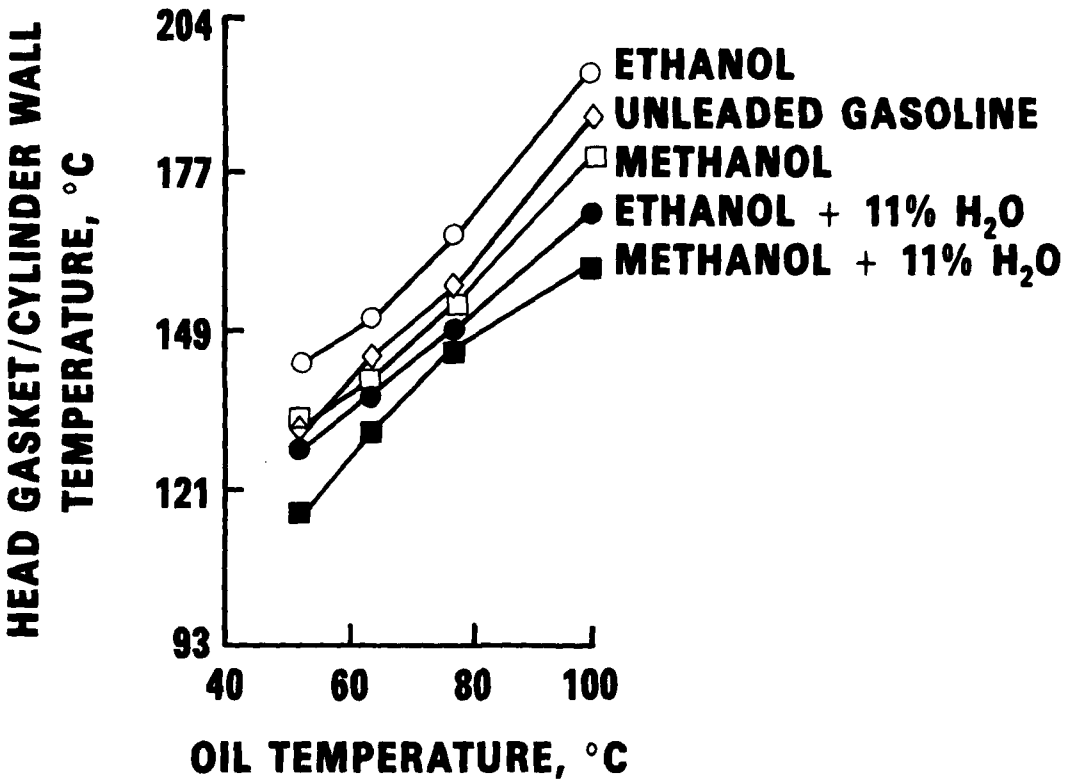

FIGURE 15. 2.3-LITER ENGINE HEAD GASKET/CYLINDER WALL TEMPERATURES WITH VARIOUS FUELS AND LUBRICANT A

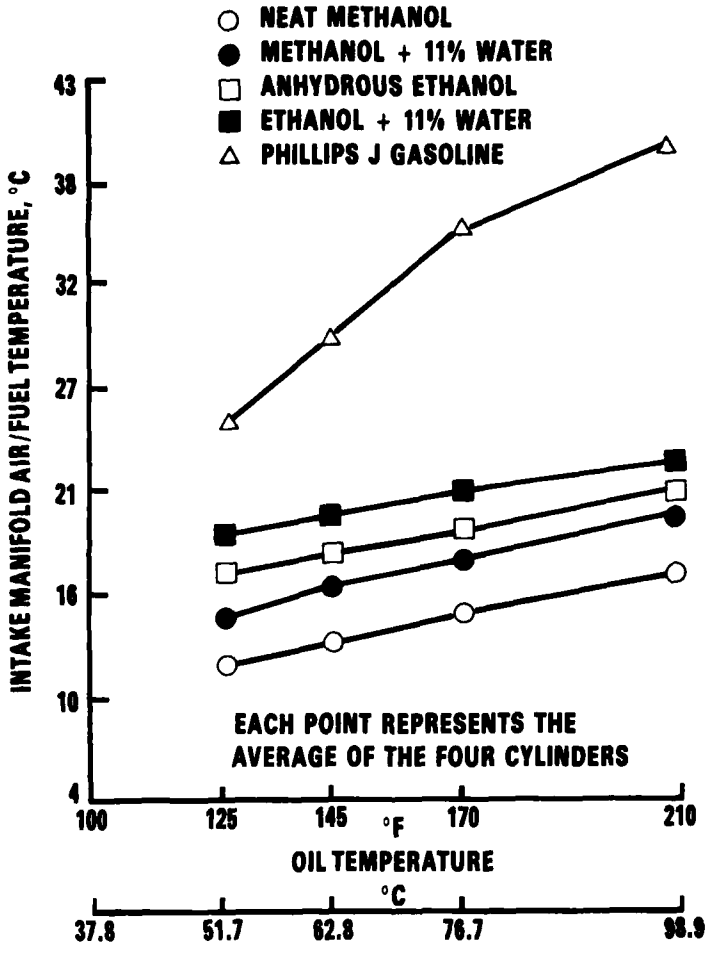

FIGURE 16. 2.3-LITER ENGINE MANIFOLD AIR/FUEL TEMPERATURES WITH VARIOUS FUELS AND LUBRICANT A

TABLE 18. CYLINDER NUMBER ORDER FOR TYPICAL WEAR AND TEMPERATURE

	Cylinder No.			
	Most →			Least
Top Cylinder	1	4	2 and	3
Bore Wear, mm	0.21	0.08	0.07	0.06
	Coolest →			Hottest
Head Gasket/Cylinder	1	2	4 and	3
Wall Temperature °C	99	104	128	134
	Coolest →			Hottest
Intake Manifold A/F	1	4	2 and	3
Mixture Temp, °C	16	17	18	18

the water pump. This change in temperature appears to contribute to the variation in top bore between cylinders.

The air/fuel mixture temperatures were hottest with Phillips J unleaded gasoline and cooler in descending order with ethanol/water, anhydrous ethanol, methanol/water and neat methanol. The air/fuel mixture temperatures were coldest in intake No. 1, while No. 4 was warmer, and Nos. 2 and 3 were hotter (typical results given in Table 18). It is interesting to note that this is the same order of the top bore wear, with No. 1 having the most wear, No. 4 having less, with Nos. 2 and 3 having the least. From these changes in air/fuel temperatures, it appears that fuel distribution is another contributing factor in top bore wear.

A series of 20-hour steady-state tests (Table 19) was then performed to observe whether increased intake air temperatures with methanol or the vaporization of methanol could reduce engine iron wear accumulation. Lubricant A was used for these investigations with engine oil-in temperature at 51.7°C (125°F). The first test was conducted with exhaust gas heating the intake manifold rather than engine coolant. This increased the average air/fuel intake manifold temperature from 10.2°C (50.4°F) to 19.9°C (67.8°F), so

TABLE 19. AIR/FUEL INTAKE TEMPERATURE WITH NEAT METHANOL

	Inlet Air Temp., °C (°F)	Engine Oil-in Temperatures 51.7°C (125°F)	98.9°C (210°F)
Coolant-heated intake manifold, avg	29.4 (85)	10.2 (50.4)	15.6 (60.1)
Exhaust-heated intake manifold, avg	29.4 (85)	19.9 (67.8)	20.8 (69.4)
Heated-intake air, avg	93.3 (200)	44.4 (112)	ND
Exhaust-heated fuel vaporizer, avg	29.4 (85)	47.8 (118)	50.2 (122.4)
Exhausted-heated fuel vaporizer plus heated intake air, avg	93.3 (200)	72.8 (163)	ND

ND = Not Determined

apparently no significant increase in vaporization was achieved. Also, no decrease in iron wear occurred, as the data were within the range of previous 20-hour tests (Figure 17).

Next, the carburetor intake air was increased to 93.3°C (200°F). This increased the intake air/fuel temperature to 44.4°C (112°F) (Table 19), but did not affect the iron wear level because it again fell within the previously bounded test results (Figure 17). A fuel vaporizer was built using the exhaust gas heat to vaporize the methanol. The engine was first started with unleaded gasoline. When the exhaust-heated vaporizer was operating at sufficiently high temperature, the unleaded gasoline was turned off, and the engine switched to vaporized methanol. This arrangement appeared to operate successfully because of the increased intake air/fuel temperature without the heated intake air (Table 19). The results from using the methanol vaporizer do not appear to decrease the iron wear level as can be seen from Figure 17. It was felt that possibly incomplete vaporization or condensing of the methanol could have occurred. Therefore, the 20-hour steady-state test was conducted using the heated carburetor intake air and the exhaust-heat methanol vaporizer. This combination appeared to operate successfully because the

intake air/fuel temperature increased to 72.8°C (163°F), well above the dew point for a stoichiometric methanol/air mixture. Figure 17 shows that the iron wear level gave somewhat lower levels of 67 ppm and was outside the envelope of the previously bounded tests. From these tests, it appears that when complete vaporization of methanol is achieved, the iron wear level is reduced.

Another 2.3-liter multicylinder engine was installed in an effort to correlate the 20-hour steady-state test with the modified Sequence VD test. Lubricant A was tested at 98.9°C (210°F), 76.7°C (170°F), 62.8°C (145°F), and 51.7°C (125°F) oil-in temperatures with methanol fuel (Figure 18). This curve fell within the boundary of the previously developed curves from other tests with lubricant A and methanol. Then two lubricants were selected which had high and low 192-hour EOT lubricant iron wear levels in the modified Sequence VD test. These lubricants were run in the 20-hour steady-state test at 51.7°C (125°F) oil-in temperature.

This is below the critical oil temperature where high wear occurs with methanol fuel. Lubricant A-1 (Test 32), which had 590 ppm iron wear in the VD test, also produced a lower iron wear level in the 20-hour steady-state test than with lubricant A (Figure 18). Next, lubricant A-9 (Test 42), which accumulated 1433 ppm iron wear in the V-D test, produced a level which was in the upper limits of the area bounded by lubricant A (Figure 18). From these tests, it appears that there is a directional trend between the modified Sequence VD test and the 20-hour steady-state tests.

A 20-hour test was also conducted using a corrosion inhibitor additive in lubricant A. This inhibitor, a tolyltriazole, was effective in eliminating corrosion in FRF (fire-resistant fuels).(18) This additive was used at a concentration of 4000 ppm with no apparent decrease in iron wear concentration (Figure 18). A recommended fuel soluble corrosion inhibitor meeting MIL-I-25017 was added to the methanol fuel at a level of 0.5 vol% and tested 20 hours using lubricant A. No apparent decrease in iron wear level was observed because the results fell within the area bounded by lubricant A.

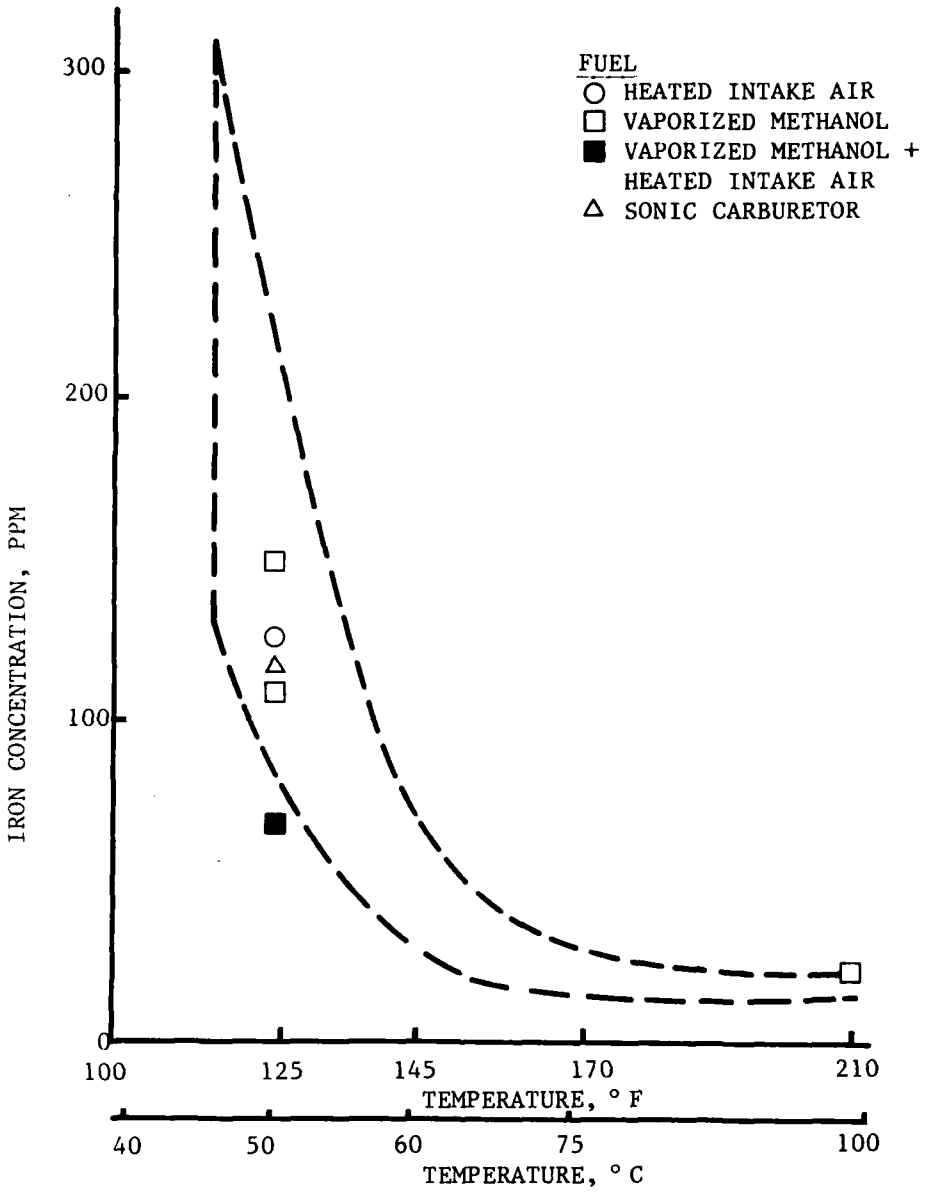

FIGURE 17. 20-HOUR STEADY-STATE TESTS USING NEAT METHANOL

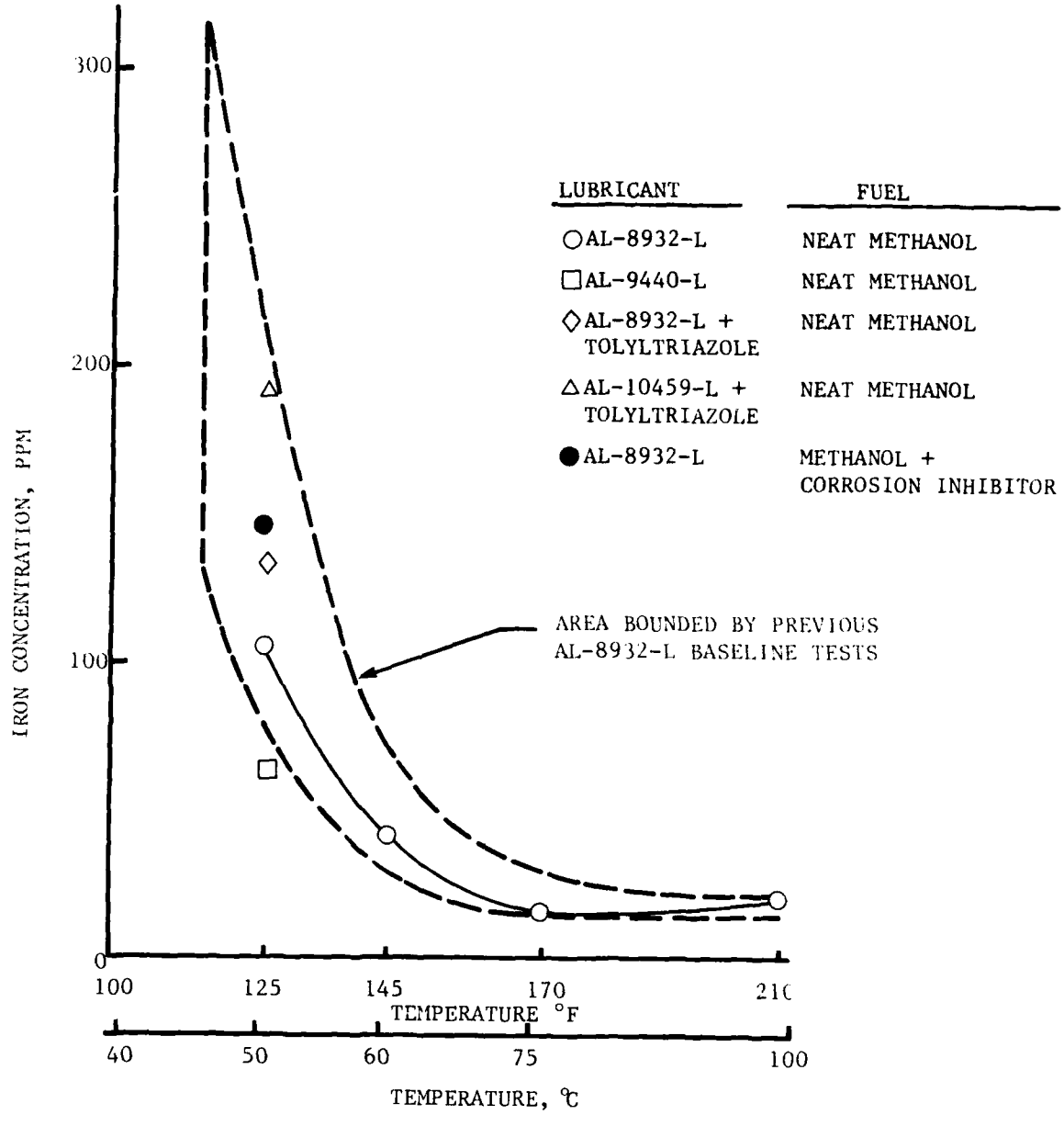

FIGURE 18. 20-HOUR STEADY-STATE TESTS USING VARIOUS LUBRICANTS AND FUEL ADDITIVES

From these data, it appears that the 20-hour steady-state test shows promise as a lubricant screening test when using alcohol fuels.

C. Proposed Mechanism

When examining the previously presented 20-hour steady-state data (Figure 19), the data indicate wear occurs as an exponential function of temperature. If wear is related to the rate of a chemical reaction, one might expect an Arrhenius-type correlation between the wear rate and the cylinder wall temperature. A mechanism is proposed which assumes that formic acid is formed from methanol combustion products in the quench layer adjacent to the relatively cool cylinder wall. The formic acid tends to react with exposed iron at the surface, forming iron formate. Eventually, the iron formate is rubbed

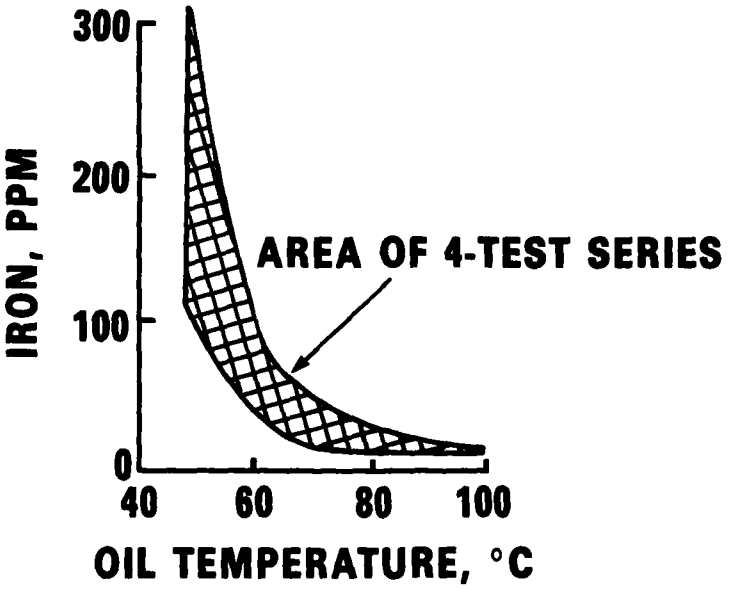

FIGURE 19. IRON CONCENTRATION VERSUS TEMPERATURE USING METHANOL AND LUBRICANT A

from the wall by the piston ring. When the cylinder wall temperature is high enough, the formic acid decomposes before iron formate can form. Two global reaction processes are proposed: (1) reaction of formic acid with iron and (2) thermal decomposition of formic acid. The decomposition reaction rate has a greater sensitivity to temperature and thus would be the controlling process in the wear mechanism. It follows that the wear rate is inversely proportional to the rate of formic acid decomposition. The decomposition probably occurs late in the combustion stroke and throughout the exhaust stroke when the cylinder wall temperature is highest. This peak cylinder wall temperature is estimated from the expression given below:

$$T_p \approx T_c + 2\,(T_a - T_c) \qquad (1)$$

where T_p is the peak cylinder wall temperature, T_c is the coolant temperature, and T_a is the average cylinder wall temperature measured at the junction of the cylinder head and block (Figure 14). The Arrhenius correlation of wear and cylinder wall temperature shown in Figure 20 is based on the same data presented in Figures 15 and 19. A least squares best fit of all the data gives a straight line of slope 1.26×10^4. The rate of decomposition of formic acid is proportional to exp $(-E/RT_p)$ where E is an activation energy and R is the universal gas constant. The wear rate is then simply proportional to exp (E/RT) and the slope of the curve shown in Figure 20 equals E/R which translates into an apparent activation energy of E = 25.2 kcal/mole. The global activation energy for the gas phase decomposition of formic acid is somewhat uncertain, but values have been measured for the heterogeneous catalytic decomposition on various surfaces. The activation energies measured on several surfaces including nickel, copper, platinum, silver, and gold ranged from 15 to 30 kcal/mole.(19) Values obtained for pure nickel, a close relative to iron, range from 20 to 25 kcal/mole. The value of 25.2 obtained is in this range and suggests that formic acid formed from combustion products decomposes on the iron cylinder wall surface. While the process of formic acid decomposition appears to explain the temperature dependence and presents a basic mechanism for wear, it is to be regarded as simply a speculation. There is much basic research yet to be done to prove the validity of the mechanism. The work presented here provides a starting point

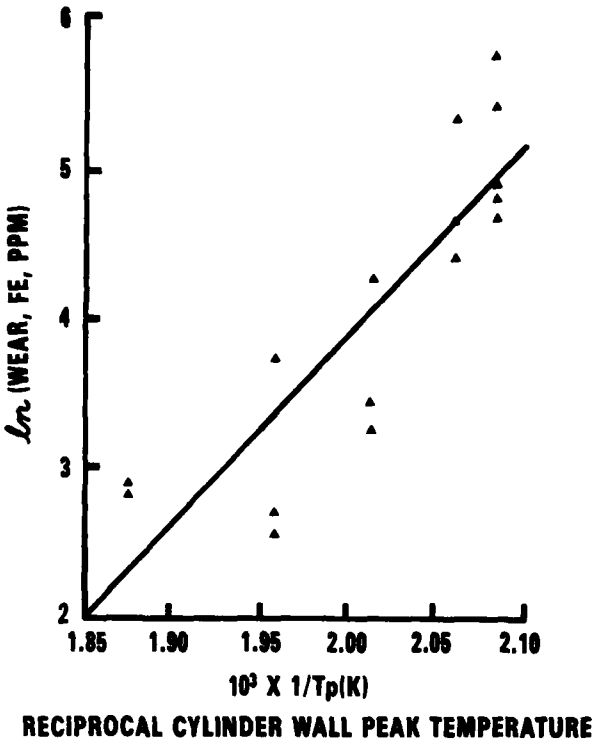

FIGURE 20. ARRHENIUS CORRELATION OF WEAR AND CYLINDER WALL TEMPERATURE.

for more fundamental studies. The next activity concentrated on gaining insight into the cause of this wear increase.

V. WEAR MECHANISM STUDIES

The extensive engine tests previously performed have established that significant ring and upper cylinder bore wear result from low-temperature operation of spark ignition engines on neat methanol. In this work, a single-cylinder CLR engine and a Ford 2.3-liter engine were used to determine the effects of operating conditions and lubricant formulation on wear. Wear, as measured by the accumulation of iron in the lubricant, was most apparent when the engine coolant and lubricant temperatures were below 70°C. At higher temperatures,

the wear characteristics of neat methanol approached those of unleaded gasoline.

Owens, et al. (11-14) suggest three possible mechanisms for the increased ring and upper cylinder bore wear:

1. The methanol or its partial combustion products react with the metal surfaces, causing metal removal through corrosive attack.
2. The high latent heat of vaporization and the relatively large quantities of methanol inducted into the engine tend to cause significant accumulations of liquid fuel on the cylinder walls. The liquid methanol could, in effect, serve as a solvent in washing the lubricant film from the cylinder wall, resulting in metal removal by adhesion and abrasion.
3. The accumulation of methanol or its combustion products in the lubricant may interfere with the lubricant and/or the additive package.

Microscopic analyses of the rings and upper ring travel areas of the cylinder liners indicated that the main cause of wear observed in the methanol-fueled engine is a corrosive attack.(11-14) This indicates that the microscopic cause of the wear is a corrosive attack of the metal surfaces by methanol or its combustion products. In order to eliminate the problem, it became apparent that a number of fundamental questions had to be addressed. These questions relate to the identification of the corrosive species and the determination of mechanisms by which these species are formed and get through the oil film to the metal surfaces. The specific objectives of the program were to (1) verify the existence of a corrosive reaction; (2) identify the chemical species responsible for the corrosion; (3) identify the mechanism by which the species are formed; (4) determine how these species arrive at the metal surfaces; and (5) propose possible solutions to the wear problem. This section is a description of a number of experiments designed specifically to address the first two objectives. However, a number of hypotheses have been developed concerning the remaining three objectives.

A. Engine Experiments

Five series of engine experiments have been performed to investigate the mechanism leading to ring and cylinder bore wear. The first four series of tests were performed using single-cylinder CLR engines and the last one was done using a four-cylinder 2.3-liter Ford engine. The results of the first three single-cylinder engine experiments were reported previously.(11) The results of these experiments (Series I, II, III) will be reviewed before describing the most recent engine work.

1. Single-Cylinder Engine Experiments--The engine used in these tests was a single-cylinder CLR engine (see Table 20 for specifications), coupled to a 22-kW (30-hp) cradled eddy current dynamometer. The engine torque was measured using a Lebow load cell. The lubricant was not a variable in any of the engine tests performed in the mechanism study.

TABLE 20. COORDINATED LUBRICANTS RESEARCH (CLR) ENGINE CHARACTERISTICS

Displacement	697 cm^3 (42.5 $in.^3$)
Bore and Stroke	9.65 cm x 9.53 cm (3.80 in. x 3.75 in.)
Compression Ratio	8.3:1
Piston	Aluminum, 3-Ring
Piston Rings	Barrel-Faced Chrome, 1st Comp. Taper Face Cast Iron; 2nd Compr. Two Chrome Rails and Expander, Oil Control
Cylinder	Replaceable Cast Iron Sleeve
Oil Capacity	0.946 liter (1 quart) (no filter)

Preliminary tests using carbureted methanol in this engine gave the first indication of the cylinder bore and ring wear problem as evidenced by both an increase in the iron content of the lubricant as well as an increase in the bore diameter and ring clearance. As indicated previously, these symptoms were characteristic only of low temperature operation of the engine. The four series of single-cylinder engine experiments are discussed below.

a. Series I - The first experiment aimed at identification of the wear mechanism consisted of operating two identical CLR engines using a common oil sump and lubricant system.(11) One engine was operated on carbureted methanol while the other was run on unleaded gasoline. Both engines were run simultaneously with identical operating conditions. The reasoning was that if lubricant degradation or contamination was the cause of the wear, both engines would show similar wear rates. At the completion of the test, both engines were dismantled and measured for wear. The cylinder bore and ring wear in the methanol engine was twice that of the gasoline engine, thus suggesting that lube oil degradation or contamination is not the controlling factor in the wear mechanism. Instead, in view of the test conditions (see Table 21), it seemed more probable that large quantities of liquid methanol

TABLE 21. OPERATING CONDITIONS FOR CLR TESTS

RPM	1550±25
Load	1.86±0.15 kW (2.5±0.2 Hp)
Equivalence Ratio	5.0±0.2
Oil Temperature	57°C (135°F)
Coolant Temperature	46°C (115°F)
Superheater Outlet Temperature	149°C (300°F)
Superheater Outlet Pressure	86 kPa(12.5 psi)

were entering the cylinder and wetting the cylinder walls, suggesting the possibility of a removal of the lubricant film and/or a direct chemical attack of the metal surfaces.

b. Series II - To investigate the role of liquid methanol, the CLR engine was fitted with both a carburetor and a methanol vaporization system.(11) The methanol vaporization system consisted of a boiler and a superheater section, both of which were heated electrically. When operated on the vaporization system, methanol vapor was supplied at the intake valve of the engine at a state which had a sufficient degree of superheat to ensure that no condensation could occur in the combustion chamber. Operating in this mode effectively eliminated the possibility of having liquid methanol present in the combustion chamber. Three 50-hour wear tests were performed using the CLR engine. The first test was a baseline test using carbureted unleaded gasoline; the second test was performed using methanol vapor; and the third test was performed using carbureted methanol. All three tests were completed at the engine operating conditions listed in Table 21. The wear rates for the unleaded gasoline test and the vaporized methanol test were essentially identical, both showing very low wear rates as indicated by the accumulation of iron in lube oil samples taken every four hours during the tests. The carbureted methanol test showed an overall higher wear rate, especially during the final twelve hours of the test. During this test, however, the water and methanol concentrations in the lube oil became excessive, with the lube oil accounting at one point for only 39 percent of sump contents.(11) It was thought that the high level of dilution may have contributed to the high wear rates, at least during the final hours of the test.

c. Series III - In this series of tests, the CLR engine was equipped with a blowby gas sampling system. The design and use of this system were reported previously.(11, 12, 20)

The results of the other CLR engine tests indicated that the wear mechanism was not due to lube oil degradation or dilution. The purpose of this test was to determine qualitatively the composition of the methanol combustion products present in the ring zone.

Preliminary analysis of samples collected from the methanol-fueled engine showed concentrations of methanol, methane, formaldehyde, formic acid, acetaldehyde, and acetic acid. It appeared that formaldehyde, formic acid, and probably methane were products of incomplete combustion of methanol. Of most concern was the formic acid, because of its potential to cause corrosion. If the formic acid is formed at the cylinder wall, or somehow migrates to the cylinder wall, it would most probably react with the cast iron liner.

d. Series IV - To further investigate the oil dilution effects, the CLR engine was used in another 50-hour wear test, again using the same operating conditions listed in Table 21. In this test (designated the simulation test) methanol and water were manually injected into the crankcase of the engine while it was running on carbureted unleaded gasoline. Efforts were made to simulate the oil dilution observed in the carbureted methanol test. It was found, however, that very large quantities of methanol and water had to be injected to maintain the levels in the crankcase, much more than suggested by the concentration-time profiles reported previously.(13) Figures 21 and 22 show the methanol and water concentration-time profiles, respectively, for both the carbureted methanol test and the simulation test. Although the concentrations obtained in the simulation test did not match the results observed in the carbureted methanol test, the levels were still extremely high and the trends were very similar.

Figure 23 is a plot of the iron concentration-time profiles for both tests. The simulation test resulted in iron concentrations comparable to the baseline test and very much lower than those observed during the carbureted methanol test. These results support the findings of the test in which a common oil system was shared by two engines. Both tests indicate that oil dilution is not a cause for the excessive cylinder bore and ring wear observed in the methanol-fueled engines.

2. Multicylinder Engine Tests--A four-cylinder 2.3-liter Ford engine was used in a series of tests designed to verify the results of the vaporized methanol tests in the CLR engine. The engine was equipped with a methanol vaporization system very similar to the one used on the CLR engine. Figure

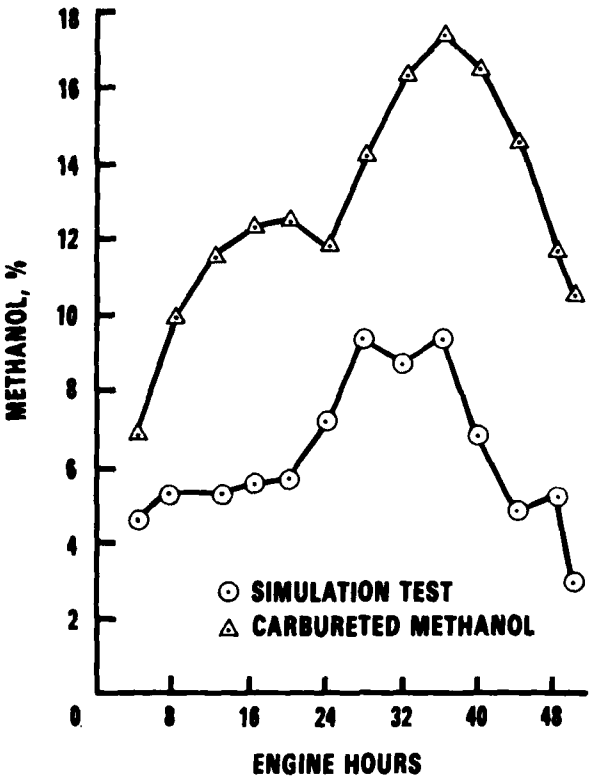

FIGURE 21. METHANOL CONCENTRATION IN LUBRICATING OIL

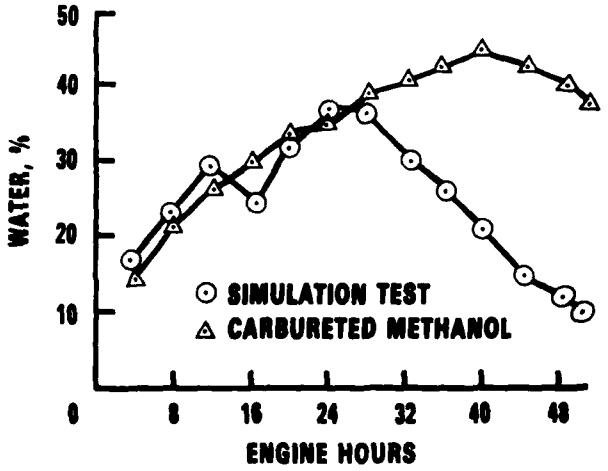

FIGURE 22. WATER CONCENTRATION IN LUBRICATING OIL

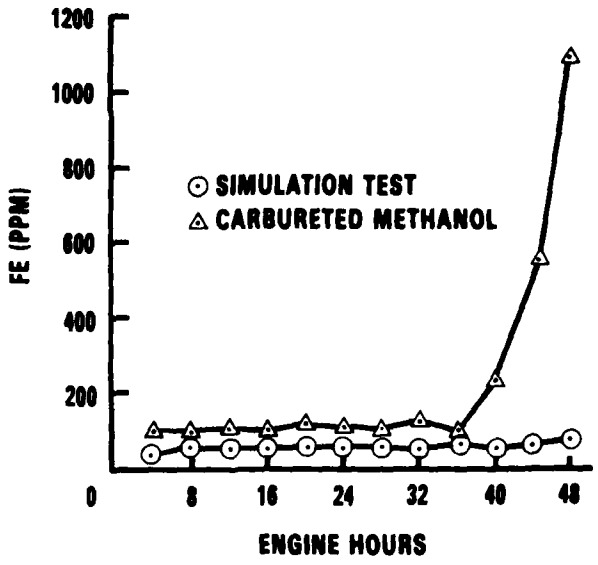

FIGURE 23. IRON WEAR METALS CONCENTRATION IN LUBRICATING OIL

24 is a schematic of the system. Table 22 is a listing of the operating conditions used during the vaporized methanol test on this engine. Figure 25 shows a compilation of data obtained from 20-hour wear tests on the 2.3-liter engine. The cross-hatched band represents the results of several tests in which various lubricant formulations were evaluated while using carbureted methanol in the 2.3-liter engine. The plot is iron concentration in the lubricating oil versus the lube oil temperature at the engine inlet from the oil cooler. The iron concentrations are those measured at the completion of

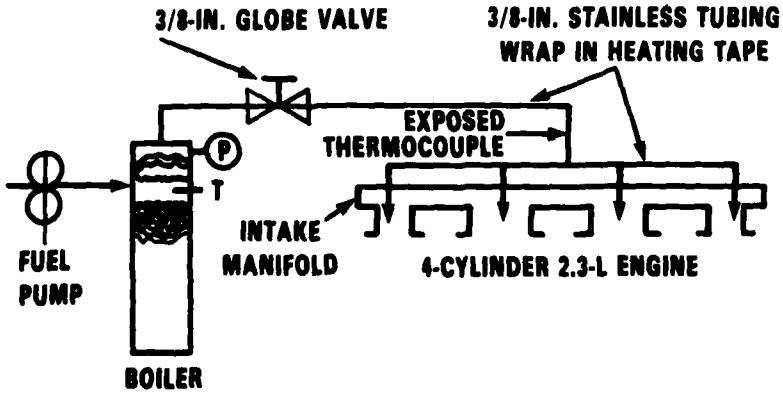

FIGURE 24. SCHEMATIC OF 2.3-LITER ENGINE VAPORIZATION SYSTEM

TABLE 22. OPERATING CONDITIONS FOR THE VAPORIZED METHANOL TESTS ON THE 2.3-LITER ENGINE

RPM	2500
Load	14.8 kW (33.3 hp)
Air/Fuel Ratio	6.5
Oil Inlet Temperature	50.5°C (123°F)
Coolant Temperature	37.7°C (100°F)
Superheater Outlet Temperature	98.9°C (210°F)
Superheater Outlet Pressure	79.3 kPa (11.5 PSIA)

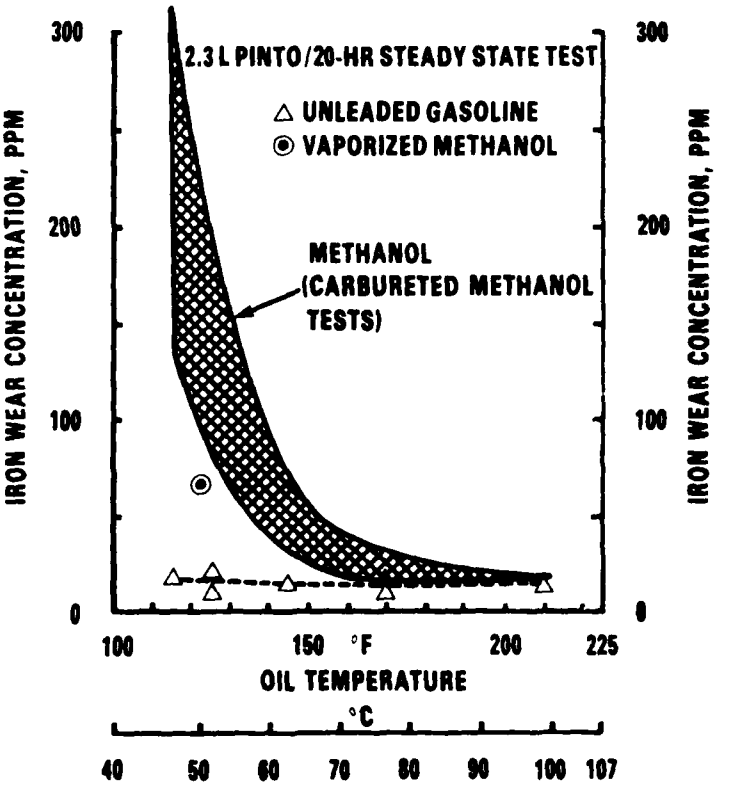

FIGURE 25. EFFECT OF OIL TEMPERATURE ON ENGINE IRON WEAR WITH METHANOL

the test. Also shown on the plot is the data point obtained from a methanol vapor test and the results of several unleaded gasoline tests. As can be seen, the result for the vaporized methanol test is below the typical wear band but higher than the unleaded gasoline test.

The vaporized methanol test results were somewhat higher than expected, based upon similar tests on the CLR engine. A possible reason for this is that it was not possible to run 20 consecutive hours. As a result, the engine was started and stopped three times over the duration of the test. During these transients, relatively large quantities of liquid methanol were inducted into the combustion chamber, possibly biasing the results toward the carbureted test results.

3. Discussion of Engine Experiments--Based upon the results of the various engine experiments, it appears that the wear mechanism is related to the presence of liquid methanol on the cylinder walls. This is suggested by the results of the methanol/vaporization tests in which the wear rates were substantially reduced when the liquid methanol was eliminated from the combustion chamber.

It would be expected that lube oil dilution by methanol or methanol combustion products would also be reduced by using vaporized methanol. This is indeed the case, but the tests with the single oil system shared by two engines and the tests in which methanol and water were injected into the lube oil both indicated that lube oil dilution and/or degradation are not the controlling factors in the wear mechanism.

Of the two remaining theories, wall washing and direct chemical attack, the direct chemical attack appears to be the most likely mechanism based upon the results of the blowby gases. In addition, it is difficult to envision how liquid methanol could sufficiently displace the lubricant film from the cylinder wall to permit metal-to-metal contact. Another consideration is that the microscopic analyses of the wear parts indicated that the metal removal was due to a corrosive reaction.

B. Spinning Disc Combustor Tests

A spinning disc combustor was constructed to examine the corrosive mechanism of wear. The device, shown schematically in Figure 26, consisted of a spinning disc atomizer mounted inside a water-cooled cast iron cylinder liner. Figure 27 is a photograph of the complete apparatus, while Figure 28 is a photograph of the disc showing its orientation inside the cylinder.

A continuous supply of methanol was introduced into a small fuel reservoir located at the center of the spinning disc. Centrifugal force generated by the rotation of the disc forced the methanol to the outside of the fuel reservoir. Small holes drilled radially from the fuel reservoir to the outside edge of the disc provided a path for the methanol to flow from the fuel

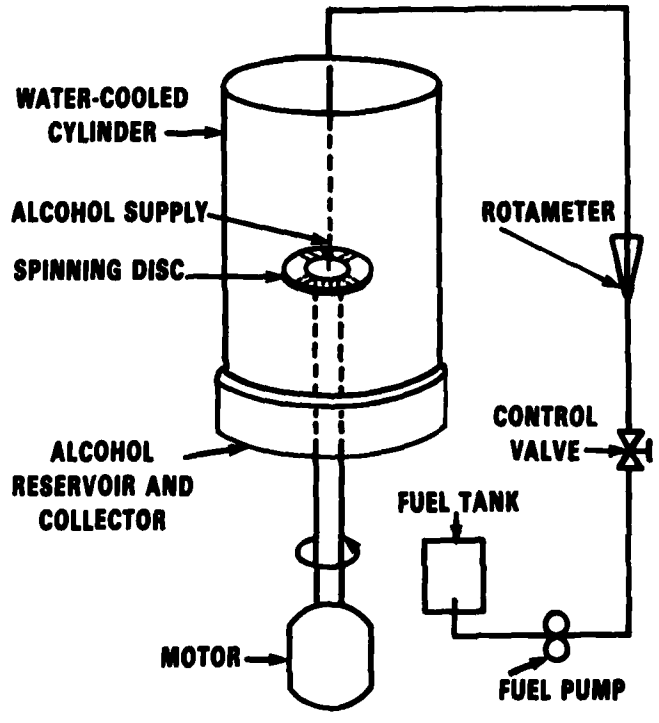

FIGURE 26. SPINNING DISC COMBUSTOR SCHEMATIC

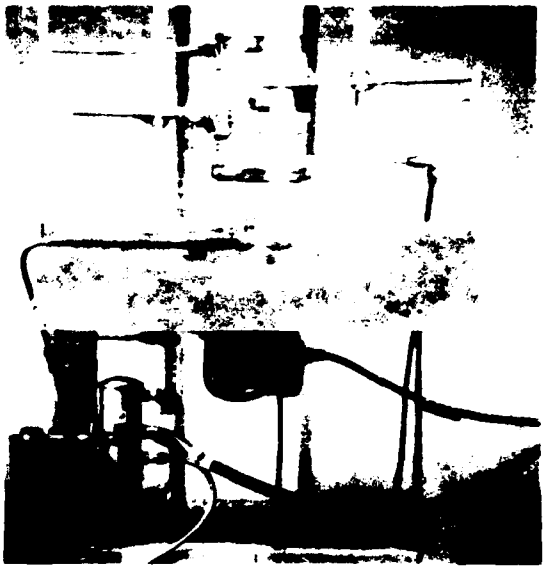

FIGURE 27. PHOTOGRAPH OF THE SPINNING DISC COMBUSTOR

FIGURE 28. PHOTOGRAPH SHOWING THE ORIENTATION OF THE DISC INSIDE THE CYLINDER

reservoir. Small holes drilled radially from the fuel reservoir to the outside edge of the disc provided a path for the methanol to flow from the fuel reservoir to the periphery of the disc. Shear stresses induced by the rotation of the disc caused the atomization of the methanol as it flowed from the small holes in the disc. The flow rate of the methanol was monitored using a rotameter installed in the supply line to the disc. Ignition was accomplished using a methane pilot flame located at the disc discharge. Once a stable self-supporting flame was established inside the cylinder at the disc discharge, the pilot flame was extinguished. The flow of combustion air was controlled by adjusting the height of the liner above the condensate reservoir located beneath the liner.

The inside surface temperature of the cylinder liner was monitored by surface thermocouples mounted at various locations inside the liner. These temperatures could be changed by controlling the flow of cooling water through a water jacket surrounding the liner. The disc was driven by a variable speed electric motor capable of more than 20,000 rpm. Speed was determined with a strobe light.

In addition to containing the flame, the cooled cylinder liner (1) quenched the burning fuel droplets as they impacted the cold wall; (2) caused condensation of some of the combustion products of the methanol; (3) provided a surface upon which a liquid boundary was formed; and (4) provided a chemically active surface upon which and/or with which the combustion products could react. The liquid products collected on the wall were allowed to drip into the condensate reservoir located beneath the cylinder. Samples thus collected were removed and analyzed for chemical composition.

Preliminary tests showed that at surface temperatures above 70°C, the collection of condensate ceased. It was observed that the liquid condensate caused severe corrosion of the cast iron cylinder. Figure 29 is a plot of the change in the diameter of the cast iron cylinder liner before and after a run in which liquid condensate was collected. Before the test, the only change in diameter was due to the normal surface roughness. After the test, however, the surface roughness had increased, and there was a large change in

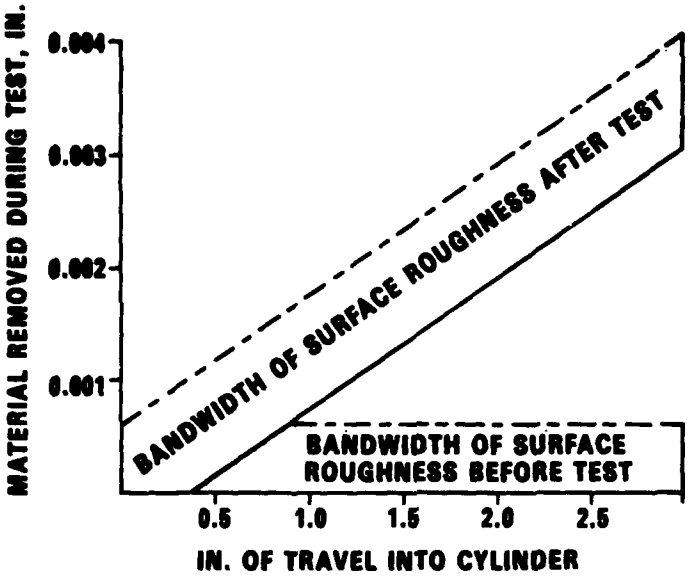

FIGURE 29. CHANGE IN CYLINDER SURFACE PROFILE

diameter due to the removal of material; these two trends are shown in Figure 29 by the increase in band width and the slope of the "after test" results. A similar test performed with the surface temperature maintained above 70°C did not show metal removal from the liner. It should be noted that the 70°C temperature limit is approximate since a uniform temperature over the entire surface of the cylinder was impossible to maintain.

Basically, two series of tests have been performed using the spinning disc. In both series, the methanol flow rate was set at 3.8 liters/hour with the disc speed at 8000 rpm.

1. Formic Acid Identification--The first series, directed at identifying formic acid in the condensate sample, was performed using the cast iron cylinder liner with a freshly honed inside surface. The liner surface temperature, in the region of the disc discharge, was maintained below 51°C.

a. Analytical methods - The condensate from the spinning disc apparatus was analyzed for water, methanol, formaldehyde, formic acid, total

acidity, and iron. Water was determined by titration with Karl Fischer reagent, and acid number was measured by titration with KOH solution to a pH of 11. Methanol, formaldehyde, and formic acid were determined by gas chromatography; a Porpak® Q column and a thermal conductivity detector were used. The iron was found in the condensate sample in the form of a rusty red-colored precipitate which could be separated from the liquid by light centrifuging. The precipitate was washed with anhydrous methanol and dried in a vacuum desiccator. The iron content was determined with an X-ray fluorescence spectrometer. A portion of the iron-containing precipitate was mixed with potassium bromide powder; this was compressed into a pellet and used as an optical absorption cell for analysis by infrared spectroscopy.

b. Results - The condensate consisted mainly of water and methanol. The amount of water in the condensate samples ranged from about 15 to 65 percent by volume depending on the cylinder wall temperature in the spinning disc apparatus. The samples were acidic (total acid number of about 1) and contained relatively small amounts of formaldehyde and rust-colored precipitate. X-ray fluorescence revealed that the rust-colored precipitate contained about 33 percent iron, which was considerably less iron than would have been expected if the precipitate was either Ferric Hydroxide, $Fe(OH)_3$ (52.3 percent iron) or Iron Oxide, Fe_2O_3 (70.6 percent iron). The infrared spectrum of the precipitate is shown in Figure 29. The strong absorption bands at 6.4 and 7.3 micrometers are characteristic of the formate iron. To confirm this analysis, the second infrared spectrum shown in Figure 30 was taken of a sample of iron formate $Fe(HCOO)_3$ that was prepared in the laboratory. The iron content of pure iron formate is 29.3 percent. The value of 33 percent found by X-ray fluorescence suggests that the rust-colored precipitate is a mixture of pure iron formate and Ferrichydroxy-diformate, $Fe(OH)(HCOO)_2$, which contains 34.3 percent iron. These results show that corrosion of the cylinder wall is due to formic acid formed in the combustion of methanol.

2. Surface Effects--The second series of tests was performed to investigate the effects of the liner surface material on the formulation of formic acid. In formulating a mechanism for the formation of formic acid, it is

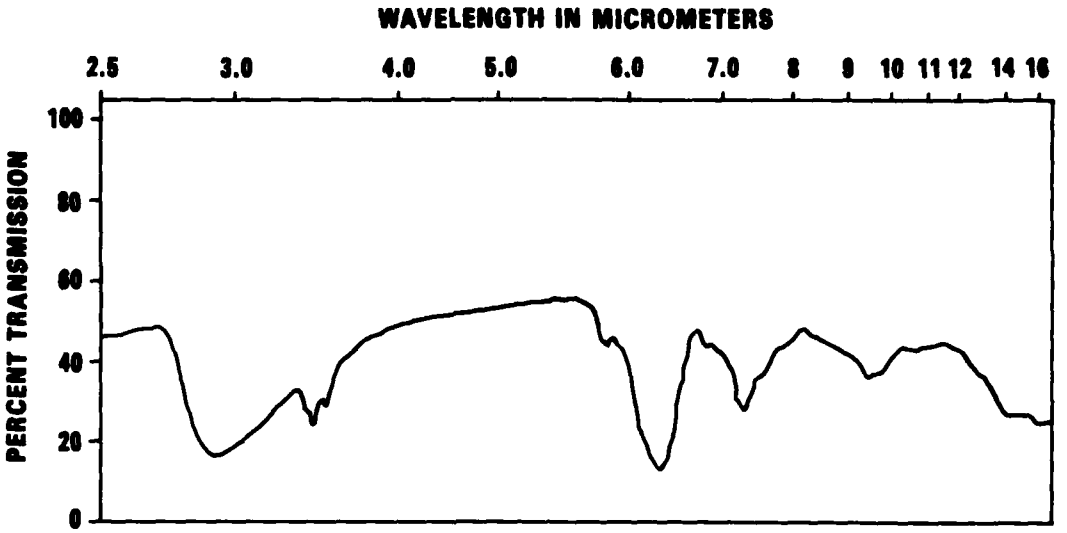

(A) PRECIPITATE IN CONDENSATE FROM SPINNING DISC EXPERIMENT

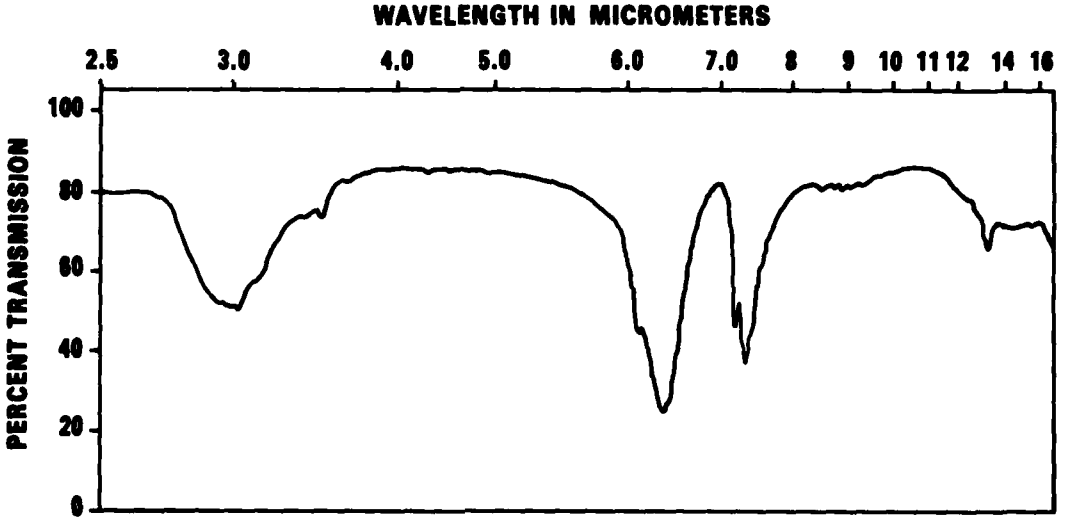

(B) IRON FORMATE PREPARED IN LABORATORY

FIGURE 30. INFRARED SPECTRA SHOWING PRESENCE OF FORMATE ION

important to consider the effects of the surface; formation may occur in the gas phase, or heterogeneous catalysis may be the predominate route. The effects of burning atomized methanol in the presence of different surfaces were examined in the spinning disc apparatus. In addition to the familiar cast iron liner, two liners, one plated with fresh nickel and one with chromium, were compared in the experiment. Condensate samples from each liner were analyzed, as described in the previous section, for possible clues to the mechanism of formic acid formation.

The conditions (wall temperature well below 50°C) were adjusted so the formation of iron formate on the cast iron liner was negligible. The formic acid would then be in the condensate, and its concentrations could be determined simply by acid-base titration. At slightly higher liner wall temperatures (approaching 70°C), the formic acid formed reacts rapidly with the cast iron.

The three liners were each run at the same conditions, with equal wall temperatures, equal fuel flow rate, and an equal amount of condensate collected in each case. The condensate samples each contained about 60 percent water with the remainder being methanol and traces of acid and formaldehyde. Titration with KOH of a portion of the condensates revealed that the acid numbers from the cast iron, nickel, and chromium liners were 1.15, 0.78, and 0.59, respectively. These results suggest that the surface plays some role in the accumulation of formic acid in the condensate. The role of the surface could be related to either chemical effects or to the physical characteristics of the surface, e.g., surface area, porosity, etc.

C. Discussion

It is apparent from the experimental results that the corrosive wear in engines operating at low temperatures on methanol is due to attack by formic acid. The formic acid appears to react rapidly with the cast iron cylinder wall to form iron formate, which eventually is rubbed from the surface by the piston ring. It seems that most of the formic acid reacts with the cylinder wall because only trace amounts of acid are found in the lubricant and blow-by.

The mechanism for the formation of formic acid is as yet uncertain. The experiments in the spinning disc apparatus suggest that the surface of the cylinder wall may play a role in the formation and/or decomposition of formic acid. If formic acid forms in the gas phase, the surface could act as a decomposition catalyst. The experimental results on the iron, nickel, and chromium liners, however, cannot be explained by catalytic decomposition because the chromium liner gave the lowest acid content in the condensate. The decreasing order of catalytic activity for decomposition is expected to be nickel, iron, and chromium.(18) Furthermore, the decomposition of formic acid is not expected to be appreciable at wall temperatures below 200°C. Over a nickel catalyst, formic acid decomposes at a measurable rate at temperatures above 200°C.(18) At lower temperatures, the reaction is relatively slow and would not be significant within the engine cycle. In the engine tests, the exhaust temperature (538°C) was essentially independent of the coolant and oil inlet temperatures, but the average cylinder wall temperature measured with a thermocouple at the junction of the cylinder head and block varied from about 90°C to 150°C depending on the fuel composition. A striking example of this was observed in the case in which the methanol contained 15 percent water; the junction temperature with this fuel was the lowest observed and the wear was the highest. The actual effects of the coolant and oil inlet temperatures on the peak wall temperature are not known, but it would appear that this temperature would be in the appropriate range for catalytic decomposition of formic acid. In a review, Mars, Schalter, and Zwietering (18) concluded that the mechanism for the decomposition of formic acid on metal surfaces involves the formation of a metal formate intermediate. The formic acid is first adsorbed on the metal surface where it reacts to form the metal formate. In this stage, the unstable formate may decompose into CO_2 and H_2 if the temperature is high enough (260°C), i.e., a wall temperature that could be achieved on the exhaust stroke of the test engine. While the spinning disc experiments show that iron formate can be formed on the cylinder wall, the engine tests indicate that wear is inversely proportional to cylinder wall temperature. This may explain the reduction in wear as the operating temperature increases, because the formate group would decompose before a significant build-up could occur. Each iron atom can react with three formic acid molecules. An iron atom must be attacked by at

least two formic acid molecules, i.e., formation of $Fe^{++}(HCOO^{-})_2$, before it becomes a stable metal salt. If only one formic acid molecule reacts, the salt is unstable in that it could react with a second acid molecule or decompose to free iron, CO_2, and H_2. It appears that when the cylinder wall temperature is high enough, e.g., 260°C, the rate of decomposition exceeds the rate of formation of the formate salts.

The mechanism for the formation of formic acid does not appear to be surface related, but this cannot be ruled out. The cylinder wall is relatively cool as the flame approaches so that the surface-catalyzed oxidation of stable combustion intermediates, such as formaldehyde, would seem to be a slow process that is unlikely to be significant in the duration of the combustion stroke. Instead, it appears that the precursors to formic acid are formed in the quench layer as the flame, rich in free radicals, approaches the wall. Formic acid is unstable at flame temperatures (22) and would not survive even if it was a combustion intermediate. When the methanol flame front enters the relatively cool quench layer, the gas becomes relatively rich with non-equilibrium concentrations of combustion intermediates and free radicals such as HCHO, CH_2OH, HCO, HO_2, H, O, and OH. (22, 23) The formyl radical, HCO, and the methylene hydroxy radical, CH_2OH, appear to be most important to the formation of formic acid. These radicals are relatively stable at the low temperatures (<400°C) expected in the quench layer. The quench layer consists of unreacted methanol and oxygen, which are essential to the formation of formic acid. The highly reactive free radicals (R) including H, O, OH, and HO_2 that diffuse into the quench layer react with methanol and formaldehyde to further increase the concentrations of CH_2OH and HCO, i.e.,

$$CH_3OH + \dot{R} = CH_2\dot{O}H + RH \quad (2)$$

and

$$HCHO + \dot{R} = \dot{H}CO + RH \quad (3)$$

Formic acid may form from either of these species in the reaction sequences given below for the $\dot{C}H_2OH$ radical.

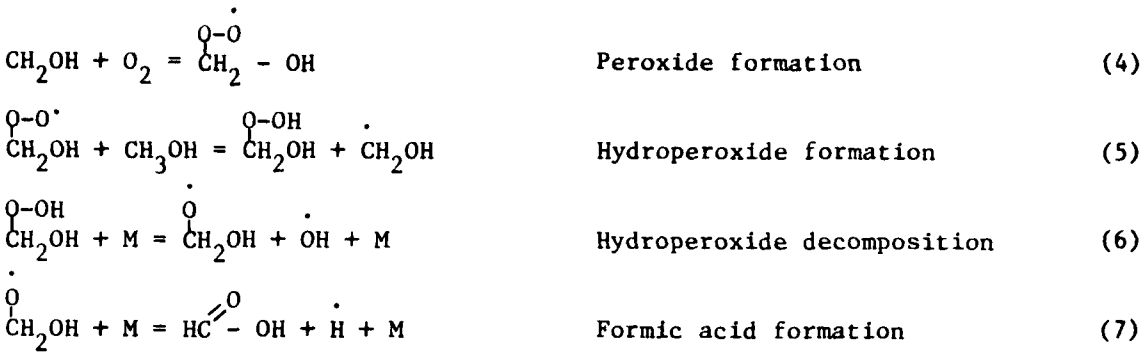

M represents all particles in the system. These reactions would occur in the boundary layer where the gas temperature is close to that of the wall. One cannot rule out the possibility that the wall may facilitate the reactions of combustion intermediates in favor of formic acid formation. However, the fact that the wall is relatively cold suggests that it would enhance radical recombination, which would inhibit the free radical reactions leading to the formation of formic acid. The kinetics of formic acid formation are only speculative at this time and should be pursued on a fundamental level in the future.

VI. SPECIAL ANALYSES

A. Inspection of Engine Parts by Eaton Corporation

The exhaust and intake valves, the camshaft, hydraulic lifters and rocker arm followers from Test 33 (lubricant A) were sent to Eaton Corporation to be examined for wear and to check their compliance with as-manufactured specifications. In addition, the 192-hour EOT used oil sample was also sent to be analyzed. These results are summarized below. Both the intake and exhaust valves were standard Ford production parts. The wear on the intake valve seat faces were considered to be minor, and overall wear on the valve stem was insignificant. The wear patterns on the tips of the valves indicate that limited rotation had occurred during operation. The most obvious characteristic noted on the exhaust valves was the dark red fillet deposits. Smaller amounts of similar-appearing deposits were also noted on the top of the valve head and on the seat faces. Energy Dispersive X-ray Analysis (EDX) con-

firmed that the deposits at each of the noted locations were of similar composition. The EDX analysis indicates that the deposit is basically iron, with lesser amounts of aluminum, phosphorus, calcium, chrome, manganese, nickel, and zinc. The phosphorus, calcium, and zinc were probably from the engine lubricant, while the aluminum was most likely from that applied to the seat face and on the top of the valve head for increased corrosion resistance. The chrome, manganese, and nickel were most likely in the form of oxides of the base material. The combustion products of methanol, which are carbon dioxide and water, typically promote the oxidation of iron and iron alloys. The aluminizing on the top of the valve heads apparently minimized oxidation at that location. Valve seat face wear was limited to the undiffused aluminized layer, similar to the intakes. Wear on the valve seat faces was considered minor. The exhaust valve tip pattern showed signs of limited rotation. Actual tip wear was virtually immeasurable. The flash chrome plating on the stems was scuffed at the head end of the valve guide contact zone. This scuffing may have been accelerated by abrasion from the iron deposits noted earlier. Overall stem wear was negligible.

All the lobes on the camshaft examined showed light polishing wear less than 0.025 mm (0.001 inch) except for the intake lobe of cylinder 4, which showed severe abrasive wear and lost approximately 0.432 mm (0.017 inch) depth of material near the nose of the lobe. The wear of the intake lobe on cylinder 4 is shown in Figure 31.

The hardness on the lobes fell within the specification. The rocker arm followers showed a light polishing wear on all the pivot sockets, valve slots and cam pads with the exception of the intake rocker arm for cylinder 4. The intake rocker arm of cylinder 4 showed severe abrasive wear on half of the cam pad and lost approximately 0.178 mm (0.007 inch) depth of material in the center of the wear zone. A comparison of the normal light wear against the heavy abrasive wear of the rocker arm of cylinder 4 is shown in Figure 32. The hardness of all the rocker arm cam pads fell within the specifications. All the lifters showed similar normal light wear on the various components of the assemblies, and no plunger sticking was observed. The leakdowns for all lifters were within the specification range. The level of metallic deposits

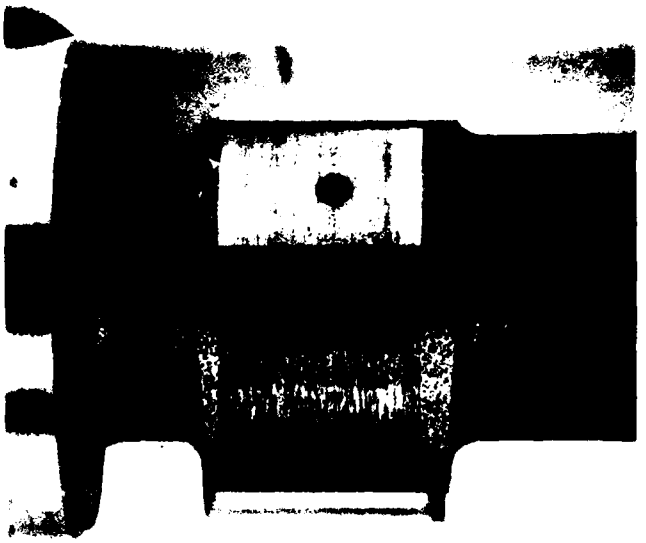

FIGURE 31. CAMSHAFT INTAKE LOBE OF CYLINDER 4

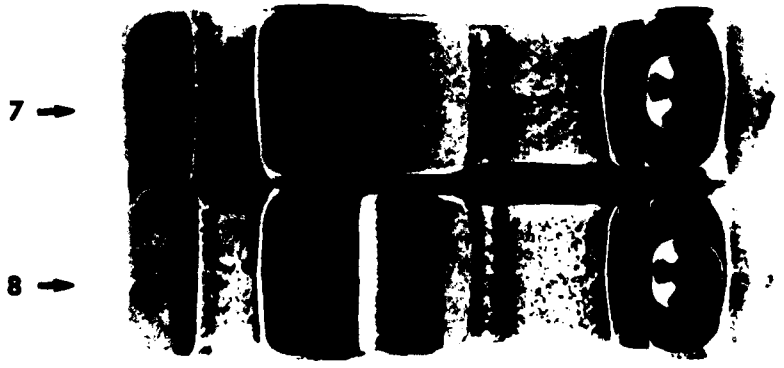

FIGURE 32. ROCKER ARMS FROM CYLINDER 4

found in the engine oil sample is higher than normally found in comparable gasoline-fueled engines, which may have contributed to abrasive wear at the cam lobe and rocker arm pad interface. The atomic absorption analysis of the engine oil compared quite favorably to that in Appendix F. The water in the oil was found to be at a normal level, and the methanol in the oil was found to be at a level comparable to gasoline dilution in a gasoline-fueled engine. The abnormally severe abrasive wear which occurred only at the intake cam lobe and rocker arm of cylinder 4 may have been influenced by the presence of the returned cylinder blowby gases. During testing, cylinder blowby gases were sampled and returned through the valve cover and onto the intake cam lobe and rocker arm of cylinder 4. At this site, water vapor condensation and other blowby gases may have strongly influenced the abnormal wear rate.

B. Inspection of Engines From a BETC Test Fleet

As part of the Bartlesville Energy Technology Center (BETC) alcohol fuels program, a low mileage accumulation fleet test was conducted in Bartlesville, OK. The test fleet consisted of eight vehicles from two different manufacturers. Six of these vehicles were operated on methanol-containing fuel, while two vehicles were fueled with unleaded gasoline (see Table 23). The

TABLE 23. BETC TEST FLEET

Vehicle ID	Manufacturer	Model	Engine Displacement, liters	Miles Accumulated	Fuel
181	Chevrolet	Chevette	1.6	6505	m1
182	Ford	Pinto	2.3	6500	m1
183	Chevrolet	Chevette	1.6	6502	m2
184	Ford	Pinto	2.3	6503	m2
185	Chevrolet	Chevette	1.6	6509	m3
186	Ford	Pinto	2.3	6500	m3
199	Ford	Pinto	2.3	6504	unleaded gasoline
200	Chevrolet	Chevette	1.6	6500	unleaded gasoline

m1 = anhydrous methanol
m2 = m1 with 10% (vol.) isopentane
m3 = m1 with 10% (vol.) isopentane + 0.32 % (wt) UKON50-HB-660

methanol-fueled vehicles were modified by closing and disabling the carburetor choke mechanism, thus enriching the fuel/air mixture by an undetermined amount. Two vehicles were operated on "neat" anhydrous methanol, while the other four methanol-fueled cars had isopentane added to the fuel as a cold-start and driveability aid. Also, two of the vehicles had a corrosion protection additive added to the fuel. All of the vehicles were lubricated with oil A (Table 1).

The methanol-fueled vehicles were operated during the period September 1978 to January 1980 and were driven 10 miles per day, 5 miles in the morning and 5 miles in the afternoon. The gasoline-fueled vehicles were operated using a similar driving cycle, but, unfortunately, during a different time period, from July 1979 to November 1980.

At the conclusion of the fleet test, AFLRL representatives were allowed to examine the engines from these vehicles. The engines were disassembled by the BETC personnel. Before-test dimensional measurements of the engines had not been made, and as a result, post-test measurements were not taken.

The engine deposits were rated using the forms and methods developed for the ASTM Sequence VD procedure, which also uses the Ford 2.3-liter engine. The procedure was modified somewhat for the 1.6-liter engine. These rating results are summarized in Table 24. The engines were all generally clean as would be expected from the low mileage accumulation. Engines 185 and 186 had a greater amount of sludge deposits, particularly in the lower part of the engine. This sludge deposit was unusual because of its distinctive green color. This deposit was probably related to the anticorrosion additive in the methanol fuel. This may also account for the reduced intake valve deposits in these two engines.

All engines had moderate varnish deposits which were generally similar, independent of the type of fuel. Engine 181 was an exception to this, however, with heavier varnish deposits on the rocker arm covers and the cylinder wall. This engine also had significant amounts of rust throughout the engine, whereas none of the other engines had any major areas of rusting.

TABLE 24. BETC TEST FLEET SLUDGE RATINGS

	Vehicle ID							
	181	182	183	184	185	186	199	200
Sludge Ratings (Merit)								
Rocker Arm Cover, Right	9.0	9.8	9.75	9.75	9.0	9.48	9.75	9.50
Rocker Arm Cover, Left	9.75	NA	9.75	NA	9.75	NA	NA	9.50
Front Seal Housing	9.75	9.95	9.75	10.0	9.10	3.15	9.67	10.0
Oil Pan	9.71	9.6	9.47	9.61	8.59	9.16	9.71	9.4
Valve Deck	9.75	9.75	9.50	10.0	9.75	9.75	9.75	9.75
Underside of Block	9.75	10.0	9.75	10.0	9.75	10.0	9.75	9.75
Oil Control Ring Clogging, Avg %	<1	<1	<1	<1	<1	<NR	<1	<1
Varnish Ratings (Merit)								
Piston Skirt, Avg	9.88	10.0	9.95	9.95	9.71	8.28	9.93	9.71
Rocker Arm Cover, Right	4.85	7.6	8.0	9.0	7.5	5.8	6.5	6.0
Rocker Arm Cover, Left	4.55	NA	8.0	NA	7.5	NA	NA	6.0
Cylinder Wall	5.59	10.0	9.75	10.0	10.0	9.17	10.0	10.0
Oil Pan	6.75	7.15	8.0	9.95	7.5	6.65	5.5	6.0
Intake Valve Deposits, Avg (Merit)	7.2	7.2	8.0	7.2	9.2	9.2	7.1	7.4

NA = Not applicable
NR = Not Rated

Since before-test measurements were not made on the engines, it was not possible to quantitatively assess the amount of engine wear. However, the piston rings from one piston were removed from each engine and examined optically. Since the piston rings had a tapered face, the width of the wear surface of the ring face was measured (see Figure 33 and Table 25). The width of this wear band was then used as an indicator of the piston ring wear. Because the two manufacturers used different ring designs, the two groups cannot be compared with each other. However, within each manufac-

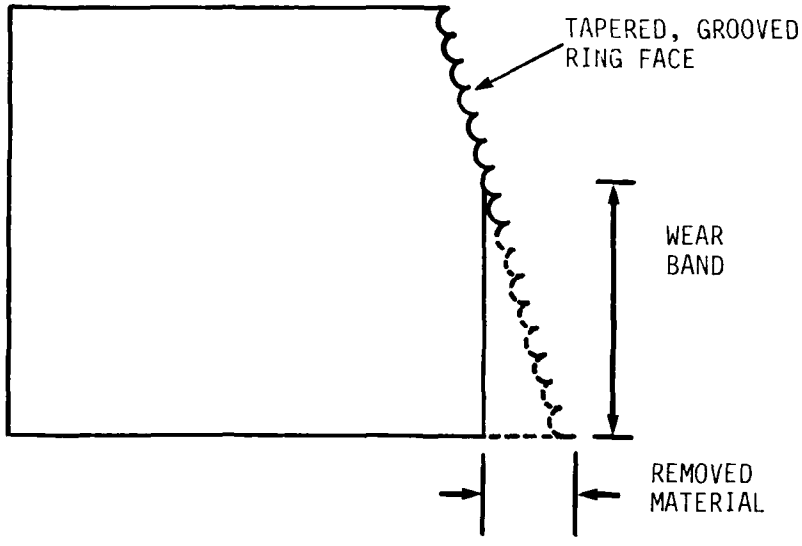

FIGURE 33. ILLUSTRATION OF COMPRESSION RING WEAR BAND

TABLE 25. WIDTH OF RING FACE WEAR SURFACE*

	Chevette				Pinto			
Engine	181	183	185	200	182	184	186	199
Cylinder No.	4	4	4	1	4	4	4	1
Wear band width	0.043	0.025	0.031	0.025	0.057	0.034	0.060	0.030
Averages		0.033		0.025		0.050		0.030

*Cast iron compression ring

turer's engine set, this method seems reasonable. From this data, it appears that, directionally, the use of methanol fuels increased the rate of piston ring wear. While it is tempting to draw other conclusions from these numbers, the small sample size would cast severe doubt on any observations. Photographs made of the ring faces at 50x and 250x magnification are shown in Figures 34 through 41.

VII. CONCLUSIONS

Initial results with the modified Sequence VD test in the 2.3-liter multicylinder engine confirmed the high wear rates observed in the CLR single-cylinder engine. However, the iron wear accumulation rates with varying lubricant formulations in the 2.3-liter engine does not agree with the rates obtained in the CLR single-cylinder engine. These engine tests show that the use of neat methanol as a fuel can result in large increases in engine wear and wear metal accumulation during low temperature operation. However, the use of anhydrous ethanol and alcohol/gasoline blends does not appear to increase engine wear over that of Phillips J unleaded gasoline. This testing also appears to indicate that neat alcohol fuels decrease the overall engine deposits relative to Phillips J unleaded gasoline. In addition, the alcohol-fueled engines appear to have more water in the used lubricant than do those fueled with Phillips J unleaded gasoline. The increased wear caused by methanol does not appear to be accompanied by major irreversible degradation of the lubricant.

From the steady-state tests, it appears that an increase in the concentration of the alcohol and water in the lubricant coincides with the increased wear rate but only when this accumulation is a byproduct of the combustion process. It appears that fuel distribution contributes to top cylinder bore wear. Also, the steady-state tests appear to indicate that the critical temperature for wear occurs when the oil temperature falls below 70°-80°C. Below this temperature, the TBN of the oil begins decreasing rapidly. The 20-hour steady-state test shows promise as a lubricant screening test when using alcohol fuels.

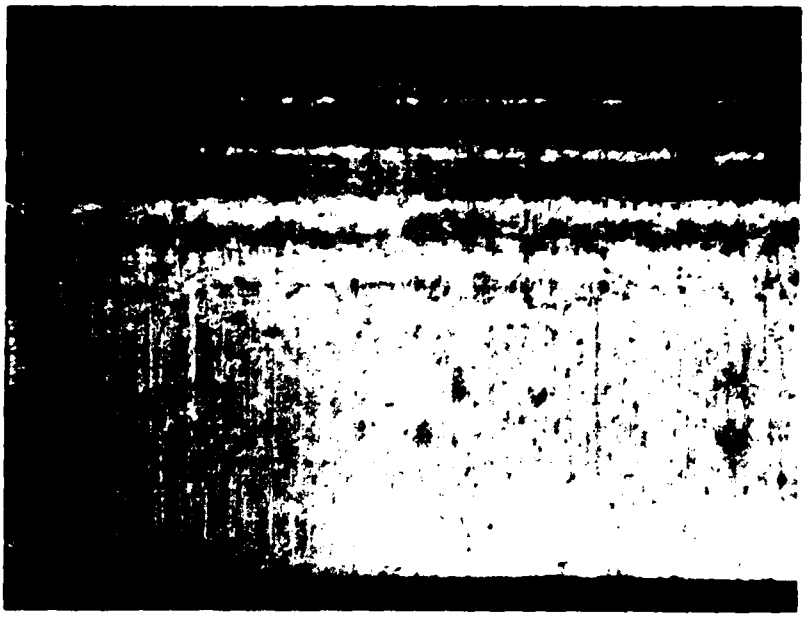

(a) 50X Magnification

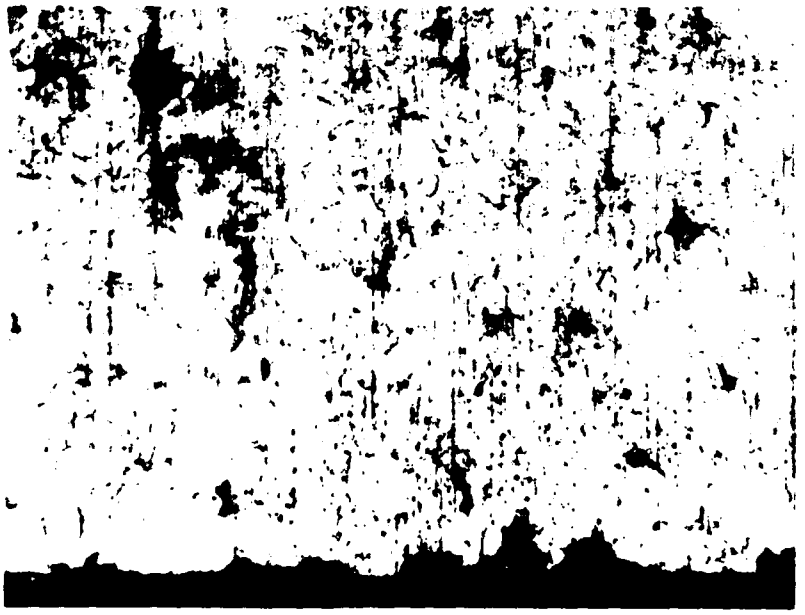

(b) 250X Magnification
Near Lower Edge

FIGURE 34. PISTON RING WEAR SURFACE--
VEHICLE NO. 181, CYLINDER 4

(a) 50X Magnification

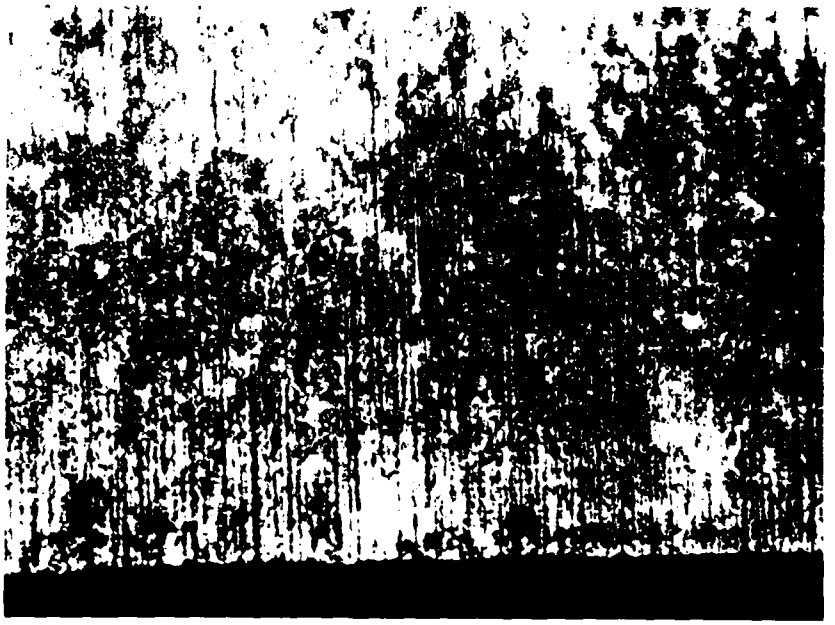

(b) 250X Magnification
Near Lower Edge

FIGURE 35. PISTON RING WEAR SURFACE--
VEHICLE NO. 182, CYLINDER 4

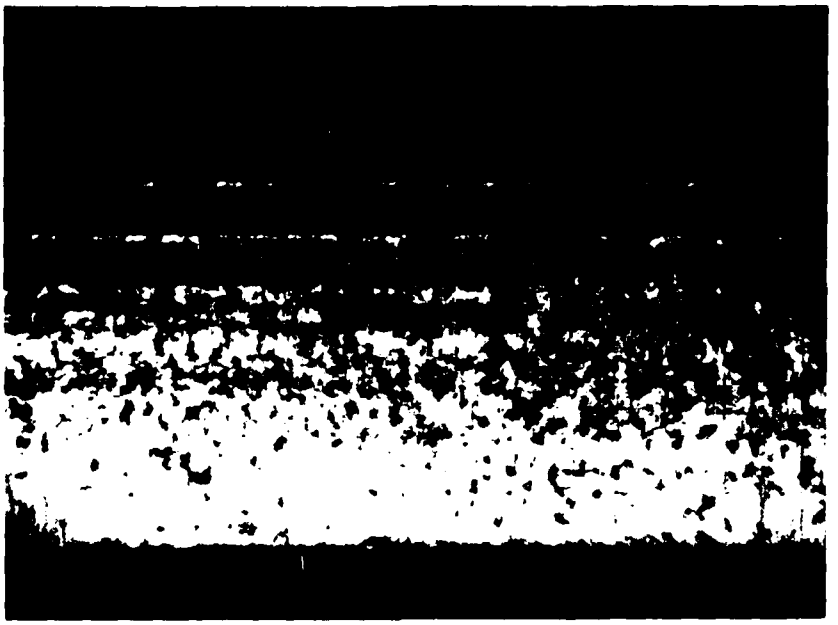

(a) 50X Magnification

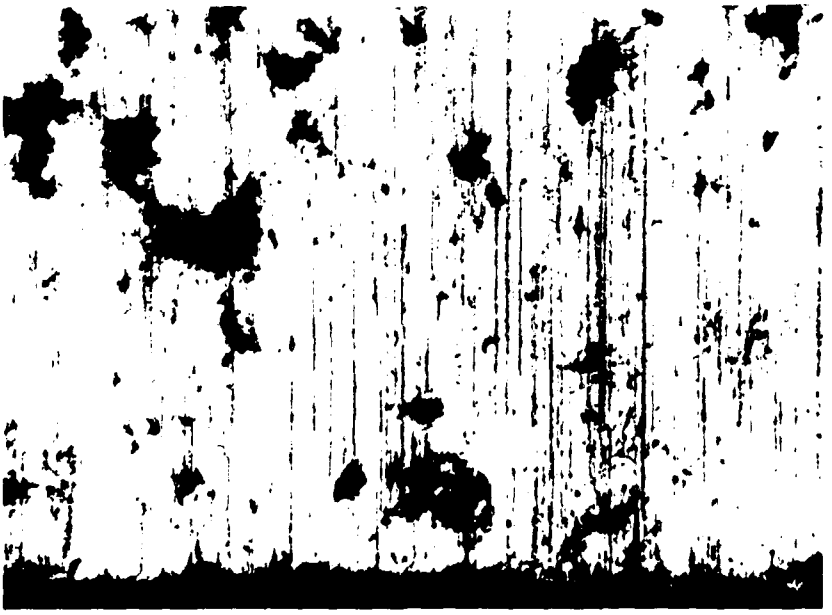

(b) 250X Magnification
Near Lower Edge

FIGURE 36. PISTON RING WEAR SURFACE--
VEHICLE NO. 183, CYLINDER 4

(a) 50X Magnification

(b) 250X Magnification
Near Lower Edge

FIGURE 37. PISTON RING WEAR SURFACE--
VEHICLE NO. 184, CYLINDER 4

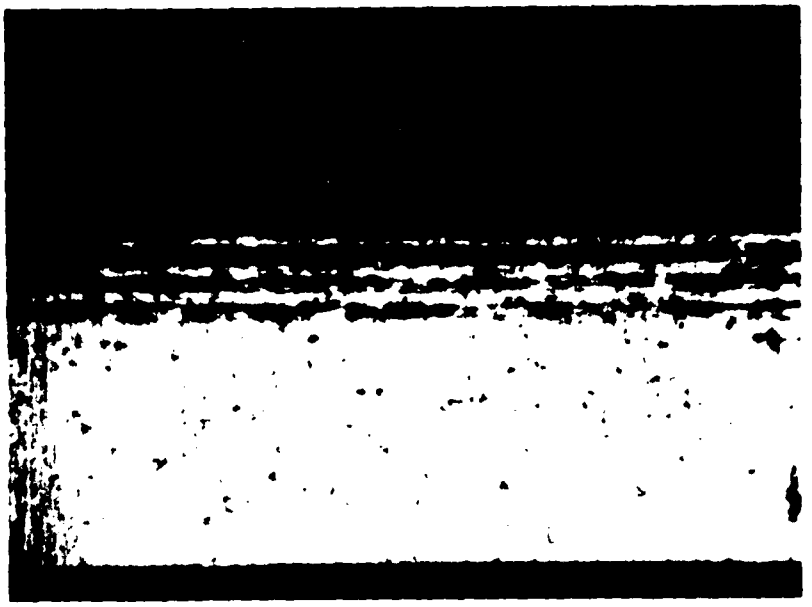

(a) 50X Magnification

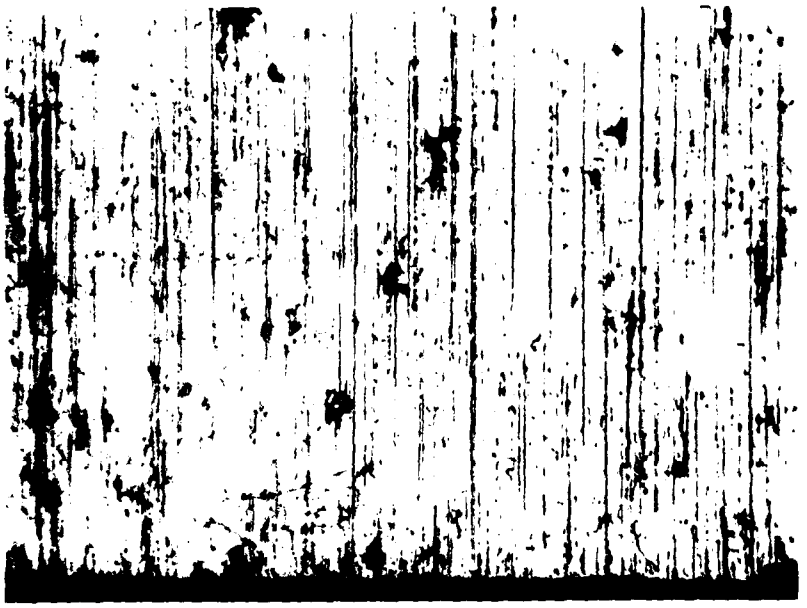

(b) 250X Magnification
Near Lower Edge

FIGURE 38. PISTON RING WEAR SURFACE-
VEHICLE NO. 185, CYLINDER 4

(a) 50X Magnification

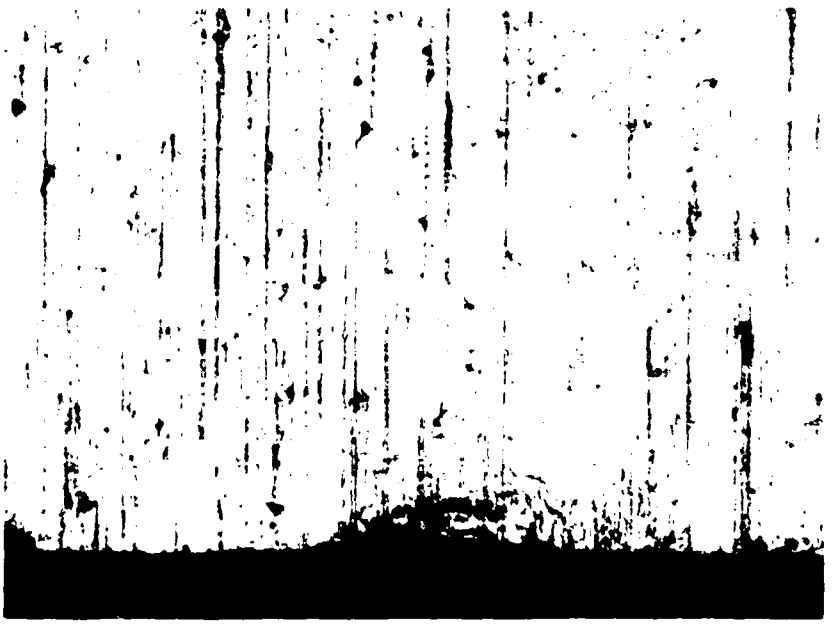

(b) 250X Magnification
Near Lower Edge

FIGURE 39. PISTON RING WEAR SURFACE--
VEHICLE NO. 186, CYLINDER 4

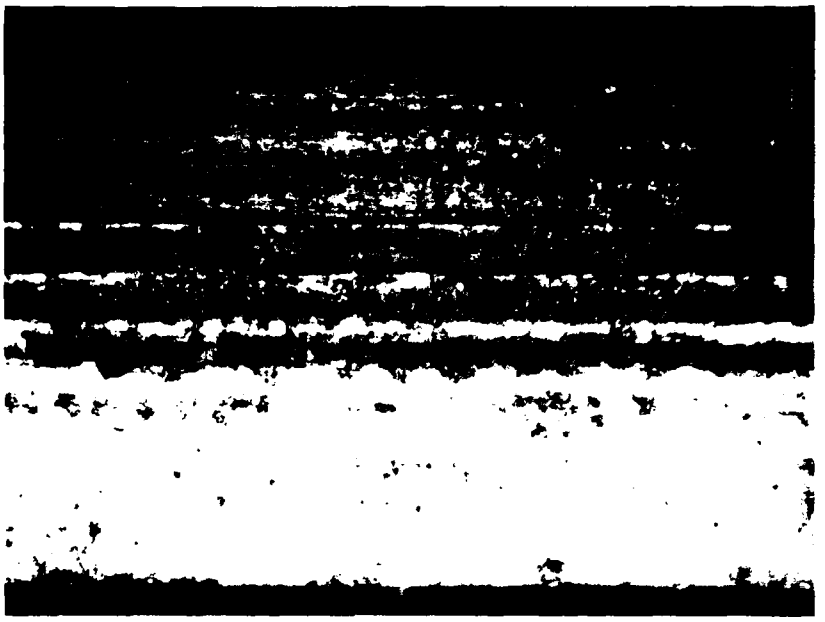

(a) 50X Magnification

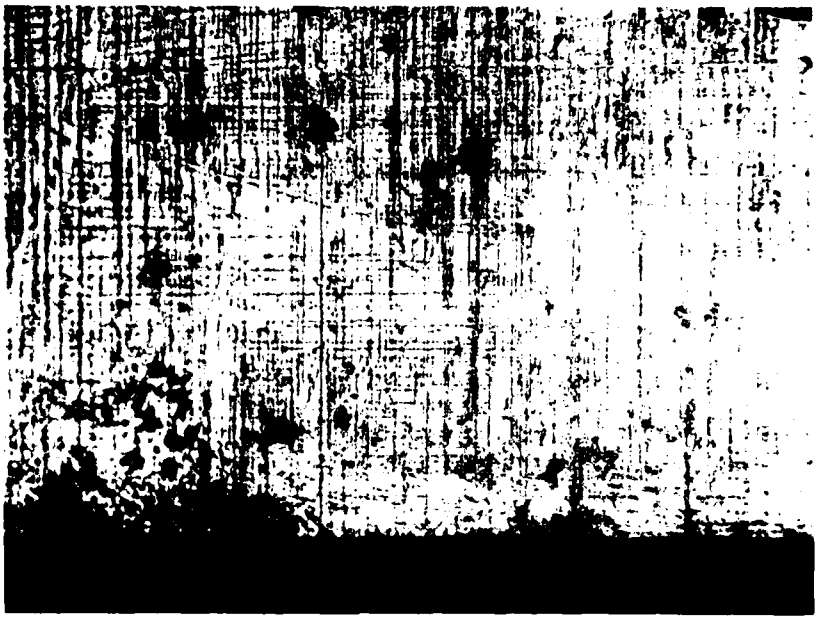

(b) 250X Magnification
Near Lower Edge

FIGURE 40. PISTON RING WEAR SURFACE--
VEHICLE NO. 199, CYLINDER 1

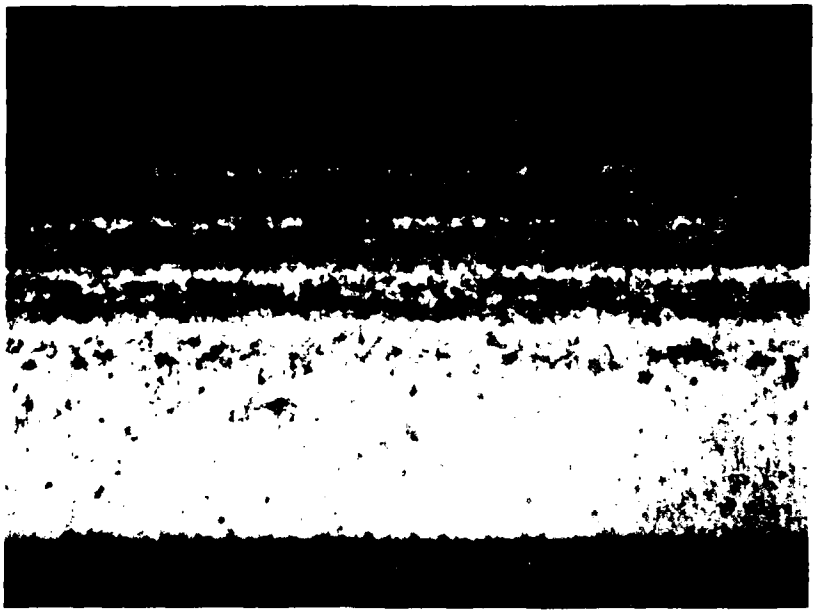

(a) 50X Magnification

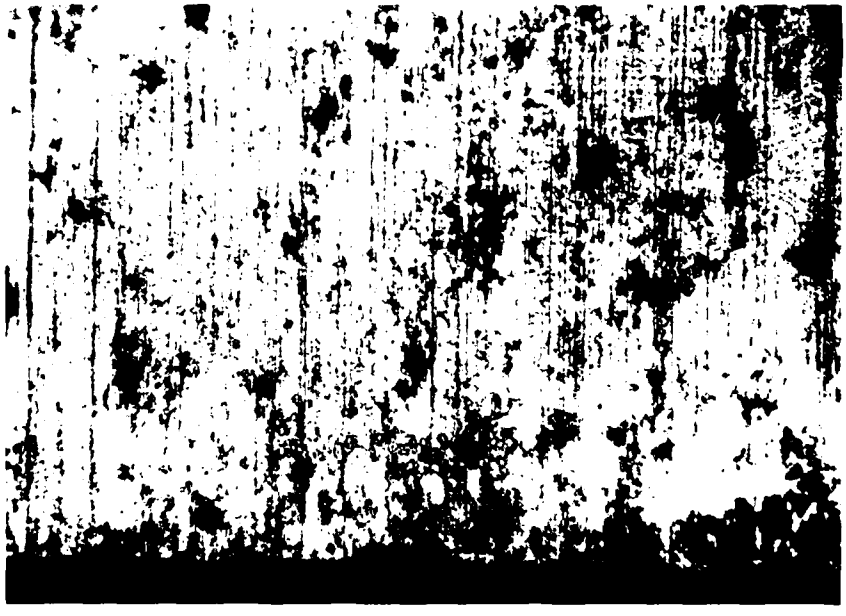

(b) 250X Magnification
Near Lower Edge

FIGURE 41. PISTON RING WEAR SURFACE--
VEHICLE NO. 200, CYLINDER 1

A temperature-dependent mechanism is proposed which assumes that formic acid is formed from methanol combustion products in the quench layer adjacent to the relatively cool cylinder wall. The formic acid tends to react with exposed iron at the surface, making iron formate. When the cylinder wall temperature is high enough, the formic acid decomposes before iron formate can form.

Lubricant A appears to be most effective in controlling methanol-related engine wear, but still not to acceptable levels. Lubricant B, which contained a magnesium-based detergent additive, had the highest top cylinder bore and top ring wear of the eleven lubricants evaluated.

The evaluations conducted with these fully formulated lubricants have indicated that the synthetic oils examined have not been beneficial in reducing the low-temperature wear related to the use of methanol fuel.

By varying the additive composition of lubricant A, it was determined that magnesium-based detergent additives were less effective in controlling methanol-related engine wear than were calcium-based additives. Lubricant dispersant chemistry also appeared to influence methanol-related engine wear. Lubricant A, which contained a phosphorus-type dispersant, had better performance with methanol fuel than did similar lubricants formulated with two different nitrogen-type dispersants. A significant increase in valve train area wear was observed with an aryl zinc-type additive when compared to the alkyl zinc-type additive. Therefore, it appears that valve train area wear resulting from aryl zinc occurs with both neat methanol fuel and unleaded gasoline. Finally, simply increasing the TBN of lubricant A by increasing its calcium content was not effective in controlling methanol-related engine wear.

Based upon the results of the engine and spinning disc experiments, it appears that the cause of the excessive cylinder bore and ring wear, encountered in methanol-fueled spark ignition engines, is due to a direct chemical attack by formic acid. The results of the spinning disc tests, in which the surface materials were varied, indicate that the surface does play

a role in the formation of formic acid. Several theories have been discussed concerning the fundamental mechanisms involved in the formation and decomposition of formic acid. The processes involved in the accumulation of formic acid on the cylinder wall have also been discussed.

VIII. REFERENCES

1. A.R. Ogston, "Alcohol Motor Fuels," Journal of the Institute of Petroleum Technologists, August 1937.

2. G. Egloff and J.C. Morrell, "Alcohol-Gasoline as Motor Fuel," Industrial and Engineering Chemistry, 28:9, p. 1080, September 1936.

3. P. Eyzat, "Utilization of Melthanol in Engine with Controlled Ignition," Revue de l'Association Francaise des Technicians du Petrole, pp. 31-35, 1974.

4. "Alcohols--A Technical Assessment of Their Application as Fuels," American Petroleum Institute Publication 4261, July 1976.

5. E. Miller, Continental Oil Company, personal communication, 1977.

6. D.L. Hagen, "Methanol as a Fuel: A Review with Bibliography," SAE Paper 770792, September 1977.

7. G.D. Ebersole and F.S. Manning, "Engine Performance and Exhaust Emissions: Methanol Versus Isooctane," SAE Paper 720692, August 1971.

8. R.D. Fleming and T.W. Chamberlain, "Methanol as Automotive Fuel Part I - Straight Methanol," SAE Paper 750121, February 1975.

9. N.D. Brinkman, "Effect of Compression Ratio on Exhaust Emissions and Performance of a Methanol-Fueled Single-Cylinder Engine," SAE Paper 770791, September 1977.

10. J.C. Ingamells and R.H. Lindquist, "Methanol as a Motor Fuel or a Gasoline Blending Component," SAE Paper 750123, February 1975.

11. E.C. Owens, H.W. Marbach, Jr., E.A. Frame, and T.W. Ryan III, "Effects of Alcohol Fuels on Engine Wear," U.S. Army Fuels and Lubricants Research Laboratory, Interim Report AFLRL No. 133, Government Accession No. AD A107136, October 1980.

12. E.C. Owens, "Methanol-Fuel Effects on Spark Ignition Lubrication and Wear," International Symposium on Alcohol Fuel-Technology-Methanol and Ethanol, Wolfsburg, Germany, November 1977.

13. E.C. Owens, H.W. Marbach, Jr., E.A. Frame, and T.W. Ryan III, "Effects of Alcohol Fuels on Engine Wear," SAE preprint 800857, June 1980.

14. E.C. Owens, H.W. Marbach, Jr., E.A. Frame, and T.W. Ryan III, "B-66 Lubrication Requirements for Alcohol-Fueled Spark Ignition Engines," IV International Symposium on Alcohol Fuels Technology, Guaruja, Brazil, October 1980.

15. D.C. Bardy, T.M. Franklin, and C.E. Roberts, "A 2.3-L Engine Deposit and Wear Test--An ASTM Task Force Progress Report," SAE preprint 780260, February 1978.

16. J.D. Tosh and J.A. Russell, "Evaluation of Environmental and Economic Benefits Through Use of Synthetic Motor Oils," U.S. Army Fuels and Lubricants Research Laboratory, Final Report AFLRL No. 91, Government Accession No. AD A045277, September 1977.

17. E.A. Frame, "Lubricants For Combating Effects of High-Sulfur Fuels," U.S. Army Fuels and Lubricants Research Laboratory, Interim Report AFLRL No. 127, Government Accession No. AD A094900, July 1980.

18. Monthly Progress Report, August 1980 and 1981 on Basic and Applied Fuels and Lubricants Research, U.S. Army Fuels and Lubricants Research Laboratory, Contract No. DAAK70-80-C-0001.

19. P. Mars, J.J.F. Schalter, and P. Zwietering, "The Catalytic Decomposition of Formic Acid," Advances in Catalysis, 14, p. 35, 1963.

20. R.D. Quillian, Jr., et al., "Cleaner Crankcases With Blowby Diversion," SAE Paper 8018, January 1964.

21. P.G. Blake and C. Hinshelwood, "The Homogeneous Decomposition Reactions of Gaseous Formic Acid," Proc. Ray. Soc. A255, p. 444, 1960.

22. D. Aronowitz, D.W. Naegeli, and I. Glassman, "Kinetics of the Pyrolysis of Methanol," J. Phy. Chem., 81, p. 2555, 1977.

23. D. Aronowitz, R.J. Santoro, F.L. Dryer, and I. Glassman, "Kinetics of the Oxidation of Methanol: Experimental Results--Semi-Global Modeling and Mechanistic Concepts," The 17th Symposium (International) on Combustion, Leads, England, 1978.

24. H.W. Marbach, Jr., E.A. Frame, E.C. Owens, and D.W. Naegeli, "The Effects of Alcohol Fuels and Fully Formulated Lubricants on Engine Wear," SAE Paper 811199, October 1981.

25. T.W. Ryan III, D.W. Naegeli, E.C. Owens, H.W. Marbach, Jr., and J.G. Barbee, "The Mechanisms Leading to Increased Cylinder Bore and Ring Wear in Methanol-Fueled SI Engines," SAE Paper 811200, October 1981.

AD-A110 021 SOUTHWEST RESEARCH INST SAN ANTONIO TX ARMY FUELS AN--ETC F/G 21/7
EVALUATION OF THE EFFECTS OF ALCOHOL FUELS ON SPARK IGNITION EN--ETC(U)
DEC 81 H W MARBACH, E C OWENS, T W RYAN DAAK70-79-C-0175
UNCLASSIFIED AFLRL-150 NL

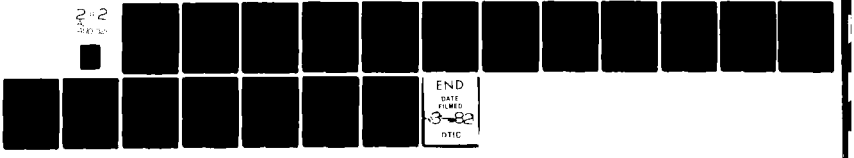

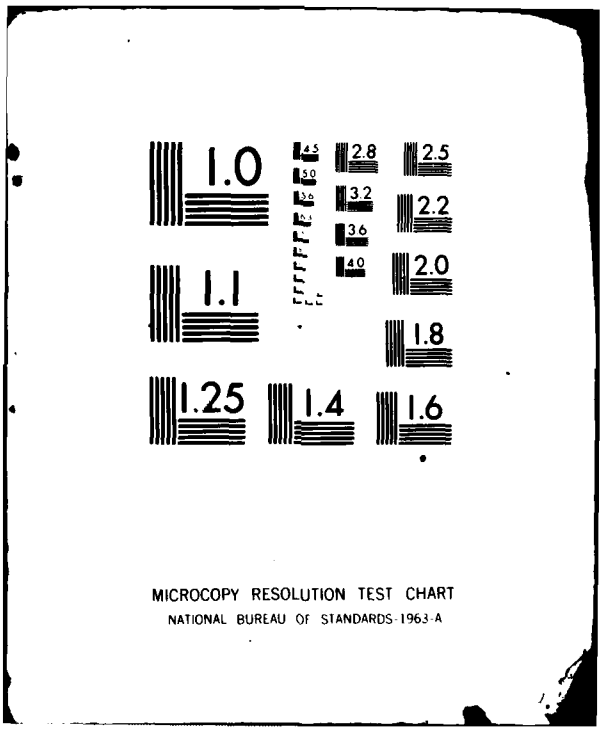
1.0
1.1
1.25
1.4
1.6
1.8
2.0
2.2
2.5
2.8
3.2
3.6
4.0
MICROCOPY RESOLUTION TEST CHART
NATIONAL BUREAU OF STANDARDS-1963-A

APPENDIX A

SEQUENCE VD TEST

OPERATING CONDITIONS

Based on Tentative Seq. V-D Test Procedure (Nov. 30, 1978)
and Applicable PV-1 Task Force Meeting Minutes

CONDITION		STAGES I	STAGES II	STAGES II
Time, min		120	75	45
Speed, rpm		2500 ± 25	2500 ± 25	750 ± 25
Load, bhp		33.5 ± 0.5	33.5 ± 0.5	1.0 ± 0.5
Oil	Cooler into engine, °F	175 ± 2	187 ± 2	120 ± 2
	Pump Gallery, psi	55 min	55 min	R(a)
	Cooling, min			10-15
Water	Jacket Output, °F	135 ± 2	155 ± 2	120 ± 2
	Flow, gpm	15.0 ± 0.5	15.0 ± 0.5	
Carb. Air	Temperature, °F	80 ± 2	80 ± 2	85 ± 5
	Humidity, grains/lb	80 ± 5	80 ± 5	80 ± 5
	Pressure, in. H_2O	0.2 ± 0.1	0.2 ± 0.1	0.2 ± 0.1
Blowby Rate, cfm		1.8 ± 0.2(b)		
Crankcase Pressure, in. H_2O		R(c)	R	R
Ignition Timing, °BTC		46	46	10
Fuel Pressure, psi		4-6	4-6	4-6
Exhaust Back Pressure, in. H_2O		8.0 - 12.0	8.0 - 12.0	0 - 3.0
EGR		ON (d)	ON	OFF
Exhaust Gas Analysis	O_2%	1.0 ± 0.2	1.0 ± 0.2	0.7 max
	CO%	1.0 max	1.0 max	6.5 ± 0.5
	NO/NO_x, ppm		R (e)	

Note: Engine operation should be maintained as close as possible to the mid-range values shown above.

(a) R = Record, not a controlled parameter.
(b) Measure at midpoint of Stage I.
(c) Normally should be 0.2 to 1.2 positive.
(d) Automatic operation; function of EGR valve diaphragm must be confirmed.
(e) Measurement once each 24 hours is required.

APPENDIX B

SUMMARY OF RESULTS

OF NEW LUBRICANT PROPERTIES

APPENDIX B. NEW LUBRICANT PROPERTIES

Oil Code	ASTM Test Method	A	B	C	D	E	F	G	H	I	J	K
40°C, cSt	D 445	68.9	65.4	106.0	26.3	71.8	97.0	56.0	30.1	96.1	125.9	77.4
100°C, cSt	D 445	11.7	10.3	11.8	5.9	11.8	13.9	10.0	5.9	14.4	14.7	12.2
Viscosity Index	D 2270	165	144	99	179	160	146	166	142	155	118	155
Total Acid No., mg KOH/g	D 664	2.5	2.3	2.0	0.2	2.4	3.3	3.0	2.3	2.5	3.1	0.16
Total Base No., mg KOH/g	D 664	9.7	5.9	9.4	7.6	8.0	6.8	6.3	5.0	3.6	7.4	0.12
Flash Point, °C	D 92	208	218	246	244	215	209	224	232	198	230	221
Sulfated Ash, wt%	D 874	1.37	0.95	1.41	1.45	1.41	0.99	1.05	1.07	0.93	1.07	1.08
Elements, wt%												
Ba	XRF	Nil	Nil	Nil	0.84	Nil	Nil	Nil	0.24	Nil	Nil	Nil
Ca	XRF	0.37	Nil	0.35	Nil	0.37	0.26	0.24	0.03	0.17	0.20	0.28
Mg	AA	Nil	0.11	Nil	Nil	Nil	Nil	Nil	0.09	Nil	Nil	Nil
Zn	XRF	0.14	0.19	0.13	Nil	0.17	0.17	0.14	0.16	0.12	0.16	0.10
P	XRF	0.17	0.15	0.08	0.01	0.17	0.13	0.13	0.13	0.09	0.11	0.11
S	XRF	0.47	0.40	0.23	0.05	0.46	0.37	0.33	0.42	0.45	0.94	0.47
N	*	0.037	0.070	0.008	0.099	0.037	0.150	0.140	0.050	0.027	0.070	0.032

AA = Atomic Absorption Method
XRF = X-Ray Fluorescence Method
* = Chemiluminescent Method

APPENDIX C

SUMMARY OF RESULTS

OF ENGINE MEASUREMENTS AND

USED LUBRICANT PROPERTIES

APPENDIX C. SUMMARY OF RESULTS OF ENGINE MEASUREMENTS AND USED LUBRICANT PROPERTIES

Lubricant Code	A	A	B	C	D	E	F	G	H	I	J	K
Test No.	PV1-7,12, 33	PV1-5,15, 20	PV1-2	PV1-9	PV1-11	PV1-13	PV1-23	PV1-24	PV1-25	PV1-31	PV1-38	PV1-30
Test Hours	192	192	152	192	192	120	192	192	192	192	192	192
Fuel	Methanol	Phillips J	Methanol	Methanol	Methanol	Methanol	Methanol	Methanol	Methanol	Methanol	Methanol	Methanol
Wear Measurements												
Top Bore Wear Avg, mm	0.0660	0.0051	0.1422	0.0660	0.0914	0.0889	0.0457	0.0787	0.0076	0.0965	0.0305	
Mid Bore Wear Avg, mm	0.0025	0.0025	0.0203	0.0025	0.0000	0.0076	0.0000	0.0000	0.0025	0.0178	0.0025	
Top Ring End Gap Loss Avg, mm	0.178	0.025	0.355	0.152	0.127	0.203	0.203	0.330	0.356	0.305	0.178	
2nd Ring End Gap Loss Avg, mm	0.102	0.076	0.152	0.127	0.127	0.127	0.152	0.152	0.152	0.076	0.152	
Rod Bearing Loss Avg, g	0.0341	0.0327	0.0221	0.0195	0.0410	0.0127	0.0945	0.0476	0.0521	0.0203	0.0191	0.0308
Cam Follower Loss Avg, g	0.0559	0.0005	0.0555	0.3036	0.5033	0.2676	0.2848	0.2736	0.2052	0.1242	0.1276	0.0623
Cam Lobe Wear Avg, mm	0.0635	0.0102	0.0051	0.1727	0.1727	0.1753	0.1422	0.1295	0.1041	0.0991	0.1016	
Exhaust Valve Guide Wear, mm	0.1041	0.0356	0.0889	0.0000	0.1219	0.0178	0.1346	0.0686	0.1448	0.0610	0.0940	
Intake Valve Guide Wear, mm	0.0152	0.0127	0.0305	0.0279	0.0102	0.0051	0.0356	0.0025	0.0279	0.0330	0.0305	
Deposition Rating												
Sludge Rating Avg	9.74	9.80	9.90	9.43	9.69	9.75	9.72	9.70	9.70	9.60	9.60	9.48
Varnish Rating Avg	9.59	8.63	9.94	9.82	9.32	9.84	8.96	9.61	8.94	8.53	9.98	9.85
Piston Varnish Rating Avg	9.90	7.91	9.90	9.10	9.12	9.58	0.92	9.48	9.90	8.82	9.97	9.86
Intake Valve Deposit Rating	8.61	6.42	9.30	9.00	8.15	8.62	8.32	8.62	9.65	8.58	8.61	8.95
Used Oil Properties												
Viscosity at 40°C, cSt	66.3	56.4	60.7	122.6	65.4	68.0	112.3	51.5	31.5	72.1	125.1	69.2
Viscosity at 100°C, cSt	10.4	9.4	9.4	13.0	10.0	10.3	14.3	9.0	6.0	10.8	13.7	10.4
Viscosity Index	145	149	135	99	138	137	130	155	137	139	106	136
TAN	4.41	4.07	7.41	4.00	4.05	3.65	5.6	4.1	6.8	0.25	4.79	4.10
TBN (D 664)	1.73	2.26	0.21	2.94	1.62	3.59	1.1	0.9	0.4	2.11	0.0	1.09
Flash Point, °C	190	163	---	228	210	202	210	198	180	200	223	188
Pentane Insols Meth.	0.28	0.53	1.98	1.79	0.09	0.34	0.21	0.27	1.78	0.31	1.60	0.41
Toluene Insols Meth.	0.16	0.22	1.33	1.58	0.07	0.27	0.19	0.24	1.46	0.34	1.38	0.34
Percent Water	0.41	0.22	0.20	0.42	0.29	0.50	0.13	0.37	0.50	0.22	0.10	0.41
EOT Wear Metals, ppm*												
Chrome	8	5	17	8	12	11	17	16	24	11	7	
Copper	26	14	17	14	10	17	64	37	57	46	39	
Iron	806	102	1710	1400	1850	1590	1827	1415	1795	1440	1580	
Magnesium**	Nil	Nil	Nil	Nil	Nil	Nil	36	25	1044	171	17	
Silicon	22	Nil	Nil	Nil	Nil	48	55	21	60	48	20	
Tin	Nil	Nil	Nil	40	Nil	37	46	22	38	40	20	
Lead	69	53	110	70	108	50	322	135	210	158	49	
Oil Consumption, kg	1.9686	1.3835	1.6874	1.9323	4.4996	1.5604	1.5740	2.5492		2.3859	1.7055	6.23

Notes: * By Atomic Absorption.
** Magnesium not determined until test No. 23.

APPENDIX D

SUMMARY OF TESTS PERFORMED WITH THE 2.3-LITER ENGINE

APPENDIX D

Test No. PVI-	Lubricant Code	AFLRL Lube Code	Fuel	Test Procedure
1	A	8932	Methanol	Mod. V-D
2	B	7338	Methanol	Mod. V-D
3	FREO-200-3	LO-1351	Phillips-J	Mod. V-D
4	A	8932	Blend	Mod. V-D
5	A	8932	Phillips-J	Mod. V-D
6	A	8932	Blend	Mod. V-D
7	A	8932	Methanol	Mod. V-D
8	C	7326	Methanol	D
9	C	7326	Methanol	Mod. V-D
10	A	8932	Ethanol	Mod. V-D
11	D	8925	Methanol	Mod. V-D
12	A	8932	Methanol	Mod. V-D
13	E	9092	Methanol	Mod. V-D
14	A	8932	Blend	Mod. V-D
15	A	8932	Phillips-J	Mod. V-D
16	A1	9288	Bad Methanol	D
17	A	8932	Various	20-Hr. S-S
18	A2	9289	Bad Methanol	D
19	A	8932	Bad Methanol	D
20	A	8932	Phillips-J	Mod. V-D
21	A2	9475	Methanol	N.C.
22	A5	9292	Methanol	N.C.
23	F	9249	Methanol	Mod. V-D
24	G	8924	Methanol	Mod. V-D
25	H	9560	Methanol	Mod. V-D
26	A6	9836	Methanol	Mod. V-D
27	A	8932	Various	20-hr. S-S
28	A7	9837	Methanol	Mod. V-D
29	A1	9288	Methanol	Mod. V-D
30	K	10874	Methanol	Mod. V-D
31	I	10107	Methanol	Mod. V-D
32	A1	9440	Methanol	Mod. V-D
33	A	8932	Methanol	Mod. V-D
34	A1	10122	Methanol	Mod. V-D
35	A8	10120	Methanol	Mod. V-D
36	A9	10121	Methanol	Mod. V-D
37	A3	9290	Methanol	Mod. V-D
38	J	10320	Methanol	Mod. V-D
39	A	8932	Various	20-Hr. S-S
40	A4	9291	Methanol	Mod. V-D
41	A10	10461	Methanol	Mod. V-D
42	A9	10459	Methanol	Mod. V-D
43	A11	10460	Methanol	Mod. V-D
44	Various	Various	Methanol	20-Hr. S-S

D = Discarded, not completed; stopped before 48 hours
N.C. = 192 hrs. not completed

APPENDIX E

SUMMARY OF RESULTS

OF NEW LUBRICANT PROPERTIES

APPENDIX E. NEW LUBRICANT PROPERTIES

Oil Code	ASTM Test Method	A	Batch 1 A1	Batch 2 A1	Batch 3 A1	A2	A3	A4	A5
40°C, cSt	D 445	68.9	63.4	65.8	58.2	66.1	77.8	68.9	66.7
100°C, cSt	D 445	11.7	11.2	11.3	10.4	11.5	11.9	10.6	10.8
Viscosity Index	D 2270	165	166	165	170	170	148	141	167
Total Acid No., mg KOH/g	D 664	2.47	2.03	2.28	2.55	2.58	1.98	2.08	2.03
Total Base No., mg KOH/g	D 664	9.73	8.93	9.75	9.89	7.25	9.53	9.11	9.71
Flash Point, °C	D 92	208	214	207	205	203	208	208	208
Sulfated Ash, wt%	D 874	1.37	1.40	1.43	1.44	1.04	1.42	1.40	1.42
Elements, wt%									
Ba, XRF		Nil	Nil	Nil	Nil	Nil	Nil	Nil	Nil
Ca, XRF		0.37	0.37	0.37	0.38	Nil	0.37	0.40	0.37
Mg, AA		Nil	Nil	Nil	Nil	0.22	Nil	Nil	Nil
Zn, XRF		0.14	0.13	0.13	0.13	0.11	0.13	0.13	0.13
P, XRF		0.17	0.11	0.11	0.10	0.14	0.09	0.10	0.10
S, XRF		0.47	0.47	0.48	0.46	0.43	0.44	0.47	0.46
N, *		0.037	0.088	0.088	0.090	0.069	0.094	0.072	0.094

AA = Atomic Absorption Method
XRF = X-Ray Fluorescence Method
* = Chemiluminescent Method

APPENDIX E. NEW LUBRICANT PROPERTIES

Oil Code	ASTM Test Method	A6	A7	A8	Batch 1 A9	Batch 2 A9	A10	A11
40°C, cSt	D 445	64.7	63.8	53.6	62.9	67.3	88.3	72.1
100°C, cSt	D 445	11.1	11.1	9.8	10.9	11.5	10.3	11.1
Viscosity Index	D 2270	166	167	170	167	166	97	146
Total Acid No., mg KOH/g	D 664	2.52	2.47	2.39	2.61	1.95	2.30	2.26
Total Base No., mg KOH/g	D 664	7.54	14.57	7.48	8.22	7.20	9.31	8.97
Flash Point, °C	D 92	206	210	209	199	217	234	214
Sulfated Ash, wt%	D 874	1.07	1.90	1.40	1.41	1.39	1.35	1.34
Elements, wt%								
Ba, XRF		Nil	Nil	Nil	NIl	Nil	Nil	Nil
Ca, XRF		Nil	0.54	0.38	0.38	0.37	0.36	0.37
Mg, AA		0.18	Nil	Nil	Nil	Nil	Nil	Nil
Zn, XRF		0.11	0.12	0.13	0.13	0.12	0.12	0.11
P, XRF		0.15	0.15	0.11	0.11	0.08	0.14	0.14
S, XRF		0.52	0.50	0.38	0.42	0.47	0.67	0.51
N, *		0.030	0.031	0.034	0.090	0.064	0.025	0.022

AA = Atomic Absorption Method
XRF = X-Ray Fluorescence Method
* = Chemiluminescent Method

APPENDIX F

SUMMARY OF RESULTS

OF ENGINE MEASUREMENTS AND

USED LUBRICANT PROPERTIES

APPENDIX F. EXPERIMENTAL ADDITIVE PACKAGES IN CONVENTIONAL LUBRICANTS

Lubricant Code	A	A-2	A-5	A-6	A-7	A-1	A-1	A-1	A-8	A-9	A-3	A-4	A-10	A-9	A-11
Test No. PVl-	7, 12, 33	21	22	26	28	29	32	34	35	36	37	40	41	42	43
Lubricant Code AL-	8932	9475	9292	9836	9837	9288	9440	10122	10120	10121	9200	9291	10461	10459	10460
Wear Measurements															
Top Bore Wear Avg, mm	0.0660	0.1194	0.1194	0.1118	0.0533	0.0152	0.0356	0.0610	0.0889	0.0356	0.0356	0.0533	0.0432	0.0457	0.0457
Mid Bore Wear Avg, mm	0.0025	0.0025	0.0000	0.0025	0.0127	0.0025	0.0025	0.0000	0.0025	0.0076	0.0000	0.0013	0.0051	0.0013	0.0025
Top Ring End Gap Loss Avg, mm	0.178	0.305	0.356	0.432	0.254	0.051	0.102	0.279	0.279	0.152	0.254	0.254	0.152	0.178	0.203
2nd Ring End Gap Loss Avg, mm	0.102	0.152	0.203	0.127	0.076	0.051	0.051	0.152	0.152	0.114	0.178	0.102	0.102	0.102	0.127
Rod Bearing Loss Avg, g	0.0341	0.0499	0.0598	0.0366	0.0152	0.0218	0.0148	0.0192	0.0413	0.0189	0.0204	0.0188	0.0153	0.0160	0.0104
Cam Follower Loss Avg, g	0.0559	0.0176	0.2360	0.0242	0.0967	0.0035	0.0309	0.0077	0.0801	0.0308	0.1923	0.0138	0.1610	0.2295	0.1469
Cam Lobe Wear Avg, mm	0.0635	0.0483	0.1092	0.4572	0.0254	0.0051	0.0330	0.0178	0.1118	0.0356	0.0864	0.0229	0.0914	0.0991	0.1321
Exhaust Valve Guide Wear, mm	*0.1041*	*0.0457*	*0.1245*	0.0279	0.1219	0.0381	0.2946	0.1473	0.0914	0.1168	0.1956	0.1194	0.1295	0.1168	0.1803
Intake Valve Guide Wear, mm	0.0152	0.0127	0.0457	0.0330	0.0178	0.0178	0.0127	0.0305	0.02794	0.0229	0.0330	0.0178	0.0229	0.0330	0.0279
Deposition Rating															
Sludge Rating Avg	9.74	9.22	9.70	9.72	9.71	9.61	9.65	9.73	9.51	9.70	9.66	9.73	9.57	9.72	9.69
Varnish Rating Avg	9.59	8.90	8.50	9.77	9.11	9.03	9.28	9.43	8.55	9.90	9.05	9.88	9.13	9.25	9.46
Piston Varnish Rating Avg	9.90	9.85	9.74	9.86	9.67	8.59	9.95	9.84	9.22	9.57	9.98	9.44	9.72	9.50	9.84
Intake Valve Deposit Rating	8.61	9.02	8.62	8.50	8.90	6.45	8.25	8.62	9.62	8.02	8.50	9.05	8.82	8.92	8.72
Used Oil Properties															
Viscosity @ 40°C, cSt	66.3	*	*	64.2	64.1	52.9	62.5	59.4	54.2	63.5	69.2	71.5	109.8	62.6	64.6
@ 100°C, cSt	10.4	*	*	9.7	10.2	9.7	9.6	9.4	8.5	9.8	10.2	10.4	11.9	9.4	9.5
Viscosity Index	145	*	*	134	147	170	135	141	132	138	132	131	97	131	128
TAN	4.41	*	*	7.71	4.32	4.72	5.22	5.00	3.76	3.86	4.24	4.13	4.05	3.94	4.21
TBN (D 664)	1.73	*	*	1.42	3.58	2.56	0.89	1.32	1.13	2.72	2.11	1.84	0.99	1.54	0.81
Flash Point, °C	190	*	*	206	200	155	222	209	204	206	205	216	236	205	211
Pentane Insols Meth.	0.28	*	*	2.56	0.20	3.93	0.89	0.41	1.96	0.59	0.10	0.52	0.72	1.24	0.15
Toluene Insols Meth.	0.16	*	*	1.65	0.14	1.68	0.68	0.29	1.70	0.49	0.10	0.42	0.59	0.88	0.12
Percent Water	0.41	*	*	0.90	0.38	0.16	0.24	0.26	0.28	0.22	0.20	0.20	0.20	0.30	0.25
Oil Consumption, lb	1.969	Nil	1.08	2.90	2.24	1.43	1.99	1.49	1.26	2.30	1.28	1.70	1.71	1.19	1.83
Wear Metals, ppm															
Chrome, AA	8	29	Nil	8	9	2	9	80	10	5	10	13	18	15	17
Copper, AA	26	28	59	27	24	9	25	84	37	16	29	19	20	44	25
Iron, XRF	806	1734	2242	1440	881	126	599	1413	1456	442	1580	585	1157		1258
Lead, AA	69	Nil	177	200	10	46	74	73	150	6	52	22	218	123	22
Magnesium, AA	Nil	Nil	Nil	8	Nil	Nil	10	12	18	8	27	12	15	26	Nil
Silicon, AA	22	Nil	Nil	38	Nil	Nil	28	42	38	Nil	Nil	Nil	<20	51	43
Tin, AA	Nil	Nil	Nil	25	90	9	Nil	35	Nil	Nil	Nil	Nil	<20	<20	Nil

* Sample discarded

DISTRIBUTION LIST

DEPARTMENT OF DEFENSE

DEFENSE DOCUMENTATION CTR
CAMERON STATION 12
ALEXANDRIA VA 22314

DEPT OF DEFENSE
ATTN: DASA(MRA&L)-ES(MR DYCKMAN) 1
WASHINGTON DC 20301

COMMANDER
DEFENSE LOGISTICS AGY
ATTN DLA-SME (MRS P MCLAIN) 1
CAMERON STATION
ALEXANDRIA VA 22314

COMMANDER
DEFENSE FUEL SUPPLY CTR
ATTN: DFSC-T 1
CAMERON STA
ALEXANDRIA VA 22314

COMMANDER
DEFENSE GENERAL SUPPLY CTR
ATTN: DGSC-SSA 1
RICHMOND VA 23297

DEPARTMENT OF THE ARMY

HQ, DEPT OF ARMY
ATTN: DALO-TSE 1
DAMA-CSS-P (DR BRYANT) 1
DAMA-ARZ (DR CHURCH) 1
DAMA-SMZ 1
WASHINGTON DC 20310

CDR
U.S. ARMY MOBILITY EQUIPMENT
R&D COMMAND
Attn: DRDME-GL 10
FORT BELVOIR VA 22060

CDR
US ARMY MATERIAL DEVEL&READINESS
COMMAND
ATTN: DRCLDC (MR BENDER) 1
DRCMM-SP (LTC O'CONNER) 1
DRCQA-E (MR SMART) 1
DRCDE-DG (MR MCGOWAN) 1
DRCIS-S (MR SPRAGUE) 1
DRCIS-C (LTC CROW) 1
5001 EISENHOWER AVE
ALEXANDRIA VA 22333

CDR
US ARMY TANK-AUTOMOTIVE CMD
ATTN DRSDA-NW (TWVMO) 1
DRSTA-RG (MR HAMPARIAN) 1
DRSTA-NS (DR PETRICK) 1
DRSTA-J 1
DRSTA-G (COL MILLS) 1
DRSTA-M 1
DRSTA-GBP (MR MCCARTNEY) 1
WARREN MI 48090

DIRECTOR
US ARMY MATERIAL SYSTEMS
ANALYSIS AGENCY
ATTN DRXSY-CM 1
DRXSY-S 1
DRXSY-L 1
ABERDEEN PROVING GROUND MD 21005

CDR
US ARMY APPLIED TECH LAB
ATTN DAVDL-ATL-ATP (MR MORROW) 1
DAVDL-ATL 1
FORT EUSTIS VA 23604

HQ, 172D INFANTRY BRIGADE (ALASKA)
ATTN AFZT-DI-L 1
AFZT-DI-M 1
DIRECTORATE OF INDUSTRIAL
OPERATIONS
FT RICHARDSON AK 99505

CDR
US ARMY GENERAL MATERIAL &
PETROLEUM ACTIVITY
ATTN STSGP-FT (MS GEORGE) 1
STSGP-PE 1
STSGP (COL HILL) 1
NEW CUMBERLAND ARMY DEPOT
NEW CUMBERLAND PA 17070

CDR
US ARMY ARRCOM, LOG ENGR DIR
ATTN DRSAT-LEM (MR MENKE) 1
ROCK ISLAND ARSENAL IL 61299

CDR
US ARMY COLD REGION TEST CENTER
ATTN STECR-TA (MR HASLEM) 1
APO SEATTLE 98733

CDR
US ARMY RES & STDZN GROUP
(EUROPE)
ATTN DRXSN-E-RA 1
BOX 65
FPO NEW YORK 09510

HQ, US ARMY AVIATION R&D CMD
ATTN DRDAV-D (MR CRAWFORD) 1
DRDAV-N (MR BORGMAN) 1
DRDAV-E (MR LONG) 1
P O BOX 209
ST LOUIS MO 63166

CDR
US ARMY FORCES COMMAND
ATTN AFLG-REG (MR HAMMERSTROM) 1
AFLG-POP (MR COOK) 1
FORT MCPHERSON GA 30330

CDR
US ARMY ABERDEEN PROVING GROUND
ATTN STEAP-MT 1
STEAP-MT-U (MR DEAVER) 1
ABERDEEN PROVING GROUND MD 21005

CDR
US ARMY YUMA PROVING GROUND
ATTN STEYP-MT (MR DOEBBLER) 1
YUMA AR 85364

MICHIGAN ARMY MISSILE PLANT
OFC OF PROJ MGR, XM-1 TANK SYS
ATTN DRCPM-GCM-S 1
WARREN MI 48090

MICHIGAN ARMY MISSILE PLANT
PROG MGR, FIGHTING VEHICLE SYS
ATTN DRCPM-FVS-SE 1
WARREN MI 48090

PROJ MGR, M60 TANK DEVELOPMENT
ATTN DRCPM-M60-E 1
WARREN MI 48090

PROG MGR, M113/M113A1 FAMILY
OF VEHICLES
ATTN DRCPM-M113 1
WARREN MI 48090

PROJ MGR, MOBILE ELECTRIC POWER
ATTN DRCPM-MEP-TM 1
7500 BACKLICK ROAD
SPRINGFIELD VA 22150

OFC OF PROJ MGR, IMPROVED TOW
VEHICLE
US ARMY TANK-AUTOMOTIVE R&D CMD
ATTN DRCPM-ITV-T 1
WARREN MI 48090

CDR
US ARMY EUROPE & SEVENTH ARMY
ATTN AEAGC-FMD 1
APO NY 09403

PROJ MGR, PATRIOT PROJ OFC
ATTN DRCPM-MD-T-C 1
US ARMY DARCOM
REDSTONE ARSENAL AL 35809

CDR
THEATER ARMY MATERIAL MGMT
CENTER (200TH)
DIRECTORATE FOR PETROL MGMT
ATTN AEAGD-MM-PT-Q (MR PINZOLA) 1
ZWEIBRUCKEN
APO NY 09052

CDR
US ARMY RESEARCH OFC
ATTN DRXRO-EG 1
DRXRO-CB (DR GHIRARDELLI) 1
P O BOX 12211
RSCH TRIANGLE PARK NC 27709

DIR
US ARMY R&T LAB
ADVANCED SYSTEMS RSCH OFC
ATTN MR D WILSTED 1
AMES RSCH CTR
MOFFITT FIELD CA 94035

CDR
TOBYHANNA ARMY DEPOT
ATTN SDSTO-TP-S 1
TOBYHANNA PA 18466

DIR
US ARMY MATERIALS & MECHANICS
RSCH CTR
ATTN DRXMR-EM 1
WATERTOWN MA 02172

CDR
US ARMY DEPOT SYSTEMS CMD
ATTN DRSDS 1
CHAMBERSBURG PA 17201

CDR
US ARMY WATERVLIET ARSENAL
ATTN SARWY-RDD 1
WATERVLIET NY 12189

CDR
US ARMY LEA
ATTN DALO-LEP 1
NEW CUMBERLAND ARMY DEPOT
NEW CUMBERLAND PA 17070

CDR
US ARMY GENERAL MATERIAL &
PETROLEUM ACTIVITY
ATTN STSGP-PW (MR PRICE) 1
SHARPE ARMY DEPOT
LATHROP CA 95330

CDR
US ARMY FOREIGN SCIENCE & TECH
CENTER
ATTN DRXST-MT1 1
FEDERAL BLDG
CHARLOTTESVILLE VA 22901

CDR
DARCOM MATERIAL READINESS
SUPPORT ACTIVITY (MRSA)
ATTN DRXMD-MS 1
LEXINGTON KY 40511

HQ, US ARMY T&E COMMAND
ATTN DRSTE-TO-O 1
ABERDEEN PROVING GROUND, MD 21005

HQ, US ARMY ARMAMENT R&D CMD
ATTN DRDAR-SCM-OO (MR MUFFLEY) 1
DRDAR-TST-S 1
DOVER NJ 07801

HQ, US ARMY TROOP SUPPORT &
AVIATION MATERIAL READINESS
COMMAND
ATTN DRSTS-MFG (2) 1
DRCPO-PDE (LTC FOSTER) 1
4300 GOODFELLOW BLVD
ST LOUIS MO 63120

DEPARTMENT OF THE ARMY
CONSTRUCTION ENG RSCH LAB
ATTN CERL-EM 1
P O BOX 4005
CHAMPAIGN IL 61820

HQ
US ARMY TRAINING & DOCTRINE CMD
ATTN ATCD-SL (MR RAFFERTY) 1
FORT MONROE VA 23651

DIRECTOR
US ARMY RSCH & TECH LAB (AVRADCOM)
PROPULSION LABORATORY
ATTN DAVDL-PL-D (MR ACURIO) 1
21000 BROOKPARK ROAD
CLEVELAND OH 44135

CDR
US ARMY NATICK RES & DEV CMD
ATTN DRDNA-YEP (DR KAPLAN) 1
NATICK MA 01760

CDR
US ARMY TRANSPORTATION SCHOOL
ATTN ATSP-CD-MS 1
FORT EUSTIS VA 23604

CDR
US ARMY QUARTERMASTER SCHOOL
ATTN ATSM-CD-M 1
ATSM-CTD-MS 1
ATSM-TNG-PT (COL VOLPE) 1
FORT LEE VA 23801

HQ, US ARMY ARMOR SCHOOL
ATTN ATSB-TD 1
FORT KNOX KY 40121

CDR
US ARMY LOGISTICS CTR
ATTN ATCL-MS (MR A MARSHALL) 1
FORT LEE VA 23801

CDR
US ARMY FIELD ARTILLERY SCHOOL
ATTN ATSF-CD 1
FORT SILL OK 73503

CDR
US ARMY ORDNANCE CTR & SCHOOL
ATTN ATSL-CTD-MS 1
ABERDEEN PROVING GROUND MD 21005

CDR
US ARMY ENGINEER SCHOOL
ATTN ATSE-CDM 1
FORT BELVOIR VA 22060

CDR
US ARMY INFANTRY SCHOOL
ATTN ATSH-CD-MS-M 1
FORT BENNING GA 31905

CDR
US ARMY AVIATION CTR & FT RUCKER
ATTN ATZQ-D 1
FORT RUCKER AL 36362

DEPARTMENT OF THE NAVY

CDR
NAVAL AIR PROPULSION CENTER
ATTN PE-71 1
PE-72 (MR D'ORAZIO) 1
P O BOX 7176
TRENTON NJ 06828

CDR
NAVAL SHIP ENGINEERING CTR
CODE 6101F (MR R LAYNE) 1
WASHINGTON DC 20362

CDR
DAVID TAYLOR NAVAL SHIP R&D CTR
CODE 2830 (MR G BOSMAJIAN) 1
CODE 2831 1
ANNAPOLIS MD 21402

JOINT OIL ANALYSIS PROGRAM -
TECHNICAL SUPPORT CTR 1
BLDG 780
NAVAL AIR STATION
PENSACOLA FL 32508

DEPARTMENT OF THE NAVY
HQ, US MARINE CORPS
ATTN LPP (MAJ SANBERG) 1
LMM (MAJ GRIGGS) 1
WASHINGTON DC 20380

CDR
NAVAL AIR SYSTEMS CMD
ATTN CODE 52032E (MR WEINBURG) 1
CODE 53645 1
WASHINGTON DC 20361

CDR
NAVAL AIR DEVELOPMENT CTR
ATTN CODE 60612 (MR L STALLINGS) 1
WARMINSTER PA 18974

CDR
NAVAL RESEARCH LABORATORY
ATTN CODE 6170 (MR H RAVNER) 1
CODE 6180 1
CODE 6110 (DR HARVEY) 1
WASHINGTON DC 20375

CDR
NAVAL FACILITIES ENGR CTR
ATTN CODE 1202B (MR R BURRIS) 1
CODE 120B (MR BUSCHELMAN) 1
200 STOVALL ST
ALEXANDRIA VA 22322

CHIEF OF NAVAL RESEARCH
ATTN CODE 473 (DR R MILLER) 1
ARLINGTON VA 22217

CDR
NAVAL AIR ENGR CENTER
ATTN CODE 92727 1
LAKEHURST NJ 08733

CDR
NAVY FACILITIES ENGRG CMD
CIVIL ENGR SUPPORT OFC
CODE 15312A (ATTN EOC COOK) 1
NAVAL CONSTRUCTION BATTALION CTR
PORT HUENEME CA 93043

CDR, NAVAL MATERIAL COMMAND
ATTN MAT-08T3 (DR A ROBERTS) 1
CP6, RM 606
WASHINGTON DC 20360

CDR
NAVY PETROLEUM OFC
ATTN CODE 40 1
CAMERON STATION
ALEXANDRIA VA 22314

CDR
MARINE CORPS LOGISTICS SUPPORT
BASE ATLANTIC
ATTN CODE P841 1
ALBANY GA 31704

DEPARTMENT OF THE AIR FORCE

HQ, USAF
ATTN RDPT 1
WASHINGTON DC 20330

HQ AIR FORCE SYSTEMS CMD
ATTN AFSC/DLF (LTC RADLOF) 1
ANDREWS AFB MD 20334

CDR
US AIR FORCE WRIGHT AERONAUTICAL LAB
ATTN AFWAL/POSF (MR CHURCHILL) 1
AFWAL/POSL (MR JONES) 1
WRIGHT-PATTERSON AFB OH 45433

CDR
USAF SAN ANTONIO AIR LOGISTICS CTR
ATTN SAALC/SFQ (MR MAKRIS) 1
SAALC/MMPRR (MR ELLIOT) 1
KELLY AIR FORCE BASE, TX 78241

CDR
US AIR FORCE WRIGHT AERONAUTICAL LAB
ATTN AFWAL/MLSE (MR MORRIS) 1
AFWAL/MLBT 1
WRIGHT-PATTERSON AFB OH 45433

CDR
USAF WARNER ROBINS AIR LOGISTIC CTR
ATTN WR-ALC/MMIRAB-1 (MR GRAHAM) 1
ROBINS AFB GA 31098

OTHER GOVERNMENT AGENCIES

US DEPARTMENT OF TRANSPORTATION
ATTN AIRCRAFT DESIGN CRITERIA BRANCH 2
FEDERAL AVIATION ADMIN
2100 2ND ST SW
WASHINGTON DC 20590

US DEPARTMENT OF ENERGY
ALTERNATIVE FUELS UTILIZATION BRANCH
ATTN: MR. E.E. ECKLUND 1
MR. R.D. FLEMING 1
MAIL CODE 5H-044
FORRESTAL BUILDING
WASHINGTON DC 20585

DIRECTOR
NATL MAINTENANCE TECH SUPPORT CTR 2
US POSTAL SERVICE
NORMAN OK 73069

US DEPARTMENT OF ENERGY
BARTLESVILLE ENERGY RSCH CTR
DIV OF PROCESSING & THERMO RES 1
DIV OF UTILIZATION RES 1
BOX 1398
BARTLESVILLE OK 74003

SCI & TECH INFO FACILITY
ATTN NASA REP (SAK/DL) 1
P O BOX 8757
BALTIMORE/WASH INT AIRPORT MD 21240

NASA-LEWIS RESEARCH CENTER
ATTN: MR. R.P. MIGRA 1
MR. G.M. PROK 1
MAIL STOP 500/122
21000 BROOKPARK ROAD
CLEVELAND, OH 44135

U.S. DEPARTMENT OF ENERGY
BARTLESVILLE ENERGY TECHNOLOGY CENTER
ATTN: MR. J.E. ALLSUP 1
P.O. BOX 1398
BARTLESVILLE, OK 74003

OTHER AGENCIES

MUELLAR ASSOCIATES, INC.
ATTN: MR. T.J. TIMBARIO 1
1900 SULPHUR SPRING ROAD
BALTIMORE, MD 21227

SOUTHWEST RESEARCH INSTITUTE
ATTN: MR. JOHN RUSSELL 1
MR. J.D. TOSH 1
POST OFFICE DRAWER 28510
6220 CULEBRA ROAD
SAN ANTONIO, TX 78284

COORDINATING RESEARCH COUNCIL
ATTN: MR. A.E. ZENGAL 1
219 PARAMETER CENTER PARKWAY
ATLANTA, GA 30346

SYSTEMS CONTROL, INC.
ATTN: MR. R. CARLSON
ENVIRONMENTAL ENGINEERING DIVISION
421 EAST CERRITOS AVENUE
ANEHEIM, CA 92805

AEROSPACE CORPORATION
ATTN: MR. R.D. RAYMOND 1
SUITE 4000
L'ENFANT PLAZA, SW
WASHINGTON, DC 20024

UNIVERSITY OF WISCONSIN
ATTN: P.S. MYERS 1
DEPT. OF MECHANICAL ENGINEERING
750 UNIVERSITY AVENUE
MADISON, WI 53706

UNIVERSITY OF MISSOURI - ROLLA
ATTN: R.T. JOHNSON 1
MECHNICAL ENGINEERING DEPT.
ROLLA, MO 65401

UNIVERSITY OF SANTA CLARA
ATTN: R.K. PEFLEY 1
DEPT. OF MECHANICAL ENGINEERING
SANTA CLARA, CA 95053

SUNTECH GROUP
ATTN: A.F. TALBOT 1
P.O. BOX 1135
MARCUS HOOK, PA 19061

PENN STATE UNIVERSITY
ATTN: MR. S.S. LESTZ 1
MECHANICAL ENGINEERING DEPT.-302
UNIVERSITY PARK, PA 16802

TEXAS A&M UNIVERSITY
ATTN: T.R. LALK 1
MECHANICAL ENGINEERING DEPT.
COLLEGE STATION, TX 77843


ILMED
8